13th International Conference

Beam Injection Assessment of Microstructures in Semiconductors

BIAMS

2016 Versailles

Abstract Book

5-9 June 2016, Versailles, FRANCE

UNIVERSITÉ DE VERSAILLES ST-QUENTIN-EN-YVELINES

université PARIS-SACLAY

HORIBA Scientific

îledeFrance

attolight™

NanoSaclay

MATELECT LTD

nano-K DES ATOMES FROIDS AUX NANOSCIENCES

cnrs

BIAMS - Versailles 2016

The 13th International Conference BIAMS continues a successful series of conferences which started in Meudon, France, in 1988. It is our honor and pleasure to welcome again the BIAMS conference in the Paris region. It is organized by GEMaC, a joint laboratory of University of Versailles St Quentin and CNRS, involved in Solid State Physics researches.

The BIAMS conference gathers scientists from all over the world to present advances in the field of the physical characterization of semiconductors by means of beam injection and related methods. Application fields are broad: photovoltaic, micro- and nano- electronics, device degradation, semiconductor defects, reverse engineering, nanophotonics, quantum optics, ...

BIAMS has gained an excellent reputation for high quality scientific presentations and discussions, and also for the warm atmosphere of its academic interaction among physicists, materials scientists and technologists working in this field, which offers an ideal place for networking.

Versailles is a recent university city which benefits from the scientific dynamism of Paris region. Versailles is just an hour from the old city center of Paris. Otherwise, you will enjoy the historic atmosphere of Versailles city with its famous gardens and castle.

We very much hope that you will find the conference both enjoyable and valuable.

Julien Barjon (Conference Chair) and the organizing committee.

Scope and Topics

Focused at the nanoscale, electron and ion beams provide a local probe particularly-suited for investigating semiconductor microstructures, nanostructures and defects. Their application for semiconductor characterization are the principal topics of this conference. The core of this meeting is cathodoluminescence (CL) and electron beam-injection current (EBIC) analysis, but not exclusively and the following topics are included :

Semiconductor characterization methods:

Electron beam characterization methods: cathodoluminescence, EBIC, TEM, STEM, EBSD, ...

Light characterization methods: spatially resolved PL, microRaman, OBIC, ...

Scanning Probe Microscopy: STM, AFM and SNOM techniques

Ion beams and other microscopy characterization techniques

Application of these methods to the study of:

Photovoltaic materials and devices

Point and extended defects, impurities, interfaces ...

Heterostructures, quantum structures, devices ...

2D crystals, nanomaterials, nanowires, nanotubes,...

Optical and electronic properties of defects, microstructures and nanostructures

Committees

International Program Committee

BARJON Julien, Université de Versailles Saint-Quentin-en-Yvelines, France
BREITENSTEIN Otwin, MPI of Microstructure Physics, Halle, Germany
CAVALLINI Anna, University Bologna, Italy
DONGWAN Kim, University of Korea, Korea
KITTLER Martin, IHP Frankfurt & IHP/BTU Joint Lab Cottbus, Germany
LEIPNER Harmut S. (advisory), University of Halle, Germany
PHILLIPS Matt, University of Technology, Sydney, Australia
PIQUERAS Javier, University Complutense, Madrid, Spain
SEKIGUCHI Takashi, National Institute for Materials Science Tsukuba, Japan
SIEBER Brigitte, Université des Sciences et Techniques de Lille, France
TABET Nouar, Qatar Energy and Environment Research Institute, Qatar
TOMOKAGE Hajime, Fukuoka University, Japan
YAKIMOV Eugene, Institute of Microelectronics, Chernogolovka, Russia
ZAMORYANSKA Maria, Ioffe Institute, St Petersburg, Russia

Local Committee

BARJON Julien (Chairman), GEMaC, Versailles
COLLIN Stéphane, LPN, Marcoussis
DONATINI Fabrice, Institut Nél, Grenoble
KOCIAK Mathieu, LPS, Orsay
SIEBER Brigitte, USTL, Lille
ARNOLD Christophe, GEMaC, Versailles
AUPETIT OCHIN Danièle, GEMaC, Versailles
GALTIER Pierre, GEMaC, Versailles
LUSSON Alain, GEMaC, Versailles
ROUX Corinne, GEMaC, Versailles
STENGER Ingrid, GEMaC, Versailles
VILAR Christèle, GEMaC, Versailles

Conference venue

About Versailles

Located at only 20 km from Paris, Versailles is a city which was built by French History and in particular under the period of King Louis XIV. Versailles is famous woldwide for the "Chateau de Versailles" which is the symbol of french power and force during the 18th century. Gardens "à la française", "Galerie des Glaces" show majesty and luxury which were part of the french empire at that time. Versailles has been also a refuge for the government, not only during the french Revolution, but also during "La Commune de Paris" in 1870 and the 3rd Republic. The related constructions are also of high interest : Salle du Jeu de Paume, Hôtel de la Préfecture, Salle des Congrès...

For further information on Versailles, please consult the Tourist information center website:
http://www.versailles-tourisme.com/en/accueil.html.

Access information

The conference will be held on the campus of sciences of Versailles city at the following address :
45 avenue des Etats Unis, 75000 Versailles, France

General map

The different locations of events during the conference are shown on the general map on the next page. All are accessible by walking or bus.

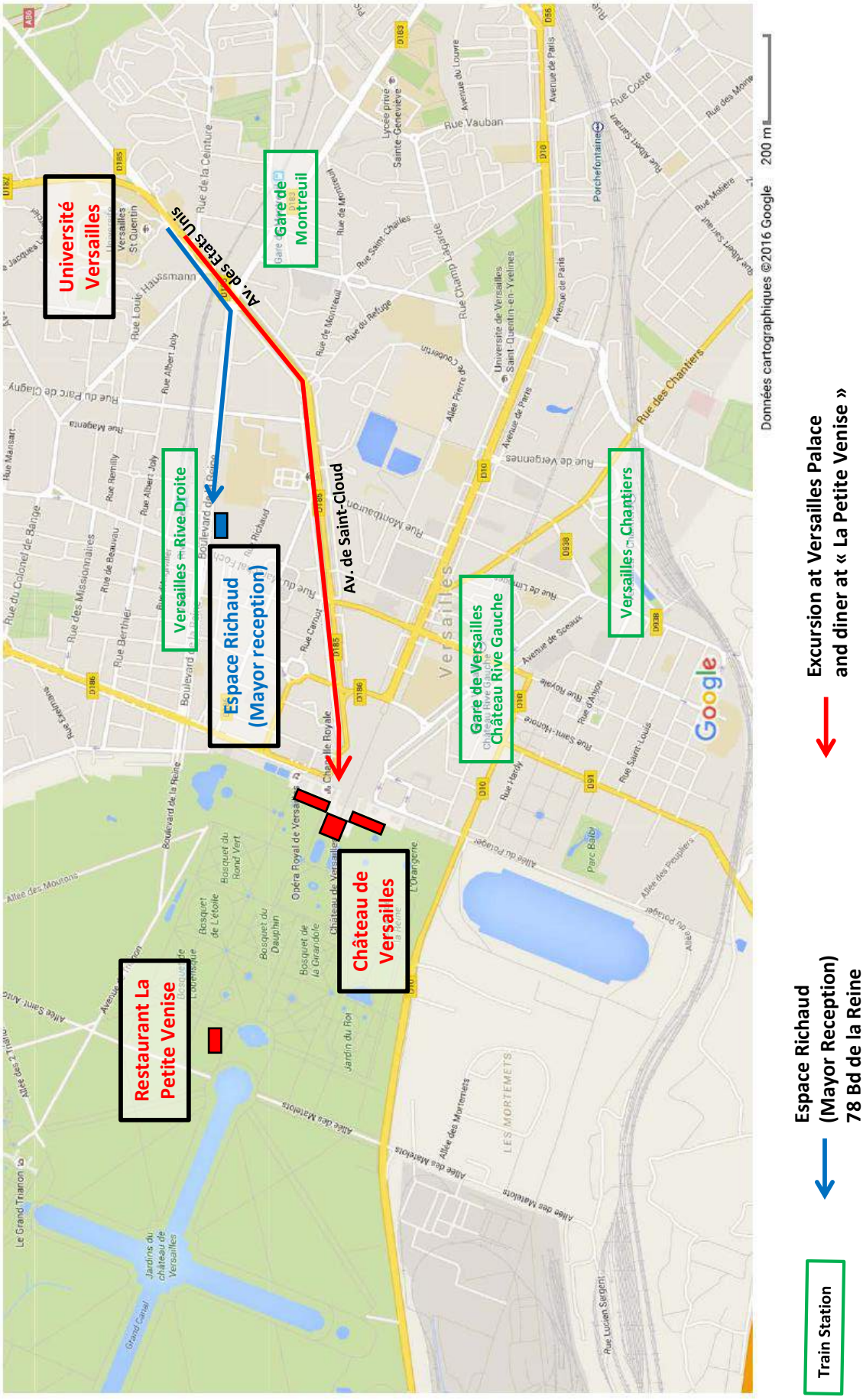
Université Versailles
Av. des Etats Unis
Gare de Montreuil
Av. de Saint-Cloud
Versailles – Rive Droite
Espace Richaud (Mayor reception)
Versailles – Chantiers
Gare de Versailles Château Rive Gauche
Château de Versailles
Restaurant La Petite Venise
Excursion at Versailles Palace and diner at « La Petite Venise »
Espace Richaud (Mayor Reception) 78 Bd de la Reine
Train Station
Données cartographiques ©2016 Google 200 m

How to get to Versailles from the airports ?

The airports of Paris are: Roissy Charles-de-Gaulle airport (CDG): 43 km from Versailles and Orly airport (ORY): 30 km from Versailles.

Coming by taxi:

- From Charles de Gaulle airport : travel time : from 40 to 120 minutes depending on traffic, average fare : from 70 to 110 €.
- From Orly airport : travel time : from 20 to 40 minutes depending on traffic, average fare: from 40 to 50 €.

Coming by public transport:

- From Charles de Gaulle airport : travel time: 1h20, fare : 15.7 €.
- From Orly airport : travel time: 1h, fare : 15 €.

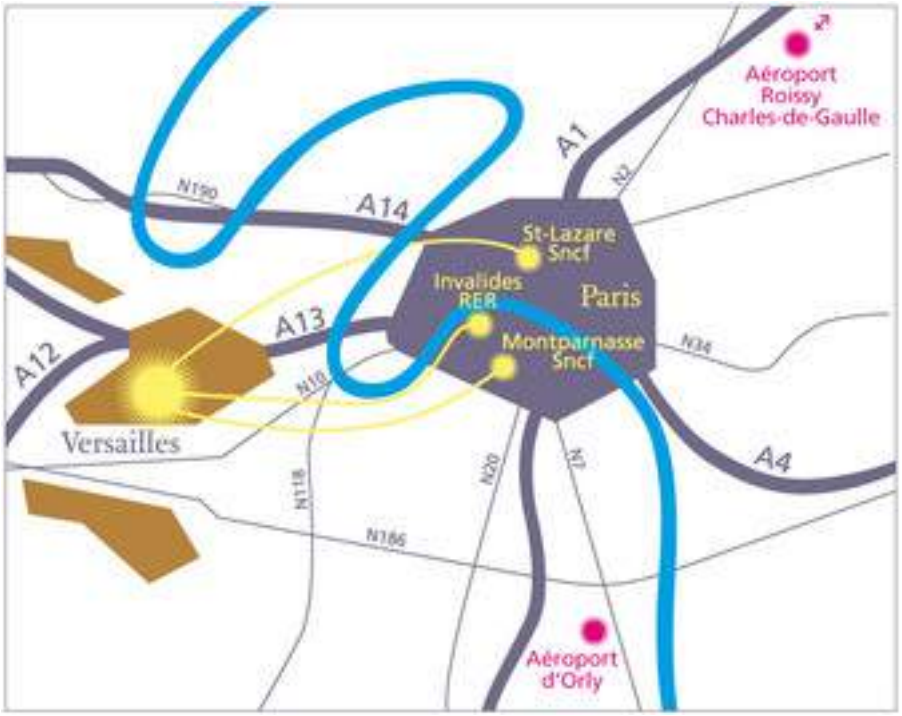

On the Campus

BIAMS 2016 is located in FERMAT building (1st block on the left after the entrance).

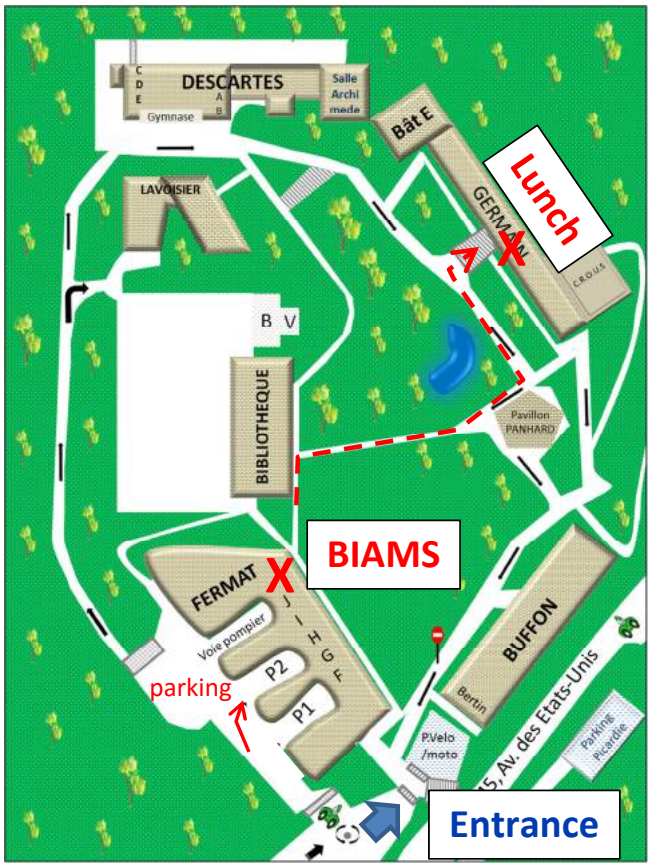

Fermat building

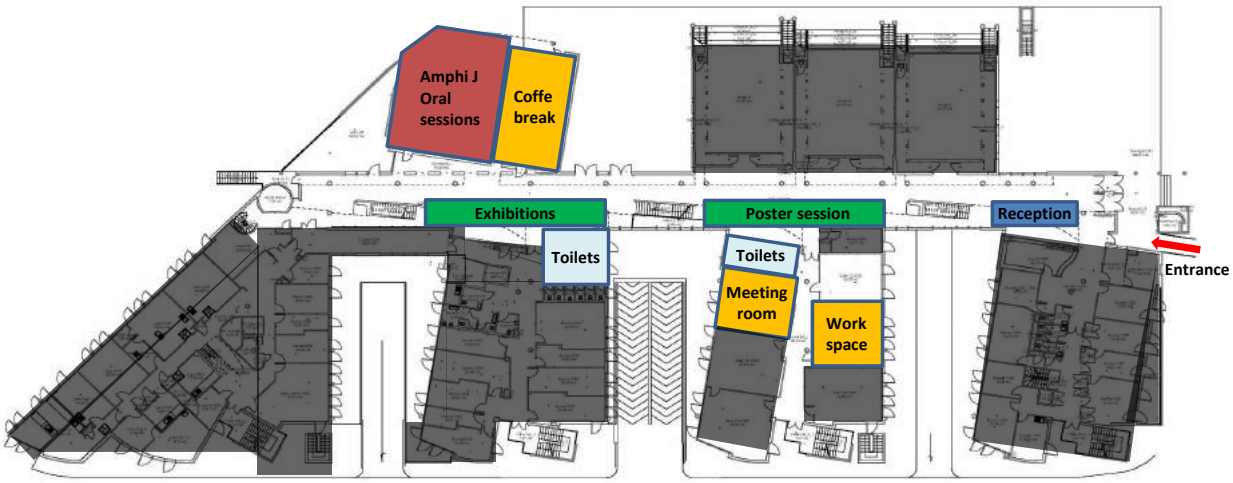

How to get around Versailles city ?

The nearest train station from Versailles university is Montreuil (SNCF) in Versailles. Be careful not to confuse with Montreuil city in the east of Paris region. Note that Versailles city is accessible by 3 different lines from Paris : Transilien train from Gare St Lazare (direct to Montreuil SNCF), RER C from Invalides, or even Transilien train from Gare Montparnasse.

Note that Versailles University is accessible by Phebus line R (unavailable on sunday) from the two nearest train stations Montreuil and Versailles Chantier. Versailles University is also accessible by Phebus lines E, F, O and Y. Only the Phebus line F is available on sunday.

Practical information

Presentations

Invited talks are 30 min + 10 min discussion.

Contributed talks are 15 min + 5 min discussion.

The maximum poster size is 100 cm wide and 150 cm high.

Lunches and coffee breaks

We offer lunch for every participants from Monday to Wednesday, as well as coffee breaks. A packed lunch will be distributed on Thursday noon at the end of the conference.

Registration

Registration will start from Sunday 5^{th}, 16:00 to 19:00, inside Fermat building at the campus UVSQ. It will continue on Monday, 8:00 am.

Website

The conference website is `http://biams2016.sciencesconf.org/`.

Contact

Please email us at: biams2016@sciencesconf.org.

Social program

Mayor reception

The Mayor reception will take place at Espace Richaud, 78 Bd de la Reine at 18:00 on Monday evening. It is open to all participants. This place is about 20 minutes by walk from the campus. Some refreshments and "amuse gueules" will be offered at the end of the reception.

Visit of Versailles Palace

The visit of Versailles Palace is scheduled for all BIAMS participants on Wednesday afternoon and starts at 16:15 until 18:00 ; this tour in small groups will be commented by guides in English. Versailles Palace is 30 minutes (2 km) by walk from University campus. After the visit, on your free time, you can enjoy the nice gardens with many fountains and sculptures in the famous "bosquets", until the conference dinner inside the garden.

Conference dinner

The conference dinner will take place in the gardens of Versailles Palace at the restaurant "La Petite Venise". It is located in the gardens close to "Apollon fountain" and the beginning of "Grand Canal". The conference diner is from 19:30 to 23:00. It is included in the registration fee for all participants. A special bus will be available for attendee's way back, to reach Versailles city center, train stations and the university campus.

Proceedings

Accepted papers will be published in a conference volume of EDP Sciences: MATEC Web of Conferences.

All papers published in the conference proceedings will be made available in an Open Access format at the website of MATEC Web of Conferences specializing in Materials science, Engineering & Chemistry. All published papers will be indexed Google Scholar, CAS, Compendex, Inspec, DOAJ, CPCI (Web of Science), Scopus and presented in a dedicated online issue. They will be peer reviewed.

At least one author of each article should attend the conference.

Manuscript submission

A maximum of two articles per author is accepted. 8 pages are allowed to invited talks and 6 pages to contributed oral and poster presentations. Manuscripts shorter than 4 printed pages are not acceptable.

Instructions for authors are available at http://www.matec-conferences.org/for-authors

Word template to be downloaded: 170 x 250 mm paper size, one column format

The paper should be **submitted before the end of June 2016** (.pdf only). Before making your PDF, please check PDF guidelines.

All submitted articles should report original, previously unpublished research results, experimental or theoretical. Articles submitted to the conference should meet these criteria and must not be under consideration for publication elsewhere.

To submit your paper, please go into the section "MY SPACE > Submissions" of the conference website (http://biams2016.sciencesconf.org/user/submissions) and follow the wizard instructions.

Sponsors

Companies

HORIBA Scientific

attolight™

MATELECT LTD

Public institutions

îledeFrance

nano-K Réseau Francilien DES ATOMES FROIDS AUX NANOSCIENCES

NanoSaclay Laboratoire d'Excellence en Nanosciences et Nanotechnologies

UNIVERSITÉ DE VERSAILLES ST-QUENTIN-EN-YVELINES

université PARIS-SACLAY

cnrs

General planning

	Sunday 5	Monday 6	Tuesday 7	Wenesday 8	Thursday 9
8h00 - 8h50		Registration			
8h50		Opening session			
9h00		Araujo	Al-Jassim	Jacopin	Donghwan
9h20					
9h40		Tallaire	Mohammad	Schué	Veselov
10h00		Phillips	Peretzki	Medvedev	Schwartz
10h20		Roque	Fazio Maria	Portail	Sekiguchi
10h40		Coffee break	Coffee break	Coffee break	Coffee break
11h00		Toth	Zamoryankaya	Niklas	Haegel
11h20					
11h40		Kaminski	Martin	Schmidt	Cremades
12h00		Bondarenko	Cho	Sieber	Jimenez
12h20 - 14h00		Lunch	Lunch	Lunch	Closing session
14h00		Pavesi	Tchernycheva	Coenen	
14h20					
14h40		Breitenstien	Donatini		
15h00		Yakimov	Müller		
15h20		Orlov	Liu		
15h40		Coffee break	Coffee break		
16h00	Reception and Welcome Party	Kociak	Poster Session	Versailles Palace Visit	
16h20					
16h40		Mester			
17h00					
17h20					
17h40					
18h00		Mayor Reception			
18h20					
18h40					
19h00					
19h20				Conference Banquet	
19h40					
20h00					
20h - 23h					

Cathodoluminescence	LBIC, EBIC and CL	Photovoltaic materials	Plasmonic	Nano-materials
Beam-induced modifications	Excitation processes	Miscellaneous	Devices	

PROGRAM

Sunday June, 5

16:00-19:00	Registration and welcome party at Versailles university

Monday June, 6

	8:00-8:50	Registration	
	8:50-9:00	Opening remarks	
MoA	09:00-10:40	**Cathodoluminescence - part 1** Chair: Anna Cavallini, *University Bologna, Italy*	23
MoA-1	09:00-09:40	Input of cathodoluminescence in the semiconductor field: A review over the last 30 years **Daniel Araujo (Invited)** *Universidad de Cádiz, Dpto de Ciencia de los Materiales (Spain)*	24
MoA-2	09:40-10:00	Dislocation Engineering in CVD Diamond Evidenced by Cathodoluminescence Imaging **Alexandre Tallaire** *Laboratoire des Sciences des Procédés et des Matériaux (France)*	25
MoA-3	10:00-10:20	Nitrogen Incorporation in ZnO Nanowires **Matthew Phillips** *University of Technology Sydney (Australia), Technical University Berlin (Germany)*	26
MoA-4	10:20-10:40	Nanocharacterization collocated of defects and luminescence in InGaAs/GaAs quantum wells **Joyce Roque** *Departement Technologies Silicium, Service Caractérisation des Matériaux et des Composants (France), Laboratoire des Technologies de la Microélectronique (France)*	27
	10:40-11:00	Coffee break (20min)	
MoB	11:00-12:20	**Beam-induced modifications** Chair: Eugene Yakimov, *Institute of Microelectronics, Chernogolovka, Russia*	29
MoB-1	11:00-11:40	Electron Beam Induced Chemical Processing and Characterization of Semiconductors **Milos Toth (Invited)** *University of Technology, Sydney (Australia)*	30
MoB-2	11:40-12:00	Effect of Proton Fluence on the Properties and Concentrations of Radiation Defects in High-Purity FZ Si **Pawel Kaminski** *Institute of Electronic Materials Technology (Poland)*	31
MoB-3	12:00-12:20	Optical properties of silicon modified by He ion beam **Anton Bondarenko** *St. Petersburg State University, faculty of Physics (Russia)*	32

	12:20-14:00	Lunch break (100min)	
MoC	14:00-15:40	**LBIC and EBIC** Chair: Takashi Sekiguchi, *National Institute for Materials Science Tsukuba, Japan*	33
MoC-1	14:00-14:40	LBIC in Tellurides for X-ray Detection: Transport Properties and Electric Field Reconstruction **Maura Pavesi (Invited)** *Dipartimento di Fisica e Scienze della Terra - Univ. of Parma (Italy)*	34
MoC-2	14:40-15:00	New Methods for Evaluating Luminescence Images of Silicon Solar Cells **Otwin Breitenstein** *Max Planck Institute of Microstructure Physics (Germany)*	35
MoC-3	15:00-15:20	Room Temperature Dislocation Glide in GaN Enhanced by E-beam Irradiation **Eugene Yakimov** *Institute of of Microelectronics Technology RAS (Russia)*	36
MoC-4	15:20-15:40	Study of Dislocation Trails in Si by the LBIC and EBIC Methods **Valeri Orlov** *Institute of of Microelectronics Technology RAS (Russia), Institute of Solid State Physics RAS (Russia)*	37
	15:40-16:00	Coffee break (20min)	
MoD	16:00-17:00	**Excitation processes** Chair: Martin Kittler, *IHP Frankfurt & IHP/BTU Joint Lab Cottbus, Germany*	39
MoD-1	16:00-16:40	Time-correlated Cathodoluminescence of defect centers in diamond and hBN **Mathieu Kociak (Invited)** *Laboratoire de Physique des Solides (France)*	40
MoD-2	16:40-17:00	Theoretical and experimental studies of cathodoluminescence excitation processes **Aleksandr Mester** *Ioffe Institute (Russia)*	41
	18:00-20:00	Mayor reception at Espace Richaud	

Tuesday June, 7

TuA 09:00-10:40 **Photovoltaic materials** 43
Chair: Otwin Breitenstein, *MPI of Microstructure Physics, Halle, Germany*

TuA-1 09:00-09:40 Luminescent, structural and chemical properties of defects in MBE- and CSS-grown CdTe films for solar cell applications 44
Mowafak Al-Jassim (Invited)
National Renewable Energy Laboratory (United States)

TuA-2 09:40-10:00 Photoluminescence Study of Charge Transfer Dynamics in Perovskite Solar Cells 45
Istiaque Hossain Mohammad
Qatar Environment and Energy Research Institute (Qatar)

TuA-3 10:00-10:20 Electron beam induced current investigations on the nanoscale at a complex oxide pn-heterojunction 46
Patrick Peretzki
UniGoe (Germany)

TuA-4 10:20-10:40 Electrical characterization at the nanoscale of Si-based thin films for photovoltaic applications 47
Maria Antonietta Fazio
University of Bologna (Italy)

10:40-11:00 Coffee break (20min)

TuB 11:00-12:20 **Cathodoluminescence - part 2** 49
Chair: Javier Piqueras, *University Complutense, Madrid, Spain*

TuB-1 11:00-11:40 Radiative center properties in wide bandgap semiconductors 50
Maria Zamoryanskaya (Invited)
Ioffe Institute (Russia)

TuB-2 11:40-12:00 Temperature-dependent Cathodoluminescence: Quantifying Thermal Quenching at the Microscopic Level 51
Lisa Martin
Center for Nano- and Biophotonics, Ghent University (Belgium), LumiLab, Department of Solid State Sciences, Ghent University (Belgium)

TuB-3 12:00-12:20 Cross-sectional CL observation for Oxynitride phosphors 52
Yujin Cho
National Institute for Materials Science (NIMS) (Japan)

12:20-14:00 Lunch break (100min)

TuC 14:00-15:40 **EBIC and CL** 53
Chair: Nouar Tabet , *Qatar Energy and Environment Research Institute, Qatar*

TuC-1	14:00-14:40	Electron beam induced current and cathodoluminescence investigation of InGaN/GaN core-shell nanowire light emitting diodes **Maria Tchernycheva (Invited)** *Institut d'Electronique Fondamentale (France)*	54
TuC-2	14:40-15:00	Comparison of three e-beam techniques for electric field imaging and carrier diffusion length measurement on the same nanowires **Fabrice Donatini** *Institut NEEL, CNRS, University of Grenoble Alpes (France)*	55
TuC-3	15:00-15:20	Luminescence properties and strain distribution within single GaN-based core-shell micropillars analyzed by nanoscale resolved cathodoluminescence spectroscopy and electron backscatter diffraction **Marcus Müller** *Institute of Experimental Physics, Otto-von-Guericke-University Magdeburg (Germany)*	56
TuC-4	15:20-15:40	Exciton Dynamics on a Single Dislocation in GaN by Picosecond Cathodoluminescence **Wei Liu** *Institute of Physics, Ecole Polytechnique Fédérale de Lausanne (Switzerland)*	57
	15:40-16:00	Coffee break (20min)	
TuP	16:00-18:00	**Poster Session**	83

Wednesday June, 8

WeA 09:00-10:40 **Cathodoluminescence - part 3** 59
Chair: Matthew Phillips, *University of Technology, Sydney*

WeA-1 09:00-09:40 Hopping of Bound Excitons in Zno Microwires Probed by Time-Resolved CL 60
Gwénolé Jacopin (Invited)
Institute of Physics, Ecole Polytechnique Fédérale de Lausanne (Switzerland)

WeA-2 09:40-10:00 Excitonic Luminescence of BN Materials 61
Léonard Schué
Laboratoire d'étude des microstructures (France), Groupe d'Etude de la Matière Condensée (France)

WeA-3 10:00-10:20 Cathodoluminescent Signature of Dislocation Reactions in GaN 62
Oleg Medvedev
St. Petersburg State University (Russia)

WeA-4 10:20-10:40 Cathodoluminescence of ensemble and single InGaN quantum disk-in-nanowires made by selective area sublimation 63
Marc Portail
Centre de Recherche sur l'HétéroEpitaxie et ses Applications (France)

10:40-11:00 Coffee break (20min)

WeB 11:00-12:20 **Miscellaneous** 65
Chair: Maria Zamoryanskaya, *Ioffe Institute, St Petersburg, Russia*

WeB-1 11:00-11:40 STM-luminescence spectroscopy of defects and impurities in oxides 66
Niklas Nilius (Invited)
University of Oldenburg (Germany)

WeB-2 11:40-12:00 Nanoscale cathodoluminescence of an InGaN single quantum well intersected by individual dislocations 67
Gordon Schmidt
Institute of Experimental Physics, Otto-von-Guericke-University Magdeburg (Germany)

WeB-3 12:00-12:20 Enhanced Ultraviolet Luminescence of ZnO Nanorods Treated by High-Pressure Water Vapor Annealing 68
Brigitte Sieber
UMET (France)

12:20-14:00 Lunch break (100min)

WeC 14:00-14:40 **Plasmonic** 71
Chair: Matthieu Kociak, *Laboratoire de Physique des Solides, France*

WeC-1	14:00-14:40	Angle-resolved cathodoluminescence spectroscopy for nanophotonics **Toon Coenen (Invited)** *DELMIC BV (Netherlands)*	72
	16:15-18:00	Castle visit	
	18:00-19:30	Garden visit (free time)	
	19:30-23:00	Conference dinner (inside the garden)	

Thursday June, 9

ThA	09:00-10:40	**Devices** Chair: Hajime Tomokage, *Fukuoka University, Japan*	73
ThA-1	09:00-09:40	A Study on Degradation of Perovskite Solar Cells and Materials **Kim Donghwan (Invited)** *Korea University (South Korea)*	74
ThA-2	09:40-10:00	Novel Technique for the Investigation of Internal Optical Loss in High-Power Laser Heterostructures **Dmitrii Veselov** *Ioffe Physico-Technical Institute (Russia)*	75
ThA-3	10:00-10:20	Huge Intensity gain of Group-IV LEDs on Si substrates by using MQW **Bernhard Schwartz** *Institut für Physik, Brandenburgische Technische Universität Cottbus-Senftenberg (Germany)*	76
ThA-4	10:20-10:40	Fountain Detectors Are Go - Low Energy Secondary Electron Imaging for Various Semiconductors **Takashi Sekiguchi** *Nano Device Characterization Group, National Institute for Materials Science (Japan)*	77
	10:40-11:00	Coffee break (20min)	
ThB	11:00-12:20	**Nano-materials** Chair: Brigitte Sieber, *Université des Sciences et Techniques de Lille, France*	79
ThB-1	11:00-11:40	Dual Probe Imaging: Combining Electron Beam Excitation and Near Field Scanning Optical Microscopy to Visualize Carrier Transport **Nancy Haegel (Invited)** *National Renewable Energy Laboratory (United States)*	80
ThB-2	11:40-12:00	Beam injection techniques in the control and micropatterning of phase transitions in TiO2 nanoparticles **Ana Cremades** *Universidad Complutense de Madrid (Spain)*	81
ThB-3	12:00-12:20	Cathodoluminescence study of photonic structures fabricated by dry etching on InP with InAsP quantum wells **Juan Jimenez** *Humboldt-Universit ät zu Berlin (Germany)*	82

Poster Session , Tuesday June, 7 (16:00-18:00)

ABSTRACTS

Monday June, 6 - MoA - Oral Session

09:00-10:40

Cathodoluminescence - part 1

Chair: Anna Cavallini, *University Bologna, Italy*

Input of cathodoluminescence in the semiconductor field: A review over the last 30 years

D.Araujo[1], F. Lloret[1] and J.C. Piñero[1] and P. Villar[1]
[1] Departamento de Ciencia de los Materiales e IM y QI, Universidad de Cádiz, 11510 Puerto Real (Cádiz), Spain
*E-mail: daniel.araujo@uca.es

Cathodoluminescence (CL) was first reported on diamond crystals by Crookes in 1879. However, this technique took its rise with the development of the scanning electron microscope (SEM). Then its development took place in parallel to electron beam induced current (EBIC), both resulting from the generation of electron-hole (e-h) pairs under the high energetic bombardment of electrons of the SEM electron beam. Indeed, the first observation of charge collection phenomena in SEM was observed by Everhart [1] in 1958 who noted that the beam induces a large difference in the back current of a p-n junction. Just before, the first light emission observation in a SEM was demonstrated by K.C.A. Smith in 1956 [2].

Even though CL can also be applied to other materials than semiconductors, for example for ceramics where different phase can be mapped and analyzed, most of the work has been carried out on semiconducting materials and devices. Different theoretical approximations of carrier diffusion in bulk semiconductor, including surface recombinations, were published at the end of the 70' [3,4]. This poses the basis for a quantification approach of CL and EBIC analysis. Other two qualitative steps, to further the possibilities of the technique, are the development of time resolved approach [5,6] and the arrival on the market of field effect electron guns (FEG). The latter improves beam brightness, beam spot size and allows to lower the energy beam analysis. This makes possible to analyze with higher accuracy the carrier dynamics and also to reach a 3D knowledge of the photon induced emission through CL-TEM tomography [7].

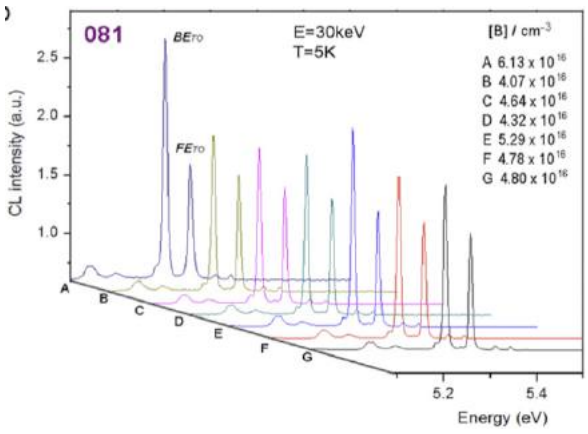

Recent results on the carrier behavior in diamond materials will be finally presented: dopant quantification and carrier transport analysis. This shows that CL is still a unique tool for the semiconductor material analysis.

Fig.1: CL spectra recorded on differently boron doped diamond samples. The FE^{TO} and BE^{TO} intensity ratio allows to deduce the doping level.

[1] T.E. Everhart, PhD dissertation, Cambridge University (1958)
[2] K.C.A. Smith, PhD dissertation, Cambridge University (1956)
[3] F. Berz and H.K. Kuiken, Solid State Electron. **19**, 437 (1976)
[4] C.J. Wu and D.B. Wittry, J. Appl. Phys. **49**, 2827 (1978)
[5] M. Merano, S. Sonderegger, A. Crottini, S. Collin, P. Renucci, E. Pelucchi, A. Malko, M.H. Baier, E. Kapon, B. Deveaud, and J.D. Ganiere, Nature **438**, 479 (2005)
[6] C. Díaz-Guerra, J. Piqueras, A. Castaldini, A. Cavallini, and L. Polenta, J. Appl. Phys. 94, 2341 (2003)
[7] A. C. Atre, B. J. M. Brenny, T. Coenen, A. García-Etxarri, A. Polman & J. A. Dionne, Nature Nanotechnology 10, 429–436 (2015)

Dislocation Engineering in CVD Diamond Evidenced by Cathodoluminescence Imaging

A. Tallaire[1], A. Boussadi[1], O. Brinza[1], J. Barjon[2], J. Achard[1]
[1] LSPM-CNRS, Université Paris 13, 99 avenue JB Clément, 93430 Villetaneuse, France
[2] GEMaC-CNRS, Université Versailles Saint-Quentin
*alexandre.tallaire@lspm.cnrs.fr

In the past decade, tremendous improvements in the crystalline quality and purity of Chemically Vapour Deposited (CVD) diamond films have been achieved. Millimetre-thick crystals with an area close to 1 cm² have been made commercially available by several suppliers, opening the way to new applications in optics and electronics. However synthetic single crystal diamond still suffers from a relatively high dislocation density typically in the 10^4-10^7 cm^{-2} range [1]. Dislocations thread through the grown CVD films perpendicularly to the surface, along the <001> direction. They affect current leakage in power devices, generate background fluorescence, or induce strain and unwanted birefringence in optical components. To achieve an optimal performance, new strategies and technologies aiming at suppressing dislocations are thus highly required.

Recently we found that it is possible to deviate threading dislocations by 45° so that they align along the <110> directions. This was achieved by homoepitaxial growth on diamond substrates having inclined planes, such as pyramidal-shape diamonds with 20° angles [2]. We explored this principle in order to confine dislocations in the lateral sectors of the grown crystal, thus allowing a reduction of their densities in the top (001) face.

Cathodoluminescence (CL) is a powerful technique to image dislocations in diamond. By recording the free-exciton emission of the crystal at 235 nm and low-temperature (110 K) dislocations become visible as dark spots or lines since they behave as efficient non-radiative recombination centers (Fig. 1). We used this technique to evaluate dislocation propagation direction and density, which has allowed us developing dislocation engineering strategies.

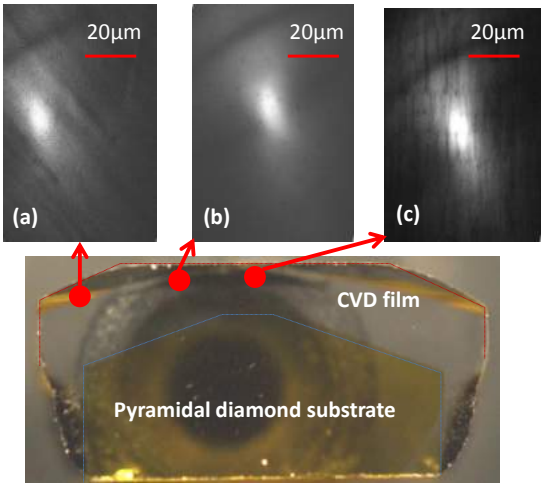

Fig. 1. CL images acquired at different locations (red spots) on the cross-section of a CVD film grown on a pyramidal-shape substrate. (a) 45° inclined dislocations, (b) dislocation-free area, (c) straight dislocations.

[1] M. Naamoun, A. Tallaire, F. Silva et al. physica status solidi (a), 209 (2012) 1715-1720.
[2] A. Tallaire, J. Achard, O. Brinza et al. Diam. & Relat. Mat., 33 (2013) 71-77.

Nitrogen Incorporation in ZnO Nanowires

M.R. Phillips[1*], L. Zhu[1], M.N. Lockrey[1], C. Ton-That[1], S. Khachadorian[2], S. Schlichting[2], N. Jankowski[2] and A. Hoffmann[2]
[1]School of Mathematical and Physical Sciences, University of Technology Sydney, Sydney, Australia
[2]Institut für Festkörperphysik, Technische Universität Berlin, Berlin, Germany
*matthew.phillips@uts.edu.au

Cathodoluminescence (CL) spectroscopy, Raman spectroscopy and X-ray absorption near-edge spectroscopy (XANES) have been used to investigate the chemical states of nitrogen species incorporated in ZnO. The use of ZnO nanowires (diameter ~150 nm and length ~1um grown by chemical vapour techniques) enabled uniform nitrogen doping. Nitrogen incorporation was achieved by thermal annealing in a nitrogen plasma at 300°C using a 230 V cathode bias, where the doping level was governed by the plasma treatment time ranging up to 120 min.

CL spectra from as-grown nanowires exhibited a strong donor bound D^oX emission at 3.36 eV and LO phonon replicas with a 72 meV spacing. Depth-resolved CL confirmed that the entire nanowires were saturated with N after 120 min. Following nitrogen plasma annealing, the intensities of the 3.23 and 3.31 eV peaks increase considerably relative to the D^oX peak. The enhancement of the 3.31 eV peak following long exposure times is attributable to excitons bound to extended structural defects. The CL emission peak at 3.23 eV has been attributed to shallow molecular N_2 acceptor in a donor-acceptor pair transition as evidenced by a blue shift of this peak with increasing electron beam excitation power.

XANES established that nitrogen plasma annealing produces three N-related defects in the nanowires: nitrogen on an oxygen site N_O, free N_2 that is loosely bound to the ZnO lattice and N_2 on a zinc site $(N_2)_{Zn}$ with signature XANES peaks at P1 (400.0 eV), and P2 (400.7 eV) and P3 (404.5 eV), respectively. As the plasma annealing time increases, the P2 component is enhanced relative to P1 and P3, indicating more nitrogen is present as molecular species with increasing annealing time. This result was supported by Raman spectroscopy that revealed signature emission lines for lattice bound molecular nitrogen. The work establishes a direct link between the emission at 3.23 eV and the concentration of molecular N_2 species that acts as a shallow acceptor as shown in the figure below.

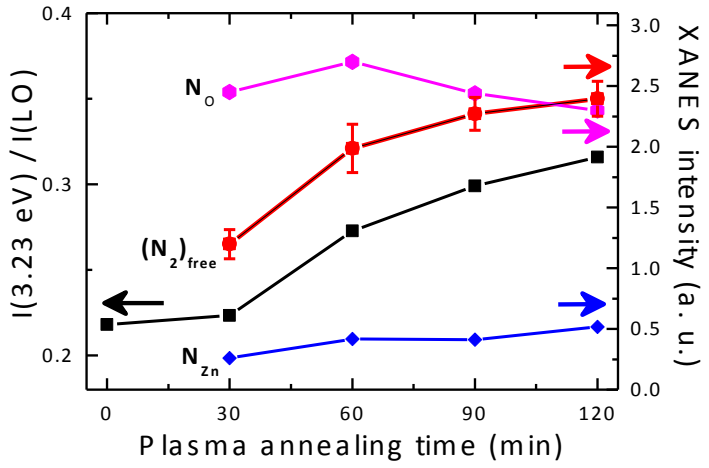

Nanocharacterization collocated of defects and luminescence in InGaAs/GaAs quantum wells

J.ROQUE[1,2]*, N.ROCHAT[1], S.DAVID[2], and F.BERTIN[1]
[1]Univ. Grenoble Alpes, F-38000 Grenoble, France
CEA-LETI, MINATEC Campus, F-38054 Grenoble, France
[2]Univ. Grenoble Alpes, LTM, F-38000 Grenoble, France
CNRS, LTM, F-38000 Grenoble, France
*Joyce.roque@cea.fr

III-V epitaxy on silicon by MOCVD (*Metal Organic Chemical Vapor Deposition)* is one important option for future electronic and optoelectronic devices integration. Unfortunately, a large number of structural defects are created in the III-V epitaxial layer and even the growth of a GaAs buffer does not prevent, dislocations to reach and cross the active regions (InGaAs/GaAs quantum wells) [1]. As such structural defects impact dramatically the device efficiency, most of studies aim at reducing the defects density but without understanding their impact on physical properties. Indeed, the most used characterizations – electrical measurements and photoluminescence – lead to spatially averaged values. In this context, we intend to develop coupled spatially resolved (at the nanoscale) characterization to understand link between the structural defects and the electronic properties of the InGaAs/GaAs quantum wells [2].

To carry out this study, two characterization techniques are coupled, Cathodoluminescence (CL) and Scanning Transmission Electronic Microscopy (STEM). CL studies give access to electronic properties (confinement effect, band structures, localization of luminescence area, intensity and wavelength position), whereas STEM/TEM permits to obtain morphological information (presence of defects, antiphase domains, variation of well width, strain measurements).

We have developed a four-step method to spatially correlate CL and STEM images. (i) platinum marks are deposited using electron beam assisted deposition in a FIB/SEM; (ii) CL mapping are done to determine the areas of interest (with significant luminescence variations); (iii) using the marks we extract a lamella (<100 nm thick) of the zone of interest by FIB; (iv) the lamella is analyzed by STEM/TEM. Analyzing the same area both CL and STEM will allow us to correlate physical properties at nanoscale and help us to understand how material characteristics modulate the optical response of InGaAs/GaAs quantum wells. We have obtained preliminary results on patterned substrates (silicon oxide trenches) [3] which show (Fig. 1) a clear correlation between the most intense CL area (yellow) and the defect free region.

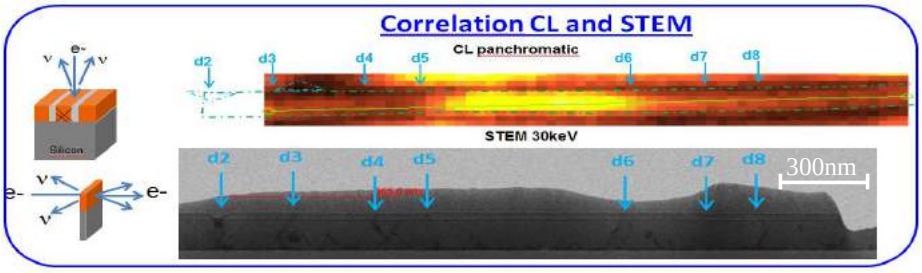

Figure 1 : Correlation between CL cartography and STEM lamella observation.

[1] D. Cherns, S.J. Henley, and F.A Ponce, Applied Physics Letters, Volume 78, pages 2691 to 2693 (2001)
[2] This work has been partially supported by the LabEx Minos ANR-10-LABX-55-01 and was performed on the Nano Characterization Platform (PFNC) of the CEA Grenoble.
[3] W. Guo, L. Date, and V. Pena, Applied Physics Letters, Volume 105, id.062101 (2014)

Monday June, 6 - MoB - Oral Session

11:00-12:20

Beam-induced modifications

Chair: Eugene Yakimov, *Institute of Microelectronics, Chernogolovka, Russia*

Electron Beam Induced Chemical Processing and Characterization of Semiconductors

M. Toth[1*]
[1]School of Mathematical and Physical Sciences, University of Technology Sydney, Ultimo, New South Wales 2007, Australia

*milos.toth@uts.edu.au

Controlled fabrication of semiconductor nanostructures is an essential step in engineering of high performance photonic and optoelectronic devices. Here I will review recent work on electron beam induced chemical processing of materials such as diamond [1], SiC [2] and hBN [3]. The beam-induced processes include deposition [4], etching (Fig. 1(a)) [1,2,5], and chemical switching of the charge state of near-surface luminescent defects [6]. They proceed through highly localized chemical reactions that are fueled by surface-adsorbed precursor molecules such as H_2O, NH_3, NF_3 and $SiC_8H_{20}O_4$ that are injected as vapors into an electron microscope. The key advantages of the techniques include cite specificity, the absence of staining and severe damage inherent to analogous focused ion beam techniques, and the ability to etch materials such as diamond (Fig. 1 (b-d)) which are resistant to conventional chemical etch methods. The techniques can therefor be used to realize practical device components for use in photonics, plasmonics, and nanofluidics. In addition, the methods can be used as surface characterization techniques capable of measuring basic properties of surface-adsorbed precursor molecules such as the adsorption energy, desorption attempt frequency, diffusion energy and diffusion pre-factor with high spatial resolution [7,8].

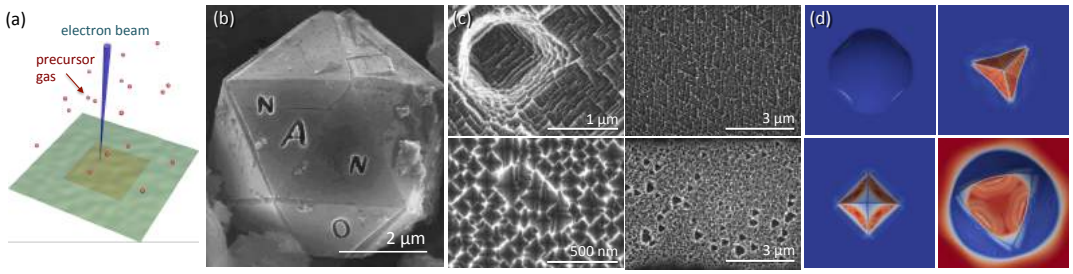

Figure 1. Isotropic and anisotropic etching of single crystal diamond. *(a) Schematic illustration of gas-mediated electron beam induced etching. (b) The word "NANO" etched into diamond, demonstrating the ability to dire-write onto a non-planar microcrystal [5]. (c) Topographic surface patterns generated on the surface of single crystal diamond through anisotropic electron beam induced chemical etching, and (d) corresponding simulations of the pattern geometries defined by the crystallographic orientation of the diamond and the chemical species of the precursor gas [1]. All processing was done at room temperature using a scanning electron microscope. Raman, photoluminescence and cathodoluminescence spectroscopy do not show any evidence of damage generated by the electron beam.*

[1] A. Martin, A. Bahm, J. Bishop, I. Aharonovich, & M. Toth, Phys. Rev. Lett. 115, 255501 (2015).
[2] A. A. Martin & M. Toth. ACS Appl. Mater. Interfaces 6, 18457–18460 (2014).
[3] T. T. Tran, K. Bray, M. J. Ford, M. Toth & I. Aharonovich. Nat. Nanotech. 11, 37 (2016).
[4] J. Bishop, C. J. Lobo, A. Martin, M. Ford, M. R. Phillips & M. Toth. Phys. Rev. Lett. 109, 146103 (2012).
[5] A. Martin, M. Toth, and I. Aharonovich, Sci. Rep. 4, 5022 (2014).
[6] T. Shanley, A. Martin, I. Aharonovich, and Milos Toth, Appl. Phys. Lett. 105, 063103 (2014).
[7] J. Cullen, C. J. Lobo, M. J. Ford & M. Toth. ACS Appl. Mater. Interfaces 7, 21408–21415 (2015).
[8] J. Cullen, A. Bahm, C. J. Lobo, M. J. Ford & M. Toth. J Phys Chem C 119, 15948–15953 (2015).

Effect of Proton Fluence on the Properties and Concentrations of Radiation Defects in High-Purity FZ Si

P. Kamiński[1]*, R. Kozłowski[1], B. Surma[1], M. Kozubal[1], A. Dierlamm[2], and M. Kwestarz[3]
[1]Institute of Electronic Materials Technology, Warszawa, Poland
[2]Karlsruhe Institute of Technology, Eggenstein-Leopoldshafen, Germany
Topsil Semiconductor Materials S.A., Warszawa, Poland
*E-mail of the corresponding author (pawel.kaminski@itme.edu.pl)

High-purity (HP) silicon, with the phosphorus concentration of ~3×10^{12} cm^{-3}, the oxygen concentration below 1×10^{16} cm^{-3} and the carbon concentration below 5×10^{15} cm^{-3}, is an important material that has recently become available for manufacturing silicon detectors used to track high-energy particles produced in proton collisions. Taking into account future hadron colliders, these detectors should be capable to operate at high fluences of fast particles being above 1×10^{14} n_{eq}/cm^2. Therefore, the development of radiation-resistant particle detectors for the future experiments is greatly needed. To achieve this objective, the wider knowledge on the electrical properties of irradiation-induced point defects and their formation mechanisms is required.

The aim of this paper is to show the properties and concentrations of radiation defect centers formed due to the irradiation with high fluences of 23-MeV protons in HP Si single crystals grown by floating zone (FZ) method. The studies were carried out using the high-resolution photoinduced transient spectroscopy (HRPITS) [1] as well as Fourier transform infrared absorption (FTIR) and photoluminescence (PL) measurements. The samples were irradiated with four proton fluences: 1×10^{14}, 5×10^{14}, 1×10^{15}, and 5×10^{15} n_{eq}/cm^2. The irradiation with each fluence resulted in the increase of the material resistivity by two orders of magnitude from ~2×10^3 to ~2×10^5 Ωcm. The defect structure of the irradiated material was found to be complex. By means of the HRPITS technique, 21 irradiation-induced traps with activation energies ranging from 30 to 590 meV were detected. It is shown that the concentrations of majority of traps nearly linearly increase with rising the fluence. The shallow traps, with activation energies of 36, 54, and 62 meV, are tentatively identified with the shallow donors formed by oxygen aggregates [2]. The concentrations of these traps increase from ~2×10^{13} cm^{-3}, for the lowest fluence, to ~8×10^{14} cm^{-3} for the highest fluence. The concentration of the 133-meV trap, tentatively attributed to the aggregate of three Si interstitials, changes from ~2×10^{13} to 5×10^{14} cm^{-3}, and the concentration of the 0.163-meV trap, associated with the vacancy-oxygen (VO) complex, ranges from ~2×10^{13} to 2×10^{14} cm^{-3}. The 273-meV trap is identified with the donor center formed by the carbon interstitial $C_i(+/0)$ and with increasing the proton fluence its concentration rises from ~2×10^{13} to 3×10^{14} cm^{-3}. Another donor center is formed by the interstitial oxygen-interstitial carbon complex (C_iO_i), observed as the 371-meV trap, whose concentration changes from ~3×10^{13} to 1×10^{15} cm^{-3}. On the other hand, the deep acceptor centers with activation energies of 360, 391, 401 meV, attributed to the tri-vacancies (V_3), tetra-vacancies (V_4) and pentavacancies (V_5) in the (2-/-) charge state, respectively, are formed. The vacancy aggregates: V_2, V_3, V_4, and V_5 in the (-/0) charge state also arise and are observed as the midgap traps with activation energies of 432, 474, 563, and 583 meV, respectively. With increasing the proton fluence from 1×10^{14} to 5×10^{15} n_{eq}/cm^2, the concentrations of the vacancy aggregates in the both charge states rise from ~1×10^{13} to ~1×10^{15} cm^{-3}.

[1] P. Kamiński, R. Kozłowski, J. Żelazko, Acta Physica Polonica A **125**, 976 (2014).
[2] J. Krupka, W. Karcz, S. A. Avdeyev, P. Kamiński, R. Kozłowski Nucl. Instr. Meth. Phys. Res. B **325**, 107 (2014).

Optical properties of silicon modified by He ion beam

A. Bondarenko[1*], Yu. Petrov[1], and O. Vyvenko[1]
[1]Faculty of Physics, St. Petersburg State University, Russia
*anton.bondarenko@spbu.ru

Modern silicon industries and governments of key countries invest actively in development of technology of economically effective production of localized light sources on silicon to be used for data transmission in next generation of processors. Due to indirect band gap of silicon the problem of development of pure silicon light emitting device (LED) with good enough performance is not so straightforward. Most of the designs that are considered by the engineers and the scientists can be divided in two groups:

1. Growth of heterostructures on silicon wafers.
2. Utilization of the luminescent properties of defects and impurities.

The second approach is much more attractive from both economic and technological point of view. One of the prominent directions in local defect engineering is the ion implantation either using lithography masks or using highly focused beams. Some papers already reports the successful designs of LEDs built on ion implanted silicon [1]. Usually as the source of the light in ion implanted silicon acts implanted ion itself (like in case of rare-earth metals), or Si-ion complexes (SiOx in casae of oxygen implantation), or even extended defects formed during the post-implantation annealing (dislocations, precipitates). Moreover, using thin layers of active material (carbon, SiO2, Si3N4, or organic films) the technology of ion beam mixing can be realized for more advanced active complexes growth during the annealing stage.

We must note that despite the technological benefits of Si LED development the investigation of properties, mechanisms, and nature of luminescence of many different kinds of extended defects in Si is of a great value for the fundamental science since we steel have more questions than answers in that field.

In present paper, we report on our results of modification of luminescent properties of silicon using the scanning He ion microscope Orion. The analysis of literature revealed that He implantation can cause appearance of many different bands in silicon luminescence spectrum in the range of wavelength of 350 1500 nm [2]. For investigation of optical properties of implanted areas and spatial resolution of the implantation, we use cathodoluminescence spectroscopy and mapping techniques. For the investigation of mechanisms of luminescence, we plan to use our original technique capable of establishing of energy levels of the defect in the band gap, which is responsible for a given luminescent band PulsedTREL [3].

[1] Sobolev N.A., Gusev O.B., Shek E.I., Vdovin V.I., Yugova T.G. and Emel'yanov A.M., Appl. Phys. Lett. **72** 3326–8 (1998)
[2] Misiuk A. and Tyschenko I.E., NATO Science Series ed. T. Tsakalakos, I.A. Ovid'ko and A.K. Vasudevan (Springer Netherlands) pp 619–38 (2003)
[3] Bondarenko A. and Vyvenko O., Proceedings of the 27th International Conference on Defects in Semiconductors, ICDS-2013 **vol 1583** (AIP Publishing) pp 46–50 (2014).

Monday June, 6 - MoC - Oral Session

14:00-15:40

LBIC and EBIC

Chair: Takashi Sekiguchi, *National Institute for Materials Science Tsukuba, Japan*

LBIC in Tellurides for X-ray Detection: Transport Properties and Electric Field Reconstruction

M. Pavesi[1,2*], A. Santi[1], M. Bettelli[2], A.Zappettini[2], and M. Zanichelli[1,2]
[1] DiFeST, Department. of Physics and Earth Sciences, Parma University, 43124 - Parma, Italy
[2] IMEM-CNR, Institute of Materials for Electronics and Magnetism, 43124 - Parma, Italy
*maura.pavesi@unipr.it

The localization of space charge on traps in the detector's volume is one of the main source of degradation of the charge collection efficiency. The onset of space charge modifies the internal electric field profile, that in the ideal case should be spatially uniform, due to the screening effect on the applied bias. Regions with little or zero electric field could appear, limiting the detector's spectroscopic performance because the lower the electric field, the fewer the number of collected photo-generated carriers as they are subject to trapping.
This phenomenon, known as polarization, causes a dramatic worsening in the spectroscopic performance. In some applications, e.g. space telescopes, the flux impinging on the detector is typically very low and the emphasis lies on the spectral performance. Other applications, e.g. medical imaging (Computed Tomography), need detectors with capability to detect a high photon flux (10^9 photons/sec mm^2), hence detectors in which the electric field does not collapse due to excessive space charge accumulation and which exhibit fast charge transits in the device.
Experimental findings and simulations have shown that the electric field inside the detector is far from the ideal uniform behavior in most of the conditions, suggesting the need of searching for a more general method to reconstruct its spatial distribution [1-3].
A method based on laser-beam induced current (LBIC) was successful used to reconstruct the spatial profile of the electric field along the thickness of a set of spectroscopic photodetectors based on tellurides (CdTe and CdZnTe). Mobility and lifetime of electrons were also deduced and compared with the mobility-lifetime product, as evaluated by fitting the charge collection efficiency curves under a suitable electric field profile model.
The method is based on a procedure of minimization built up from current transient profiles at different applied voltages, making use of the Ramo-Shockey theorem. Starting from the physical constraints imposed by the detector's thickness and the applied voltages, two expressions for each experimental transient profile integrated over the time of flight were obtained. Demanding the constancy of the photo-generated charge from each laser pulse, a minimization procedure gives a reasonable value for the carrier lifetime, but only if transients are acquired at adequately low voltages, for which the flight times is comparable to the carrier lifetime. In this way, it is possible to give an enough accurate evaluation of the lifetime. After deducing the initial photo-generated charge and μ, it is possible to derive the laws of motion, then to reconstruct the electric field.
The procedure demonstrated its applicability on a set of CdTe and CdZnTe detectors with different thicknesses and gave results in good agreement with collection efficiency measurements.
The novelty of the method lies in its semi-analytical approach, in which it is not necessary to assume any profile of the field.
We believe this method could be potentially of interest for a wide class of materials on which the transient current technique can be applicable.

[1] S. Uxa, E. Belas, R. Grill, P. Praus, and R.B. James, IEEE Trans. on Nucl. Sci. **59**, 2402 (2012)
[2] J. Franc, R. Grill, J. Kubát, E. Belas, P. Hoschl, P. Moravec, and P. Praus, Nucl. Instr. and Meth. Phys. Res. A **633**, S100 (2011)
[3] M. Zanichelli, A. Santi, M. Pavesi, and A. Zappettini, J. Phys. D: Appl. Phys. **46**, 365103 (2013)

New Methods for Evaluating Luminescence Images of Silicon Solar Cells

O. Breitenstein[1], F. Frühauf[1], and J. Bauer[1]
[1]Max Planck Institute of Microstructure Physics, Halle, Germany
*breiten@mpi-halle.mpg.de

Most methods for evaluating photoluminescence (PL) and electroluminescence (EL) images of silicon solar cells are based on the evaluation of local diode voltages within the model of independent diodes, see e.g. [1-3]. Hence, the local EL signal or the illumination-corrected PL signal (this is the PL signal at bias V minus the short-circuit PL signal [1]) was fitted to the generally valid equation $\Phi_i = C_i * \exp(V_{d,i}/V_T)$. Here i is a position index, C_i is the local scaling parameter, which depends on the local lifetime, $V_{d,i}$ is the local diode voltage in position i, and V_T is the thermal voltage. In the independent diode model, the local diode voltage $V_{d,i}$ is calculated from the applied bias V and the locally flowing current density J_i by considering a voltage drop at a series resistor $R_{s,i}$. This resistor is assumed to connect each image pixel independently to the cell terminals. By performing PL measurements at various biases and illumination intensities, the values of C_i, $R_{s,i}$, and $J_{01,i}$ (the saturation current density in position i) can be obtained separately [2,3].

It has been found already early [4] that EL- or PL-based J_{01} images do not agree with that obtained by dark lock-in thermography (DLIT). Recently the reason for this disagreement could be explained [5]. It is due to the distributed (horizontal) nature of the series resistance in solar cells, which leads in inhomogeneous cells (inhomogeneous J_{01}) to horizontal balancing currents and to a strong resistive coupling of neighboring regions. Thus, the model of independent diodes is too simple to correctly describe the local voltage drops, on which methods [1-3] rely. Therefore recently two alternative methods for evaluating PL and EL images have been proposed.

The first method was proposed already by Glatthaar et al. in 2009 [6] and is based on applying the Laplacian operator to a V_d image. This operator provides the second spatial derivative of V_d, which, for a given emitter resistivity, is proportional to the locally flowing current density. It has been found in [6] that the J_{01} data obtained by this method are systematically too low. The reason for this disagreement has been found recently: It is due to photon scattering in the light detector used for this method. This blurring has to be corrected by spatial deconvolution [7]. If this is done, the J_{01} results of PL and DLIT imaging basically agree. The most striking experimental challenge of the Laplacian method is noise, which is very critical here.

The second alternative method is not to evaluate the local diode voltages $V_{d,i}$ but rather the calibration constant C_i. It was claimed by Fuyuki et al. [8] that C_i is proportional to the diffusion length L_d. This, however, only holds for low lifetimes, for high lifetimes C_i approaches a saturation value. We recently have derived a simple approximate formula, which considers this saturation and corresponds to the Fuyuki approximation for low lifetimes [9]. First applications of this formula indicate that this method indeed allows to evaluate EL images correctly, leading to J_{01} images which agree with DLIT measured ones.

[1] T. Trupke, E. Pink, R.A. Bardos, and M.D. Abbott, Appl. Phys. Lett. **90**, 093506 (2007).
[2] M. Glatthaar et al., Phys. Status Solidi RRL **4,** 13 (2010).
[3] C. Shen et al., Solar Energy Mat. & Solar Cells **109**, 77 (2013).
[4] O. Breitenstein et al., IEEE Journal of Photovoltaics **1,** 159 (2011).
[5] O. Breitenstein et al., Solar Energy Mat. & Solar Cells **137**, 50 (2015).
[6] M. Glatthaar et al., J. Appl. Phys. **105**, 113110 (2009).
[7] F. Frühauf and O. Breitenstein, Solar Energy Mat. & Solar Cells **146**, 87 (2016).
[8] T. Fuyuki et al., J. Appl. Phys. *101*, 023711 (2007).
[9] O. Breitenstein et al., IEEE Journal of Photovoltaics, in preparation.

Room Temperature Dislocation Glide in GaN Enhanced by E-beam Irradiation

E.B. Yakimov[1,2,*], P. S. Vergeles[1], A.Y. Polyakov[2], In-Hwan Lee[3], and S. J. Pearton[4]
[1]Institute of Microelectronics Technology RAS, Chernogolovka, Russia
[2]National University of Science and Technology MISiS, Moscow, Russia
[3]School of Advanced Materials Engineering and Research Center of Advanced Materials Development Chonbuk National University, Jeonju, South Korea
[4]University of Florida, Gainesville, USA
*yakimov@iptm.ru

A question about the recombination enhanced dislocation glide (REDG) effect is very important for the design of high power laser diodes and LEDs for lighting, especially for GaN-based structures with a rather high dislocation density. In the present paper the results of REDG study in GaN under e-beam irradiation in SEM are presented. Dislocations are revealed by the electron beam induced current (EBIC) method that allows to control their displacement *in situ*. The epitaxial lateral overgrowth (ELOG) GaN samples studied were grown by MOCVD on basal plane sapphire substrates. The thickness of the seed MOCVD n-GaN templates was 2 μm, the width of the SiO_2 stripes was 12 μm and the width of the mask windows was 4 μm. The stripes were elongated along the [1-100] direction. The thickness of the ELOG film grown over this mask was 6 μm. Such thickness was chosen because in this case the depth, where the dislocation segments are inclined in respect to the growth direction (c-axis) is not too large to be revealed by the EBIC method. The Schottky barriers were prepared by Au evaporation. EBIC investigations and irradiation were carried out in a scanning electron microscope JSM-840 at room temperature and beam energy of 35 keV. Low Energy Electron Beam Irradiation (LEEBI) was carried out with the same energy and current varied from 0.1 to 50 nA.

In the samples studied a threading dislocation density in windows reaches $10^8 cm^{-2}$ while in wing regions it is about $10^6 cm^{-2}$. Besides, in the wing regions dislocation segments located in the basal plane can be revealed. Under LEEBI a noticeable movement of such segments was observed under LEEBI in the SEM, however usually only a small fraction of dislocations was able to move. Most of dislocations were immobile. A shift of threading dislocations under LEEBI was not detected. The maximum extent of the dislocation glide did not exceed a few tens of μm and this extent and a number of gliding dislocations depended on the beam current. Nevertheless, the dislocation movement was observed even at beam current of 0.1 nA. At such beam current the dislocation velocity decreases and can be evaluated as 10 nm/s. The basal dislocation movement due to LEEBI is explained by the REDG effect. Besides, a change of relative EBIC contrast of some neighboring dislocations was also observed that allows to assume that the dislocation segments can move in the direction perpendicular to the basal plane, i.e. that the REDG-driven movement of dislocation segments in prismatic planes can also occur. It could be assumed that a high density of pinning sites for dislocations are present in the structures studied. Thus, the majority of dislocations are pinned. The dislocations that are free to glide soon encounter pinning sites preventing further motion.

Study of Dislocation Trails in Si by the LBIC and EBIC Methods

V.I. Orlov[1,2]*, O.V. Feklisova[1], E.B. Yakimov[1,3], and N.A. Yarykin[1]
[1]Institute of Microelectronics Technology RAS, Chernogolovka, Russia
[2]Institute of Solid State Physics RAS, Chernogolovka, Russia
[3]National University of Science and Technology MISiS, Moscow, Russia
* orlov@issp.ac.ru

The results of investigations of the dislocation trail recombination properties in Si by the light beam induced current (LBIC) and the electron beam induced current (EBIC) methods are presented. The dislocation trails are quasi-two-dimensional defects which are formed behind moving dislocations and demonstrate a noticeable electrical activity. However, in spite of a long history of their investigation, the nature of these defects and mechanisms of their formation remain a matter of discussion. It is shown in this contribution that the complementary application of the EBIC and LBIC methods sheds a new light on this old problem. It should be noted that the main difference of these methods consists in the different penetration depth which can exceed 100 μm for LBIC. As our calculations shown, the larger penetration depth leads to an increase of the recombination contrast in case of the two-dimensional defects perpendicular to the surface. Besides, the deeper layers can be monitored without a recurring sample preparation.

The samples studied in the present work were cut from a dislocation free single crystalline p-type Si (boron concentration of 10^{14} cm^{-3}). The dislocations were introduced by the four-point bending technique, the indentations made by the diamond tip on a {111} surface being used as dislocation source. Two dislocation slip planes which are active in the used geometry are inclined to the surface normal at an angle about 20°. Such small deviation preserves the high LBIC sensitivity for the light with a rather high penetration depth. However, it allows to obtain the defect projection onto the surface and to reconstruct the three-dimensional defect structure. On the other hand, EBIC is more suitable for the quantitative measurements of the defect recombination strength in the near-surface layers and, in combination with successive chemical etching, allows to reconstruct the depth dependence of the defect strength. Besides, it is not so time consuming as LBIC one and provides the higher lateral resolution.

Such investigations allow to answer the old question about the type of dislocations which are responsible for the dislocation trail formation. It is found for a depth larger than 50 μm that only one 60°-segment of the dislocation half-loop produces the electrically active dislocation trails while the other 60° and the screw segments do not. This is fulfilled for the both acting slip planes independently of stress sign (tensile or compressive). A part of dislocations can be bent closer to the surface that leads to a misinterpretation of the trail sources. The LBIC measurements allow to separate the trails formed in the near surface layer behind the bent part of dislocation segment from those active over all slip plane swept by the unbent dislocation segment. The analysis carried out allows to assume that the dislocation trails are formed behind those 60° dislocation segments where the leading partial dislocations are of the 90°-type.

Monday June, 6 - MoD - Oral Session

16:00-17:00

Excitation processes

Chair: Martin Kittler, *IHP Frankfurt & IHP/BTU Joint Lab Cottbus, Germany*

Time-correlated Cathodoluminescence of defect centers in diamond and hBN

M. Kociak[1*], S. Meuret[1], L. H. Galvao-Tizei[1], R. Bourrellier[1], A. Zobelli[1]
[1]LPS, CNRS/Université Paris Sud, Orsay, France

*Mathieu.kociak@u-psud.fr

The interest for single photon emitters (SPE) has tremendously grown over the last decade, due to their possible application in quantum information. Point defects in semi-conductors or insulators are ideal SPE candidates, because they are schematically atomic systems well isolated from the external environment. A well-known example is the Nitrogen Vacancy (NV) defect, which has become the workhorse of quantum nanooptics [1].
Quantum properties of the light emitted by potential SPE are commonly studied by intensity interferometry of the Photoluminescence (PL) signal [2]. An intensity interferometer allows the measurement of the time correlation function $g^{(2)}(\boldsymbol{\tau})$ as a function of the delay $\boldsymbol{\tau}$. $g^{(2)}(\boldsymbol{\tau}=0)<1$ is the signature of anti-bunching of the emitted photons and therefore of the detection of a quantum state of light, and $g^{(2)}(\boldsymbol{\tau}=0)<0.5$ of single photon emission.
A drawback of PL intensity interferometry is obviously the spatial resolution limited by the diffraction limit, which makes PL not adapted to the characterisation of packed sets of SPE. On the other hand, CL is known for decades for its ability to detect light emission from point defects in high band gap semi-conductors [3]. Also, CL can be extremely well resolved spatially, in particular when it is performed in a Scanning Transmission Electron Microscope (STEM) on thin objects [4]. We have thus developed an intensity interferometric experiments adapted to a dedicated STEM-CL [5] system in order to perform time-correlated CL (TCCL).
In this talk, we will show several applications of TCCL. We will first devise the experimental evidence of antibunching in CL light in the stereotypical example of NV centers [5]. Beyond this textbook example, we will show that TCCL is perfectly adapted to the chase of novel SPEs with the example of an SPE emitting in the UV in hexagonal Boron Nitride (hBN) [6]. Then, we will discuss the case where several SPEs are excited at the same time by an electron beam [7]. In a PL experiment, this would result typically in a totally flat correlation function with $g^{(2)}(\boldsymbol{\tau})=1$. We will show that very surprisingly, $g^{(2)}(\boldsymbol{\tau})$ as measured by CL exhibits a peak at zero delay with potentially very high value ($g^{(2)}(\boldsymbol{\tau}=0) >60$), indicating bunching of the emitted photons. This effect will be described in terms of synchronized emission of several SPE excited in combination by the e-beam. As we have shown that the emitter's lifetime can be directly measured from the correlation function, I will finish by discussing the applications of the bunching effect in nanoscale lifetime measurement.

[1] I. Aharonovich et al., Nature Photon **5**, 397 (2011).

[2] A. Beveratos, et al. *Quantum Communication* (Kluwer Academic Publishers, Boston, 2002),

[3] L. Robins et al., Phys. Rev. B **39**, 13367 (1989).

[4] M. Kociak et al., Comptes Rendus Physique **15**, 158 (2014).

[5] L. H. G. Tizei and M. Kociak, Phys. Rev. Lett. **110**, 153604 (2013).

[6] R. Bourrellier et al., in Preparation (2016).

[7] S. Meuret, et al. Phys. Rev. Lett. **114**, 197401 (2015).

Theoretical and experimental studies of cathodoluminescence excitation processes

A.Y. Mester[1]*, E.Y. Flegontova[1], L.A. Bakaleynikov[1], M.V. Zamoryanskaya[1]
*mesteralex@mail.ru

The cathodoluminescence phenomenon has long been known and it is widely used in electron-probe research methods. However, cathodoluminescence excitation mechanism is fundamentally different from photoexcitation due to the fact that the electron beam energy is much greater than the band gap of any materials. The investigation of the processes leading to the cathodoluminescence is one of the most important problems in the cathodoluminescence research area.

Cathodoluminescence intensity depends on the excitation capture rate and the relaxation time. Last parameter defines duration of well-known luminescence decay. Rising of the cathodoluminescence is not instant process as well. Duration of this process depends on electron beam current and energy and on excitation capture efficiency of considered energy level. Last mentioned parameter characterizes energy level excitation rate. The main aim of this work was to study the dependencies of cathodoluminescence rising process on electron beam and material parameters.

To solve this problem experimental study and theoretical calculations were carried out. Theoretical calculations were based on the idea that cathodoluminescence is mainly excited by the secondary electrons. It means that cathodoluminescence excitation rate is connected with the number of secondary electrons in the sample-probe interaction area. This number depends on the electron beam current and secondary electron distribution in the interaction area (which is connected with the electron beam energy and material properties). Using this approach and the two-level system model the kinetic equation of cathodoluminescence intensity was derived. Using the numerical simulation method the dependencies of cathodoluminescence rising on different electron beam and material parameters were investigated. Obtained results were compared with the experimental data.

Experimental investigations were conducted on yttrium-aluminum garnet activated by thulium. Cathodoluminescence spectrum of YAG:Tm was obtained. Cathodoluminescence dynamic features were studied for 354 nm thulium luminescence line which corresponded to $^1D_2 - {}^3H_6$ transition. Cathodoluminescence rising curves were obtained for different values of the electron beam current and energy and for various thulium concentrations. Decay curves were investigated as well.

The comparison of the experimental and theoretical data showed that proposed model of cathodoluminescence excitation is in a good agreement with the experimental results.

Tuesday June, 7 - TuA - Oral Session

09:00-10:40

Photovoltaic materials

Chair: Otwin Breitenstein, *MPI of Microstructure Physics, Halle, Germany*

Luminescent, structural and chemical properties of defects in MBE- and CSS-grown CdTe films for solar cell applications

Mowafak Al-Jassim, John Moseley, Harvey Guthrey, Helio Moutinho, Steve Harvey, James Burst, Wyatt Metzger and Nancy Haegel
National Renewable Energy Laboratory, Golden, Colorado 80401, USA
mowafak.aljassim@nrel.gov

CdTe solar cells are the leading thin film solar cell technology. However, despite their near ideal bandgap, the cell efficiency is far less than the theoretical limit, and considerably less than efficiencies reported in other systems with similar bandgaps, such as GaAs. The purpose of this study is to investigate the loss mechanisms in commercial CdTe cells by comparing them with model systems. We combined scanning electron microscopy (SEM)-based cryogenic cathodoluminescence (CL) spectrum imaging and electron backscatter diffraction (EBSD) in order to map the spatial distribution of various atomic-level defects in CdTe films as a function of deposition and film processing conditions. Two different deposition techniques were used. Lattice-matched, epitaxial CdTe films were deposited on single crystal as well as polycrystalline CdTe substrates by molecular beam epitaxy (MBE). For comparison purposes, polycrystalline CdTe films were deposited using our standard close-spaced sublimation (CSS) method on glass-based substrates. Correlations between the CSL relationship, defect structure, and radiative recombination intensity at grain boundaries and intra-grain regions are then made and discussed in the context of film deposition conditions and post-deposition processing history. Further, the effect of the $CdCl_2$ passivating treatment was investigated. The distribution of Cl on grain boundaries and intra-grain dislocations was studied by time of flight SIMS (TOF-SIMS) imaging and high resolution STEM-EELS. These results were correlated with the recombination behavior of these defects as revealed by CL.

In addition to structural defect studies, this work also assesses the incorporation and three-dimensional distribution of extrinsic dopants. Both group II and group III-V dopants were used in an attempt to increase minority carrier lifetime. Cryogenic CL spectral imaging and TOF-SIMS were used to investigate the distribution of dopants as a function of annealing conditions.

Photoluminescence Study of Charge Transfer Dynamics in Perovskite Solar Cells

Mohammad I. Hossain[1], Abdelhak Belaidi[1], Nouar Tabet[1], Giulia Grancini[2], Md Khaja Nazeeruddin[2]

[1]Qatar Environment and Energy Research Institute, Hamad Bin Khalifa University (HBKU), Qatar Foundation, Doha, 5825, Qatar
[2]Group for Molecular Engineering of Functional Materials, Ecole Polytechnique Fédérale de Lausanne, CH-1951 Sion, Switzerland.
Email: mhossain@qf.org.qa

The performance of perovskite based solar cells is widely governed by the charge transfer dynamics in the absorbing layer and at the interfaces with its adjacent interface electron transport and hole transport layers (ETL and HTL respectively). Photoluminescence (PL) is a powerful technique to investigate the carrier recombination in the absorbing layer as well as the carrier extraction at the interfaces. It allows the identification of the dominant recombination mechanism i.e. monomolecular (SRH), bi-molecular (band to band), and tri-molecular (Auger) which is the subject of hot debate in the literature.

In this work, Continuous Wave PL (CW-PL) , Time Resolved Photoluminescence (TRPL) and UV-Vis spectroscopy were used to characterize three different types of samples including a perovskite layer on glass, a perovskite layer coated with Spiro-OMETAD and a perovskite layer coated with fluorine-dithiophene (FDT) (a new hole transport material replacing the costly spiro-OMETAD). The perovskite layers were deposited on glass substrates using one step solution process technique followed by the deposition of HTL or ETL.

The charge dynamics at FDT/perovskite interface was investigated using CW-PL as well as TRPL. CW-PL measurements revealed a quenching effect with both types of HTL (Spiro and FDT), whereas the highest PL intensity was recorded in the case of perovskite alone. Equal excitation intensity was used to compare the absolute PL intensity. The quenching of CW-PL spectra was about 79% in the case of perovskite/FDT sample, whereas 67% quenching was measured in the case of perovskite/Spiro-OMETAD.

TRPL measurements spectra of the perovskite layer alone showed the highest lifetime with longer time of decay. The perovskite/HTL sample displayed shorter lifetime decay (7.6 ns) even at higher intensity. The faster PL quenching in the case of the FDT indicates a faster charge transfer from the perovskite absorbing layer to FDT. The UV-visible measurements on perovskite layer gave a value of 1.6eV for the optical gap in good agreement with the value commonly reported in the literature. Both the absorption and emission spectra showed very little stroke's shift confirming less vibronic relaxation. The obtained results provide valuable indications for the design of highly efficient hybrid Organic-Inorganic perovskite PV solar cells.

Electron beam induced current investigations on the nanoscale at a complex oxide pn-heterojunction

P. Peretzki[1], B. Ifland[2], C. Jooss[2], and M. Seibt[1]*
[1]IV. Physical Institute, Faculty of Physics, Georg August University Goettingen, Germany
[2]Institute of Material Physics, Faculty of Physics, Georg August University Goettingen, Germany
*mseibt@gwdg.de

The perovskite structured material $Pr_{0.67}Ca_{0.33}MnO_3$ (PCMO) combined with $SrTi_{0.998}Nb_{0.002}O_3$ (STNO) is presently explored as a model system for manganite-based pn-heterojunctions where PCMO is p-doped and STNO is n-doped. In this system, it is expected [1] that the rapid thermalization of low-energy photoexcited charge carriers can be quenched by making use of hot polaron-type correlated states with long lifetimes [2]. However, how polaron lifetimes convert into a diffusion length is presently not well understood, since the polaron mobility strongly depends on the excited state. Success in decrease of polaron thermalization would open the possibility of converting the photon energy of a broad range of the solar spectrum into electric energy. PCMO can be epitaxially grown on STNO and atomic scale PCMO-STNO interface design is expected to be crucial for controlling the charge transfer across the interface and thus photovoltaic properties.

We use quantitative electron beam induced current (EBIC) measurements in a scanning electron microscope to gather insight into the charge carrier and transport process in our material system. This imposes a challenge as the size of the space charge region, the supposed diffusion length and electron beam excitation volume are all on the nanometer scale, which is not accounted for in usual EBIC models. To conquer this challenge, we prepare our samples in a cross-section lamella geometry for EBIC measurements. Results are compared with simulations based on calculating the paths of impinging electrons by the Monte Carlo algorithm provided by CASINO [3].

In a simulated EBIC linescan across the pn-junction interface in the lamella, the proposed order of magnitude for the diffusion length in our system and its influence on the line profile is confirmed [4]. In order to test the robustness of our model, cross-section lamellae with a wedge-shape thickness profile have been prepared., An electron acceleration voltage and beam current series of linescans across the pn-interface is obtained in wedge-shape as well as constant thickness lamella geometry. By adjusting the space charge region width, the average energy loss per excited polaron pair and the diffusion length on both junction sides simulations of EBIC linescans fit well with experimental results. It is worth to note that possible 'dead layers' resulting from the lamella preparation do not significantly influence the measurement.

It is observed that the effective polaron diffusion length depends on the acceleration voltage which will be discussed in our contribution.

Acknowledgement: Funding from the Deutsche Forschungsgemeinschaft (DFG) under Grant No. SFB1073, project B02 is acknowledged.

[1] G. Saucke, J. Norpoth, C. Jooss, D. Su and Y Zhu, Phys. Rev. B **85**, 165315 (2012).
[2] P. Grossmann, I. Rajkovic, R. Moré, J. Norpoth, S. Techert, C. Jooss and K. Mann, Rev. Sci. Instrum. **83**, 053110 (2012).
[3] D. Drouin, A. R. Couture, D. Joly, X. Tastet, V. Aimez and R. Gauvin, Scanning **29**, 92-101 (2007).
[4] B. Ifland, P. Peretzki, B. Kressdorf, P. Saring, A. Kelling, M. Seibt and C. Jooss, Beilstein J. Nanotechnol. **6**, 1467-1484 (2015).

TuA-4

Electrical characterization at the nanoscale of Si-based thin films for photovoltaic applications

M. A. Fazio (1), M. Perani(1), N. Brinkmann(2), B. Terheiden(2), D. Cavalcoli(1).

(1) Department of Physics and Astronomy, University of Bologna, Italy; (2) Department of Physics, University of Konstanz, Germany.

The electrical properties of innovative Si based thin films for photovoltaic applications have been investigated at the nanoscale. Si-based solar cells actually control almost the 90% of the whole photovoltaic (PV) market; the research aims constantly to further increase efficiency and stability and to improve cost reduction [1]. The goal of this contribution is the study of Plasma Enhanced Chemical Vapor Deposition (PECVD) grown a- and nc-SiO_xN_y thin films for Silicon Heterojunction (SHJ) solar cells.

nc-SiO_xN_y and a-SiO_xN_y could substitute a-Si:H in the heteroemitter and passivation layers of the SHJ solar cell, respectively, as they already showed higher conductivity and higher optical gap the respect to a-Si:H [2, 3]. The combination of intrinsic and doped a-SiO_xN_y in the heteroemitter stack has already shown high values of open circuit voltage (733 mV) [2]. In addition, a- and nc-SiO_xN_y thin films are highly disordered and multi-phase materials whose transport properties are still debated in literature.

The aim of the present contribution is a thorough study of the conduction mechanisms at the nanoscale in these thin films, the study of the role of the nanocrystals on the macroscopic and microscopic electrical properties, the study of the influences of the film growth parameters on the nanoscale electrical properties.

Local conductive properties at the nanoscale have been investigated using conductive-Atomic Force Microscopy (c-AFM) with a platinum conductive tip of a nominal radius <20 nm, achieving high-resolution current maps obtained at constant applied bias. Current maps of nc-SiO_xN_y revealed in each sample conductive grains surrounded by an insulating matrix. Our results showed that different oxygen content affects local conductivity properties. The annealing process causes changes in crystallinity fraction as well as in conduction.

In order to achieve information on the transport mechanism, current-voltage characteristics have been performed locally under the AFM in different points of the samples with the AFM tip. The best conductive properties, i.e. symmetric local current-voltage characteristics for negative and positive bias are achieved for highly crystalline, annealed nc-SiO_xN_y samples with low O content, obtaining a maximum conductance of 10^{-7} S. On the contrary, a-SiO_xN_y showed asymmetrical IV curves with conductance values at least two orders of magnitude lower than the highly crystalline nc-SiO_xN_y samples.

The present contribution shows that c-AFM mapping is a highly effective tool in the analysis of the electrical properties of thin films, and the investigation of current flow in these highly disordered materials could help achieving a detailed insight in their electrical transport. In addition, the present results can help providing information on the best deposition parameters that can be used to obtain suitable materials for SHJ solar cells application.

[1] S. De Wolf, A. Descoeudres, Z. C. Holman and C. Ballif, Green **2**, 7 (2012).

[2] N. Brinkmann, D. Sommer, G. Micard, G. Hahn and B. Terheiden, Sol. Energ. Mat. Sol. C. **108**, 180 (2013).

[3] M. Perani, N. Brinkmann, A. Hammud, D. Cavalcoli and B. Terheiden, J. Phys. Chem. C **119**, 13907 (2015).

Tuesday June, 7 - TuB - Oral Session

11:00-12:20

Cathodoluminescence - part 2

Chair: Javier Piqueras, *University Complutense, Madrid, Spain*

Radiative recentery properties in wide bandgap semiconductors

M.Zamoryanskaya[1], E. Ivanova[1], M. Karavaev[1], Ya. Kuznetsova[1], D. Shustov[1], V. Shkoldin[1]
[1]Ioffe Institute, St.Petersburg, Russia
*zam@mail.ioffe.ru

Luminescence is one of the most sensitive methods of solid state investigation. Luminescence bands of semiconductors are related with band-band transitions, including exciton levels, shallow acceptor and donor levels and levels located within the bandgap. These levels can be associated with defects (vacancies, interstices, stacking faults) and impurities.

Luminescence can be excited by optical way, x-ray, electron beam, electric current and other types of radiation. The emission spectra depend on the specific excitation method. The intensity of emission bands primarily depends on the energy of excitation. That is why the photoluminescence technique gives the possibility to excite the radiative levels selectively, what is very important for investigation of luminescent bands nature. X-ray, electron beam, electric current excitation is similar to the photo excitation in the fundamental absorption region. But the probability of the excitation capture depends on the energy and type of excitation. That is why the ratio of emission bands intensity can be different for photo- x-ray- and cathodoluminescence.

The very important difference between the ways of luminescence excitation is the area of electron-hole generation. It depends on the penetration of exiting radiation in the sample. In case of photoluminescence it may be several microns, for x-ray excitation – centimeters. The region of cathodoluminescence generation is defined by the region of deceleration of electrons from the primary beam. The penetration depth of electrons grows approximately from 20 to 100 nm if the energy is increased from 1 to 5 keV. At the energies as large as 30 keV the penetration depth can approach 2–4 μm.

The region of deceleration of electrons from the primary beam corresponds to the region of electron–hole pair generation. In a semiconductor electron–hole pairs can diffuse within a distance, which corresponds to the diffusion length of charge carriers for a given material or structure. It means that the region of electron-hole generation is larger than the region of interaction between the electron beam and the sample. Such specifics of cathodoluminescence technique is very useful for studying nanogeterostructures.

Temperature-dependent Cathodoluminescence: Quantifying Thermal Quenching at the Microscopic Level

L.I.D.J. Martin[1,2]*, D. Poelman[1,2], P.F. Smet[1,2]
[1]LumiLab, Department of Solid State Sciences, Ghent University, Ghent, Belgium
[2]Center for Nano- and Biophotonics (NB-Photonics), Ghent University, Ghent, Belgium
*Lisa.Martin@Ugent.be

A cathodoluminescence (CL) detector attached to a scanning electron microscope (SEM) is capable of producing images with high spatial resolution, which provide information on defects in semiconductors or the age and provenance of minerals. SEM-CL can be applied to a variety of materials, especially to those compounds which are intended to emit light. These luminescent materials are ideally suited for a microscopic investigation by SEM-CL (Fig. 1).

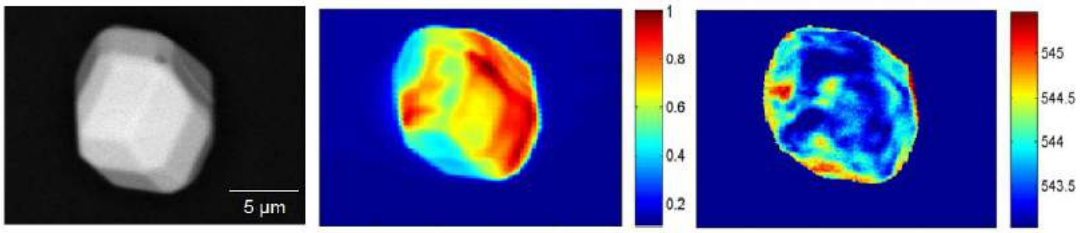

Figure 1: Backscattered electron image (left), normalized total intensity (center) and emission barycenter in nm (right) derived from a spectrally resolved CL mapping of $Lu_3Al_5O_{12}$:Ce at -25°C.

Luminescent materials, also known as phosphors, find their main application in white light emitting diodes (LEDs). LEDs are rapidly replacing incandescent and fluorescent lamps in general lighting, as well as in display back lighting. White LEDs consist of a blue emitting LED chip and one or more phosphor materials which convert part of the blue light to longer wavelengths. These phosphors should retain efficiency and color [1] while operated well above room temperature. Therefore it is important to know how temperature affects the emission spectrum and intensity.

Thermal quenching is generally measured on bulk material, whereas in this work the thermal behavior is evaluated at microscopic level by SEM-CL. A heating stage using a Peltier element is used, making it possible to investigate the sample's behavior between -25°C and 125°C. If the material is inhomogeneous or consists of multiple phases, different thermal quenching temperatures can occur in a single sample (or even within a single phosphor particle) resulting in spectrum changes upon changing temperatures [2].

With the addition of an energy-dispersive X-ray detector (EDX) the local composition and dopant concentration can be studied simultaneously. Correlating structural, compositional and luminescent information allows for identification of non-uniform doping or impurity phases, which can be used to improve synthesis methods and possibly also the overall performance of the phosphor.

[1] P.F. Smet, A.B. Parmentier, and D. Poelman, Journal of the Electrochemical Society **158**, R37-R54 (2011).
[2] P.F. Smet, J. Botterman, A.B. Parmentier, and D. Poelman, Optical Materials **35**, 1970–1975 (2013).

Cross-sectional CL observation for Oxynitride phosphors

Y. Cho[1], K. Takahashi[1], B. Dierre[2], T. Takeda[1], R.J. Xie[1], N. Hirosaki[1] and T. Sekiguchi[1]*
[1]National Institute for Materials Science (NIMS), Tsukuba, Japan
[2]Delft University of Technology, Postbus, Netherlands
*E-mail: CHO.Yujin@nims.go.jp

Rare-earth doped oxynitride phosphors are great application for white-light emitting diodes (w-LEDs) and field emitting devices (FEDs). They have outstanding thermal and chemical stability based on their stable chemical bonding structures. Moreover, wavelength tunable luminescence can be obtained by changing the rare-earth ions and their concentration in the host lattice [1]. However, due to the difficulties in terms of optimization of sintering conditions, oxynitride phosphors often contain secondary phases [2]. Investigation of such localized structures is important to understand the sintering mechanism and optimize the sintering conditions to obtain single-phase phosphors. Cross sectional polishing (CP) method using an argon ion beam is a powerful method to observe such kind of structures. Wider polishing area made enough particles to be observed, which allows to detect the minute secondary phases inside of the particles.

In this study, we performed cross-sectional CL observation of oxynitride phosphors. The luminescence and element distribution in the particles were identified by low-voltage CL microscopy and electron prove micro analyzer (EPMA). Fig.1 presents the CP-CL measurement of Ca-doped JEM ($(La,Ce)Al(Si_{6-z}Al_z)(N_{10-z}O_z)(z\sim1)$) blue-phosphors. This shows that submicron grain emits 540 nm luminescence along a large portion of the particles with dark grain boundary, while another portion emits 430 nm luminescence. The 300 nm emission is locally distributed. Based on the literature and XRD analysis, we can attribute the band centered at around 430 nm to Ce^{3+} in JEM and that at 480 nm to Ce^{3+} in α-SiAlON. The darker broad emission is originated to Ce^{3+} in β-SiAlON, and that at 310 nm to nitride-host material. This result indicated that JEM phosphor consists of many different phases agglomerated with each other. The secondary phases induced the red shift and the broadening of spectrum.

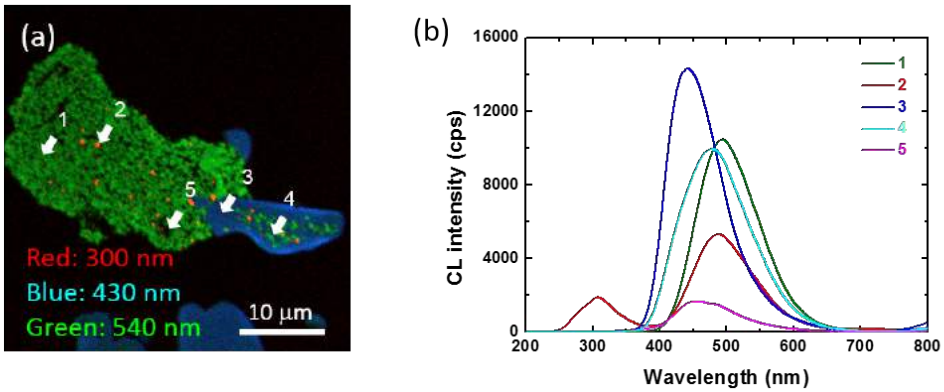

Figure1. Cross-sectional-CL images at 300 nm (red), 430 nm (blue) and 540 nm (green) (a) and local CL spectra taken at 5 kV for JEM phosphors doped 0.69 at% of Ca, respectively.

[1] R.-J. Xie, N. Hirosaki, K. Sakuma, and N. Kimura, *J. Phys. D: Appl. Phys.*, **41**, 144013 (2008).

[2] B. Dierre, X. L. Yuan, N. Hirosaki, T. Kimura, R.-J. Xie, and T. Sekiguchi, *J. Mater. Res.*, **23**, 1701 (2008).

Tuesday June, 7 - TuC - Oral Session

14:00-15:40

EBIC and CL

Chair: Nouar Tabet , *Qatar Energy and Environment Research Institute, Qatar*

Electron beam induced current and cathodoluminescence investigation of InGaN/GaN core-shell nanowire light emitting diodes

[1]Maria Tchernycheva *, [1]Hezhi Zhang, [1]Vladimir Neplokh, [1]Valerio Piazza, [1]Nan Guan, [1]François H. Julien, [2]Gwénolé Jacopin, [3]Pierre Rale, [3]Stéphane Collin, [3]Ludovic Largeau

[1] *Institut d'Electronique Fondamentale, UMR 8622 CNRS, University Paris Saclay, 91405 Orsay cedex, France*

[2] *Laboratory of Quantum Optoelectronics, Ecole Polytechnique Fédérale de Lausanne (EPFL), 1015 Lausanne, Switzerland*

[3] *LPN-CNRS, UPR20, Route de Nozay, 91460 Marcoussis, France*

* e-mail: maria.tchernycheva@u-psud.fr

Electron Beam Induced Current (EBIC) microscopy has been widely used to characterize optoelectronic devices for more than thirty years. In particular, nitride light emitting diodes (LEDs) in the form of two-dimensional (2D) films have been intensively investigated by this technique. In 2D LEDs, EBIC was used to probe the electrical activity of the device with a high resolution and to detect failures induced by material defects. Recently semiconductor nanowires have emerged as a way to boost the performance of nitride LEDs by improving the material quality [1, 2]. However, the replacement of a 2D active region by 3D nanowires increases the complexity of the device structure and impacts its electrical and optical behavior. In this context, the EBIC microscopy is vey useful to understand the device operation and to detect failures since it offers excellent spatial resolution and allows to address individual nanostructures composing the macroscopic device.

In this presentation we will briefly review the EBIC investigations of single nanowires and nanowire devices built of different materials and then we will focus on the EBIC analyses of core/shell InGaN/GaN nanowire LEDs [3]. We correlate EBIC and CL microscopies with compositional analysis to assess the material, electrical and optical properties of the wires. Individual nanowires from fully operational macroscopic LEDs are probed by EBIC under both top-view and cross-sectional imaging configurations. The electrical activity of the p-n junction on the m-planes and on the semi-polar planes is assessed. EBIC and CL maps of the nanowire cross-section show no signal dips, which confirms the absence of electrically active defects crossing the active region. EBIC profiles perpendicular to the wire elongated direction at different positions demonstrate a good homogeneity of the material parameters of GaN (doping concentrations and minority carrier diffusion lengths) along the wire axis. Coupled EBIC and CL characterizations on cleaved nanowires demonstrate the correlation between the electrical and optical signals : the reduction of the EBIC signal toward the nanowire top is accompanied by an increase of the CL intensity. This effect is interpreted as a consequence of the In and Al gradients in the quantum well and in the electron blocking layer evidenced by energy-dispersive X-ray spectroscopy (EDX), which influence the carrier extraction efficiency.

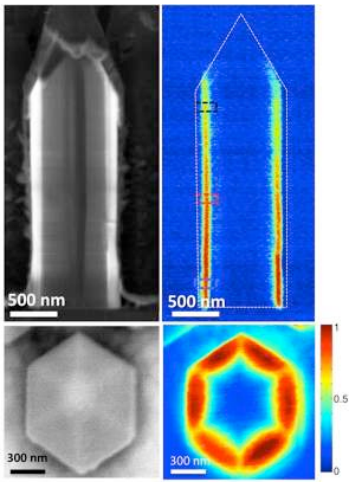

SEM and EBIC images of a core/shell NW LED in a cross-sectional and top-view geometries.

References

[1] M. Tchernycheva et al., Nano Letters 14, 2456 (2014).
[2] H. Zhang et al., Nanotechnology 26 465203A (2015).
[3] M. Tchernycheva, et al., Nanoscale 7, 11692 – 11701 (2015).

Comparison of three e-beam techniques for electric field imaging and carrier diffusion length measurement on the same nanowires

F. Donatini[1,2]*, A. De Luna Bugallo[1,2], P. Tchoulfian[1,3], G. Chicot[1,2], C. Sartel[4], V. Sallet[4] and J. Pernot[1,2,5]
[1]Univ. Grenoble Alpes, Inst NEEL, F-38042 Grenoble, France
[2]CNRS, Inst NEEL, F-38042 Grenoble, France
[3]CEA,LETI, Minatec Campus, F-38054 Grenoble, France
[4]Groupe d'Etude de la Matière Condensée (GEMAC), CNRS Université de Versailles St-Quentin, 78035 Versailles Cedex, France
[5]Institut Universitaire de France, 103 boulevard Saint-Michel, F-75005 Paris, France
*fabrice.donatini@neel.cnrs.fr

While nanowire (NW) based devices offer numerous advantages compared to bulk ones, their performances are frequently limited by an incomplete understanding of their properties, where surface effect should be carefully considered. Here, we demonstrate the ability to spatially map the electric field and determine the carrier diffusion length in NW by using an electron beam as the single excitation source. This approach is performed on numerous single ZnO NW Schottky diodes whose NW diameter vary from 85 to 350 nm. The dominant impact of the surface on the NW properties is revealed through the comparison of three different physical quantities recorded on the same NW: electron-beam induced current, cathodoluminescence and secondary electron signal. Indeed, the depletion region near the Schottky contact exhibits an unusual linear variation with reverse bias whatever the NW diameter. On the contrary, the carrier diffusion length is shown to be controlled by the NW diameter through surface recombination. This systematic comparison performed on a single ZnO NW demonstrates the power of these complementary techniques in understanding NW properties.

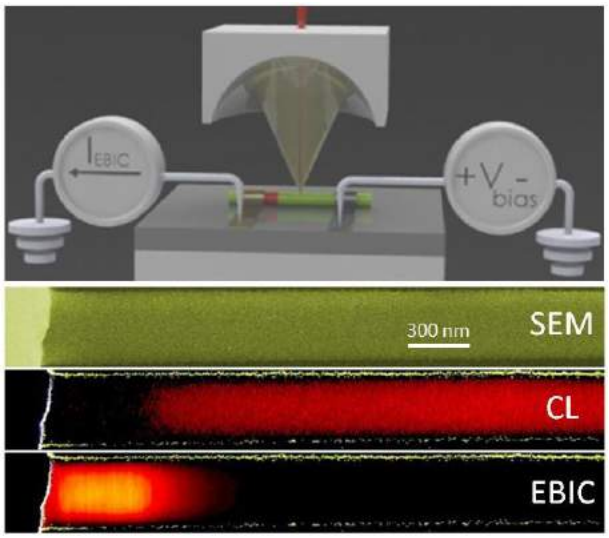

[1] F. Donatini, A. De Luna Bugallo, P. Tchoulfian, G. Chicot, V. Sallet, C. Sartel, J. Pernot, "Comparison of three e-beam techniques for electric field imaging and carrier diffusion length measurement on the same nanowires", submitted to Nano Letters in November 2015.

Luminescence properties and strain distribution within single GaN-based core-shell micropillars analyzed by nanoscale resolved cathodoluminescence spectroscopy and electron backscatter diffraction

M. Müller[1,2]*, G. Schmidt[1], S. Metzner[1], P. Veit[1], F. Bertram[1], S. Krylyuk[2,4], R. Debnath[2,5], J. Y. Ha[2,4], B. Wen[2,5], P. Blanchard[3], A. Roshko[3], A. Motayed[2,4,5], M. R. King[6], A. V. Davydov[2], and J. Christen[1]

[1]Institute of Experimental Physics, Otto-von-Guericke-University Magdeburg, Germany
[2]Materials Science and Engineering Division, National Institute of Standards and Technology, USA
[3]Quantum Electronics and Photonics, National Institute of Standards and Technology, USA
[4]Institute for Research in Electronics and Applied Physics, University of Maryland, USA
[5]N5 Sensors Inc., USA
[5] Northrop Grumman ES, Linthicum, USA
*marcus.mueller@ovgu.de

Three-dimensional GaN based core-shell micropillars provide a promising material system to improve the performance of optoelectronic devices due to a high crystal quality and an increased effective light emitting area in comparison to conventional planar devices.
Using highly spatially resolved cathodoluminescence (CL) spectroscopy directly performed in scanning transmission electron microscope (STEM), we will present a direct insight into the optical and structural properties of the individual core-shell layers on a nanoscale. In addition, electron backscatter diffraction (EBSD) was carried out to analyze the strain distribution within the micropillar.
The sample under investigation was produced by a combination of top-down and bottom-up processes. The two-step core-shell fabrication process consists of inductively coupled plasma etching of lithographically patterned GaN-on-Si templates followed by selective area growth of GaN shells using hydride vapor phase epitaxy (HVPE). The overgrowth of the etched GaN pillars produces a regular array of prismatically shaped hexagonal micropillars with a mean density of 8.8×10^5 cm^{-2} on 5×5 mm^2 chips.
Structural characterization by transmission electron microscopy (TEM) of the core-shell GaN micropillar proved an enhanced crystal quality with reduced dislocation density in the epitaxially overgrown shell region. Probing the different growth regions of the shell and the top-down processed core, a strong difference of the local optical properties is observed. The GaN core exhibits a weak CL due to a high density of threading dislocations which act as center for non-radiative recombination processes. The GaN shell grown by HVPE around the core reveals a higher CL intensity. Here, a strong incorporation of impurities during the epitaxial overgrowth by HVPE results in a high free-carrier concentration in the non-polar shell region, which is evidenced by intense (e-h) recombination. In contrast, the HVPE shell on top of the core exhibits the donor-bound exciton emission and donor-acceptor-pair (DAP) transition, indicating a lower free-carrier concentration. Furthermore, the nanoscale analysis of the strain by EBSD clearly reveals a compressively strained c-lattice parameter in the GaN shell region with respect to the GaN core.
Thus, CL imaging and EBSD analysis give a comprehensive insight in the core-shell layer architecture of the GaN micropillars and enable a direct visualization of the impurity incorporation and strain distribution within single micropillars.

Exciton Dynamics on a Single Dislocation in GaN by Picosecond Cathodoluminescence

W. Liu[1*], J. -F. Carlin[1], N. Grandjean[1] and B. Deveaud[1] and G. Jacopin[1]
[1]Institute of Physics, Ecole Polytechnique Fédérale de Lausanne (EPFL), Station3 CH-1015 Lausanne, Switzerland
*we.liu@epfl.ch

It is known that GaN-based blue LEDs with high threading dislocation density (TDD) (~10^8 cm^{-2}) can still maintain high efficiency owning to Indium fluctuation. However, when GaN-based LEDs with less Indium content working at violet to deep UV regions, the efficiency drops severely due to the high TDD[1]. Therefore, to fully exploit the potential of GaN-based LEDs, it is essential to understand the carrier dynamics around dislocations. Here, we investigate the exciton dynamics at T = 10 K on a single dislocation in bulk GaN grown by MOVPE, thanks to a picosecond time-resolved Cathodoluminescence (tr-CL) setup combining high temporal (~5 ps) and spatial (~50 nm) resolutions[2].

As shown in CL mapping (Fig. 1(a)), the CL intensity drops by 40 % when the electron beam is on the dislocation, demonstrating the non-radiative character of dislocations. By using tr-CL (Fig. 1(b)) for different points around the dislocation, we demonstrate that this reduced efficiency is characterized by two factors: (1) The intensity $I_{CL}(t=0)$ at early delay time is lower close to the dislocation (Fig. 1(c)); (2) The effective lifetime (τ_{eff}) is reduced close to the defect (Fig. 1(d)). To explain such a behavior, we propose a model based on a diffusion equation which considers a region defined by effective radius of dislocation R_{eff} [4], where the recombination is entirely non-radiative and instantaneous. The good agreement between our experimental results and the model allows us to clearly identify the effective range of dislocation defined by an effective radius $R_{eff} \approx 95$ nm.

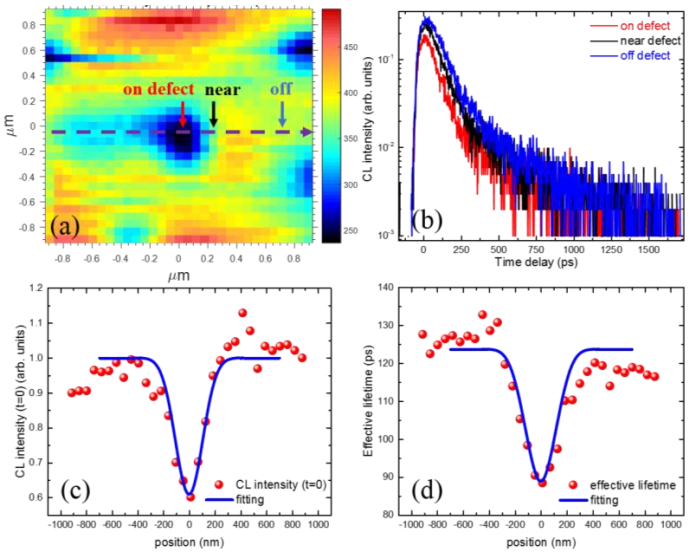

Fig. 1 (a) CL intensity (arb. units) mapping on a dislocation at 10 K; (b) tr-CL probed at different distances from the dislocation; (c) and (d) 1 dimensional mappings of $I_{CL}(t=0)$ and τ_{eff}, and fittings with parameters: diffusion length L_{diff} = 24 nm, R_{eff} = 95 nm, FWHM of injected electrons = 220 nm.

[1] S. Nakamura, Science. **281**, 956 (1998).
[2] M. Shahmohammadi, *et al.*, Nano Lett. **16**, 243 (2016).
[3] D. Gogova, *et al.*, Jpn. J. Appl. Phys. **43**, 1264 (2004).
[4] W.R. Harding, *et al.*, Electron. Lett. **12**, 503 (1976).

Wednesday June, 8 - WeA - Oral Session

09:00-10:40

Cathodoluminescence - part 3

Chair: Matthew Phillips, *University of Technology, Sydney*

Hopping of Bound Excitons in Zno Microwires Probed by Time-Resolved CL

G. JACOPIN[1]

[1] Institute of Physics, École Polytechnique Fédérale de Lausanne (EPFL), Station 3, CH-1015 Lausanne, Switzerland
Gwenole.jacopin@epfl.ch

Optimizing the electronic structures and carrier dynamics in semiconductors at atomic scale is an essential issue for innovative device applications. Besides the traditional chemical doping and the use of homo/hetero-structures, elastic strain has been proposed as a novel promising possibility. Here, we report on the direct observation of the dynamics of the excitonic transport in a ZnO microwire under pure elastic bending deformation, by using picosecond time resolved cathodoluminescence with high temporal, spatial and energy resolutions. We demonstrate that donor bound excitons can be effectively drifted by the strain-gradient in inhomogeneous strain fields, against simple views implied by their name: "donor bound exciton". Our observations are well reproduced by a drift-diffusion model taking into account the strain gradient and allow us to deduce an exciton mobility of 1400± 100 cm^2/eVs in the ZnO wire [1].

By means of Monte-Carlo simulations [2], we show that the motion of donor bound exciton can be explained by a hopping process at cryogenic temperature. Additional temperature dependent time-resolved experiments allows us to confirm this hypothesis [3]. These results provide critical information on the exciton dynamics in semiconductors, and the possible role of strain gradient in opto-electronic and sensing nano/micro-devices.

[1] X. Fu et al., Exciton drift under Uniform Strain Gradient in Bent ZnO Microwires, ACS Nano, 8, 3412 (2014).
[2] G. Jacopin et al., Hopping process of bound excitons under an energy gradient, Applied Physics Letters, 104, 042109 (2014).
[3] M. Shahmohammadi et al., Exciton hopping probed by picosecond time-resolved cathodoluminescence, Applied Physics Letters, 107, 141101 (2015).

Excitonic Luminescence of BN Materials

L. Schue[1,2], F. Fossard[1], F. Ducastelle[1], J. Barjon[2] and A. Loiseau[1]

[1]LEM, CNRS-Onera, 29 avenue de la Division Leclerc, Châtillon, France
[2]GEMAC, Université Versailles – CNRS, 45 avenue des Etats Unis, Versailles, France

Hexagonal boron nitride is a wide band gap semiconductor (~6.5 eV), which meets a growing interest for graphene engineering [1]. In particular electron mobility of graphene is shown to be preserved when graphene is supported by a h-BN film. We attempt to have a better comprehension of the optical properties of thin BN layers governed, in the 5.2-6 eV energy range, by strong excitonic effects [2,3].

In this work, we present first cathodoluminescence experiments on bulk samples synthesized through various processes. They all present the same features in the energy range 5.7–6 eV attributed to intrinsic free excitons (the so-called S series). We then tried to follow how are impacted these intrinsic emissions reducing hBN thickness. We observed a significant effect of the confinement on the luminescence analyzing defect free flakes obtained by mechanical exfoliation [4].

We then focused on the D series, emitted at lower energy (5.2-5.7 eV) and previously attributed to excitons trapped on defects such as grain boundaries [5]. We managed to localize this signal on folded flakes where the D bands are strongly enhanced along the fold and discuss its origin.

Finally, we recently have undertaken CL experiments on BN samples presenting another stacking sequence (ABC..) and we will discuss how the excitonic properties are impacted by the stacking sequence.

[1] C.R. Dean et al. Nature Nanotechnology, **5**, 722 (2010)
[2] P. Jaffrennou el al., Phys. Rev. B, **77**, 235422 (2008)
[3] Y. Kubota et al., Science, **317**, 932 (2007)
[4] L. Schue et al., accepted for publication in Nanoscale (2016)
[5] A. Pierret et al., Phys. Rev. B, **89**, 035214 (2014)

Cathodoluminescent Signature of Dislocation Reactions in GaN

Medvedev O.[1, 2*], Vyvenko O.[1], Bondarenko A.[1]
[1] V.A. Fok Institute of Physics, St. Petersburg State University
[2] IRC for Nanotechnology, Research Park, St.-Petersburg State University
*o.s.medvedev@spbu.ru

Despite of a long story of investigations of dislocations in GaN only recently it was found that screw dislocations introduced by room-temperature plastic deformation exhibited a strong characteristic luminescence [1,2]. The spectral position of the dislocation-related luminescent (DRL) line peak was reported to be near 3.3 eV in semi-insulated GaN [2], but to be 3.1-3.2 eV in low-ohmic n-type material [3,4]. TEM investigation of the dislocation core structure revealed their perfect character in semi-insulating GaN making thus the line 3.3 eV as a fingerprint for perfect, non-dissociated screw dislocations. Additional red shift of the DRL band in low-ohmic material was attributed to the presence of stacking fault ribbon in the dislocation core, i.e. due the core dissociation. Here we report new results of the further cathodoluminescence (CL) study of a-screw dislocations in GaN.

We investigated c-plane GaN single crystals grown by HVPE and MOCVD techniques with a density of grown-in dislocations of about 10^6-10^9 cm^{-2} and shallow net-donor concentration in the ranges of 10^{15}-10^{18} cm^{-3}. Additional dislocations were introduced by indentation or scratching of the sample surfaces at room temperature. CL measurements were performed in a chamber of a scanning electron microscope at the temperatures 70-300K.

In particular we discovered that while the long straight segments of a-screw dislocations radiated a set of the lines in 3.1-3.2 eV (Fig.1, dashed line) ranges their intersection points exhibited spectral features (IRL) at about 3.3eV (Fig.1, dotted line). The appearance of IRL was observed in-situ in SEM chamber as bright dots at the a-screw dislocation intersections. It was found that the number of the IRL dots increased under electron beam exposure whereas DRL vanished at these points. We proposed that the appearance of the dots exhibiting IRL is due to reactions between the crossing dislocations giving rise to their core structure transformation: initially splitted into partials became perfect in the vicinity their intersection point.

Detailed description of all obtained results will be presented at the Conference.

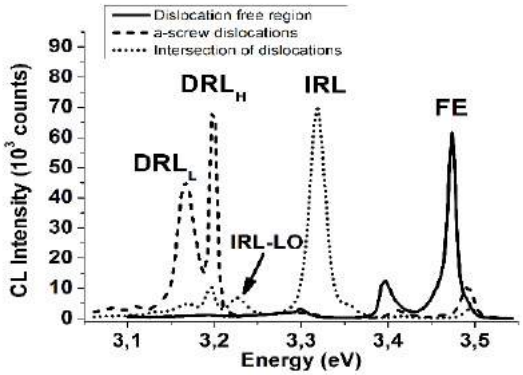

Figure 1. Cathodoluminescence spectra taken at similar conditions from: dislocation-free region (FE), straight segments of a-screw dislocations (DRL), intersections of a-screw dislocations (IRL).

References:

[1] Medvedev O, Vyvenko O, Bondarenko A and Voronenkov V 2014 *12th international workshop on Beam Injection Assessment of Microstructures in Semiconductors* (Tsukuba) p MoA4
[2] Albrecht M, Lymperakis L and Neugebauer O 2014 *Phys. Rev. B* **241201** 1–4
[3] Medvedev O S, Vyvenko O F and Bondarenko A S 2015 *Semiconductors* **49** 1181–6
[4] Huang J, Xu K, Fan Y M, Wang J F, Zhang J C and Ren G Q 2014 *Nanoscale Res. Lett.* **9**

.

Cathodoluminescence of ensemble and single InGaN quantum disk-in-nanowires made by selective area sublimation

M. Portail*, S. Vézian, V. Brändli, J. Brault, B. Alloing, J. Massies, and B. Damilano
CRHEA – CNRS UPR10, Rue Bernard Grégory, 06560 Valbonne, France
*marc.portail@crhea.cnrs.fr

III-N based low dimensionality structures, as nanowires (NWs) or quantum disks (QDisks), are a subject of important ongoing research regarding their potential interest for various fields as photonics, nanoelectronics or biosensing. Among the techniques used for their elaboration, an innovative top-down approach, the selective area sublimation (SAS), has been recently proposed. In this method, III-N NWs and QDisks are formed from conventional 2D quantum well epitaxy and selectively etched by thermal treatment using an epitaxial SiN_x nanomask [1]. This approach is a simple method which reduces the number of technological steps usually required in top down processes and reduces the only growth concern to well established 2D epitaxial processes. Furthermore, the SAS can be applied for the fabrication of QDisks with nanometer sizes (3-4 nm) in the 3 directions of space.

In this presentation, we assess the optical properties of InGaN QDisks grown by SAS using room temperature and 77K cathodoluminescence (CL). The QDisks are obtained by applying SAS method to a five period InGaN / GaN multiple quantum well and by overgrowing them with GaN. The NW density is ~$1x10^9$ cm^{-2}. CL measurements are performed in a JEOL JSM scanning electron microscopy equipped with a GATAN CL4 monochromator. Detection is achieved either on an UV enhanced CCD or a high sensitivity photomultiplier. Accelerating voltage and current probe are 3 keV and in the range of 100 pA, respectively. In order to avoid charging effect and to isolate a few NWs, a metallic mask is deposited on the sample and openings of different sizes (from 0.3×0.3 μm^2 to 10×10 μm^2) are defined by e-beam lithography. Under these conditions of operation, the QDisk emission (430-450 nm) of isolated NWs is easily identified and well separated from that of the GaN 2D buffer layer (365 nm). We will illustrate how CL is of interest for the characterization of such material and we will discuss about results obtained in pan- and mono- chromatic modes as well as hyperspectral imaging. We will also correlate these results with another local luminescence probe (micro-photoluminescence).

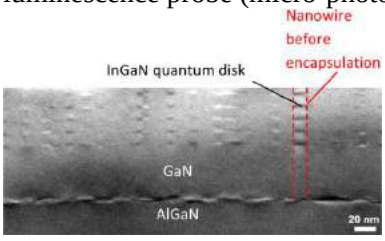

Figure 1: cross section transmission electron microscope image of InGaN QDiskss encapsulated in GaN (from [1]).

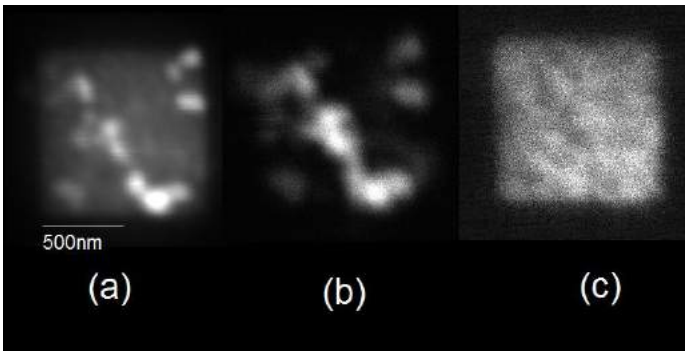

Figure 2: CL micrographs recorded at room temperature – 3 keV – 130pA – x40000 on a 1x1 μm^2 area; Panchromatic mode (a); monochromatic mode centered at 438 nm (b) and 365 m (c).

[1] B. Damilano, S. Vézian, J. Brault, B. Alloing, and J. Massies, Nano Letters, DOI:10.1024/acs.nanolett.5b04949

Wednesday June, 8 - WeB - Oral Session

11:00-12:20

Miscellaneous

Chair: Maria Zamoryanskaya, *Ioffe Institute, St Petersburg, Russia*

STM-luminescence spectroscopy of defects and impurities in oxides

Niklas Nilius
Carl von Ossietzky Universität, Institut für Physik, 26111 Oldenburg, Germany
niklas.nilius@uni-oldenburg.de

The properties of oxides are largely governed by defects and impurities in the lattice that control the carrier density in the bulk bands, act as local charge centers and provide discrete electronic states in the gap region of the material. Detail characterization of lattice imperfections is therefore import to understand the electronic and optical response of oxides and a first step to tailor oxide properties via defect engineering and doping. Optical and photoelectron spectroscopy are commonly used to study oxide properties, but have the disadvantage of a poor spatial resolution. As the nature of defects and impurities often depends on their local environment, a high-resolution technique is desirable for studies down to atomic length scales.

In my talk, I discuss how scanning tunneling microscopy can be employed to probe local oxide properties including defects and impurities. The experimental scheme relies on electron injection (10-100 eV) from the STM tip into a pre-characterized sample region and collecting the outgoing radiation with a CCD detector. To ensure high structural quality and avoid charging effects, the oxides of interest are grown in the form of thin films on single-crystalline metal supports. The strength of our approach is demonstrated for a number of model systems. MgO, an inert wide-gap insulator, exhibits fascinating optical properties along dislocation lines as well as after inserting single-ion Cr or Eu impurities. The optical response of ZnO can be varied by changing the defect landscape, i.e. by generating Zn or O vacancies, or doping the wurtzite lattice with nitrogen. Also plasmon-exciton coupling can be investigated locally, as demonstrated for TiO_2 surfaces covered with silver and gold particles. Although the technique does not reach the energy resolution of conventional optical spectroscopy, it is ideally suited to study inhomogeneous samples with high spatial resolution.

Nanoscale cathodoluminescence of an InGaN single quantum well intersected by individual dislocations

Gordon Schmidt*, Peter Veit, Sebastian Metzner, Christoph Berger, Frank Bertram, Armin Dadgar, André Strittmatter, and Jürgen Christen

Institute of Experimental Physics, Otto-von-Guericke-University Magdeburg, Germany
*Gordon.Schmidt@ovgu.de

III-nitride based heteroepitaxially grown quantum well layers contain a relatively high number of threading dislocations (TD) compared to their III-arsenide counterparts. Thus, non-radiative recombination at dislocations is expected to reduce the efficiency of light emitting devices. Nonetheless, highly efficient blue LEDs based on InGaN/GaN quantum wells have been realized and commercialized since its first demonstration by S. Nakamura *et al.* In contrast to the remarkable technical breakthroughs the physics of the most crucial component – the active medium – remains not fully understood and is still debated.

Using cathodoluminescence spectroscopy performed in a scanning transmission electron microscope (STEM-CL), we analyze the optical properties of an InGaN single quantum well (SQW) with nanometer scale resolution in very close proximity to individual threading dislocations. Embedded into GaN barriers the InGaN SQW was grown with an ammonia/group-III precursor (V/III-) ratio of 3000 at a temperature of 815 °C by metal-organic vapor phase epitaxy on a GaN/sapphire template. To avoid the interdiffusion of In and Ga atoms in the InGaN/GaN heterostructure, the barrier material was grown at relatively low temperature of 935 °C.

Cross-sectional STEM images prove the comparably high quality of the GaN/sapphire template and the InGaN SQW in general. Originating from the buffer/sapphire interface vertically running TDs show up in the STEM images and intersect with the InGaN SQW at several positions. In dislocation free domains, the SQW layer with a thickness of 1.4 ± 0.1 nm exhibits a sharp interface to the bottom GaN barrier while the upper interface has a diffuse contrast. The panchromatic CL with the highest intensity at 15 K is emitted by the SQW. The spatially averaged spectrum exhibits emission contributions from the SQW at 395 nm wavelength with distinct LO-phonon replica and near band edge emission from the GaN barriers at 357 nm wavelength.

With the high spatial resolution of our STEM-CL setup we are able to investigate the intersection of *single* dislocations with the InGaN SQW and its vicinity. Most strikingly, the SQW emission is blue-shifted by up to $\Delta E = 70$ meV in the vicinity to TDs with concurrently reduced intensity. The detailed analysis of the evolution of the excitonic SQW luminescence across a single TD reveals an asymmetric emission profile. Directly exciting the SQW on one side of the TD, the SQW CL starts to shift continuously blue more than 200 nm apart from the intersection and reaches a minimum peak wavelength of 385 nm close to the intersection point at a distance of ~40 nm. Tracking the SQW emission further across the TD, the peak wavelength continuously shifts to longer wavelengths up to 395 nm wavelength. The nature of the blue shift will be discussed in terms of local variations of strain, composition and thickness introduced by TDs.

Enhanced Ultraviolet Luminescence of ZnO Nanorods Treated by High Pressure Water Vapor Annealing (HWA)

Amer Al-Nafiey[1,2], Brigitte Sieber[2,*], Bernard Gelloz[3], Ahmed Addad[2] , Myriam Moreau[4], Julien Barjon[5], Maria Girleanu[6], Ovidiu Ersen[6], and Rabah Boukherroub[1]
[1]IEMN, UMR CNRS 8520, Université Lille 1, Villeneuve d'Ascq, France
[2]UMET, UMR CNRS 8207, Université Lille 1, Villeneuve d'Ascq, France
[3]Department of Applied Physics, Nagoya University, Nagoya, 464-8603 Aichi, Japan
[4]LASIR, UMR CNRS 8516, Université Lille 1, Villeneuve d'Ascq, France
[5]GEMaC, UMR CNRS 863, Université de Versailles St Quentin, Versailles, France
[6]IPCMS UMR CNRS 7504, Strasbourg, France
*E-mail: brigitte.sieber@univ-lille1.fr

The luminescence intensity of ZnO nanostructures is very much surface-dependent as a result of their large surface area to volume ratio. Thus, whatever the bulk luminescence intensity, the more defective the surface is, the lower the total luminescence emitted by the nanostructure. One way to reduce the density of surface defects is to anneal the nanostructures at high temperature. In such high temperature post-annealing air, oxygen and argon are the most used atmospheres. However the influence of high-pressure water vapor annealing (HWA) on ZnO nanostructures has never been reported. HWA has been successfully used to improve the photoluminescence (PL) of porous silicon [1] and silicon nanowires substrates.

In this work, we show that HWA of ZnO nanorods at a temperature as low as 260°C leads to a large enhancement of their UV luminescence [2]. The ZnO nanorods were prepared via a chemical bath deposition method at low temperature (96°C) on silicon substrates [3]. Then the samples were post-annealed for 3 h either in air, or using HWA with pressures in the range 1.3 -3.9 MPa. Figure 1 shows the PL spectra of as-grown and annealed ZnO nanorods. It is clear that while annealing in air allows the appearance of the UV band (very weak in the as-prepared samples), the HWA treatment leads to a further threefold increase of its intensity. Also the visible band is strongly decreased after post-annealing.

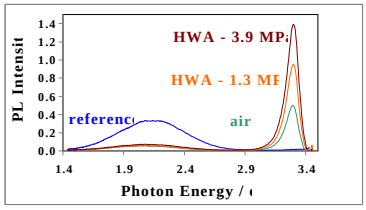

Fig. 1 PL spectra (@300 K) of as-grown and annealed ZnO nanorods.

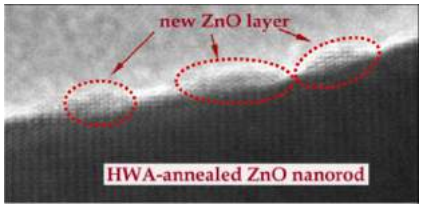

Fig 2 HRTEM image of the new ZnO layer grown on the nanorod surface after HWA annealing.

The characterization of the nanostructures using micro-Raman and cathodoluminescence spectroscopies, scanning electron microscopy, X-Ray Photoelectron Spectroscopy and high resolution transmission electron microscopy (HRTEM-Fig 2) demonstrates that the origin of the UV luminescence enhancement is due to the transformation of the $Zn(OH)_2$ surface−layer into ZnO, but also to the growth of a new thin ZnO layer at the surface of the rods (Fig 2).

[1] B. Gelloz, A. Kojima and N. Koshida, Appl. Phys. Lett. **87**, 031107 (2005)
[2] A. Al-Nafiey, B.Sieber, B. Gelloz, A.Addad , M. Moreau, J. Barjon, M.Girleanu, O.Ersen, and R.Boukherroub, J. Phys. Chem C,**120**, 4571 (2016)
[3] G. Perry, Y. Coffinier, V. Thomy and R. Boukherroub, Langmuir, **28**, 389 (2012)

Wednesday June, 8 - WeC - Oral Session

14:00-14:40

Plasmonic

Chair: Matthieu Kociak, *Laboratoire de Physique des Solides, France*

Angle-resolved cathodoluminescence spectroscopy for nanophotonics

T. Coenen[1],
[1]Delmic BV, Delft, The Netherlands
*coenen@delmic.com

In the field of plasmonics, metallic nanostructures are used to confine light to deep-subwavelength volumes. Owing to the nanoscale size of such structures it is challenging to resolve their optical properties with conventional optical microscopy. Recently, electron-beam spectroscopy techniques have emerged as powerful probes in nanoscience due to their ability to generate, probe, and control light at length scales far below the diffraction limit of light. Taking advantage of the high spatial resolution, novel techniques have appeared that combine electron beam excitation with optical spectroscopy. Spatially-resolved cathodoluminescence (CL) spectroscopy, in which the electron-beam-induced radiation is collected inside an electron microscope is one of these techniques that holds great potential for nanoscience.

For a long time CL has been used by geologists to analyze and identify minerals, but in the past two decades its scope has expanded significantly. Recently, it has been used to study the fundamental optical properties of a myriad of metallic, semiconductor, and dielectric (nano)materials in the fields of materials science and nanophotonics, including plasmonics and metamaterials. We have developed a special version of CL spectroscopy in which we can both effectively measure the emitted spectrum as well as the angular emission distribution (SPARC)[1,2]. Furthermore, we have developed a CL polarimetry technique to fully resolve the polarization of the emitted light for every angle of emission [3].

At the heart of this development is a motorized micropositioning system for the paraboloid mirror that collects the CL which can precisely overlay the mirror focus with the electron beam impact position. This alignment ensures that the CL beam coming from the paraboloid optic is perfectly parallel enabling efficient light collection and hyperspectral imaging. This alignment procedure is critical for many nanophotonic studies where the CL signals can be very low (10^{-4} photons/electron). It also allows the angle-and polarization-resolved imaging to be done in a reliable and reproducible manner.

We demonstrate how these CL techniques can be applied to variety of different materials and structures. In particular, we use it to measure the fundamental scattering properties of elementary building blocks in nanophotonics such as metallic and semiconductor nanoparticles, holes, and wires and show that interesting physical parameters can be extracted from such measurements. Of course these building blocks can be combined into more complex composite nanoantennas, metamolecules, metasurfaces, photonic crystals etc, engineered for specific applications. Also in these cases CL is a highly relevant technique that can be used to study guided mode propagation, near-field coupling, chirality, diffraction/interference, and the photonic band structure amongst others.

[1] T. Coenen, E. J. R. Vesseur, and A. Polman, Appl. Phys. Lett. **99**, 143103 (2011).
[2] T. Coenen, E. J. R. Vesseur, A. Polman, and A. F. Koenderink, Nano Lett. **11**, 3779 (2011).
[3] C. I. Osorio, T. Coenen, B. J. M. Brenny, A. Polman, and A. F. Koenderink, ACS Photon. **3**, 147 (2016).

Thursday June, 9 - ThA - Oral Session

09:00-10:40

Devices

Chair: Hajime Tomokage, *Fukuoka University, Japan*

A Study on Degradation of Perovskite Solar Cells and Materials

Seongtak Kim[1] , Seunghun Lee[1,2], Hae-Seok Lee[1], Yoonmook Kang[1], Sungeun Park[1,2] , Stefan W. Glunz[2] , Wilhelm Warta[2], Martin Schubert[2], Bernhard Michl[2], Laura Mundt[2] and Donghwan Kim[1]*

[1]Department of Materials Science and Engineering, Korea University, Seoul, Korea
[2] Fraunhofer Institute for Solar Energy Systems, Freiburg, Germany
*donghwan@korea.ac.kr

The organic-inorganic hybrid perovskite solar cells were introduced from the year of 2009 [1]. The perovskite materials have emerged as light absorbers in solar cells because they have a high absorption coefficient, a tunability of band gap, a long diffusion length and a high mobility [2-4]. Since the conversion efficiency of perovskite solar cells has reached above 22 % over the past few years [5], the long-term stability of the perovskite solar cells has to be considered for a commercialization. Recently literatures on thermal, humidity, and light stability were published [6-11]. We report on the thermal stability of methylammonium lead iodide perovskite solar cells. Although the methlyammonium lead iodide perovskite absorber was not decomposed, the solar cell performance was reduced when the temperature was raised. When the perovskite cells were heated up to 65°C, the open-circuit voltage and the effective diffusion length decreased by 20% and 50%, respectively. We propose that the degradation is caused by the thermal stress in $CH_3NH_3PbI_3$ perovskite solar cells.

[1] Kojima, K. Techima, Y. Shirai, and T. Miyasaka, J. Am. Chem. Soc, **131**, 6050 (2009)
[2] S. Sun, T. Salim, N. Mathews, M. Duchamp, C. Boothroyd, G. Xing, T. C. Sum, and Y. M. Lam, Energy Environ. Sci., **7**, 399 (2014)
[3] J. H. Noh, S. H. Im, J. H. Heo, T. N. Mandal, and S. I. Seok, Nano Lett, **13**, 1764 (2013)
[4] G. Xing, N. Mathews, S. Sun, S. S. Lim, Y. M. Lam, M. Gratzel, S. Mhaisalkar, and T. C. Sum, Science, **342**, 344(2013)
[5] http://www.nrel.gov/ncpv/images/efficiency_chart.jpg
[6] G. Niu, W. Li, F. Meng, L. Wang, H. Dong, and Y. Qiu, J. Mater. Chem. A, **2**, 705 (2014)
[7] J. M. Frost, K. T. Butler, F. Brivio, C. H. Hendon, M. V. Schilfgaarde, and A. Walsh, Nano Lett., **14**, 2584 (2014)
[8] B. Conings, J. Drijkoningen, N. Gauquelin, A. Babayigit, J. D'Haen, L. D'Olieslaeger, A. Ethirajan, J. Verbeeck, J. Manca, E. Mosconi, F. D. Angelis, and H. G. Boyen, Advanced Energy Materials, **5**, 1500477(2015)
[9] I. Deretzis, A. Alberti, G. Pellegrino, E. Semecca, F. Giannazzo, N. Sakai, T. Miyasaka, and A. L. Magna, Applied Physics Letters, **106**, 131904(2015)
[10] T. Leijtens, G. E. Eperon, S. Pathak, A. Abate, M. M. Lee, and H. J. Snaith, Nature communications, **4**, 2885 (2013)
[11] S. Ito, S. Tanaka, K. Manabe, and H. Nishino, J. Phys. Chem. C., **118**, 16995 (2014)

Novel Technique for the Investigation of Internal Optical Loss in High-Power Laser Heterostructures

D.A. Veselov[1*], I.S. Shashkin[1], A.A. Podoskin[1], S.O. Slipchenko[1],
Z.N. Sokolova[1], N.A. Pikhtin[1,2], I.S. Tarasov[1]
[1]Ioffe Institute, Saint-Petersburg, Russia
[2]Saint Petersburg State University, Saint-Petersburg, Russia
*E-mail: dmitriy90@list.ru

High-power semiconductor lasers based on separate confinement heterostructures with quantum wells suffer from internal optical loss increase with temperature [1] and pump current [2,3] rise. These phenomena strongly decrease maximum optical power, efficiency and reliability of the device.

We introduce the new method of internal optical loss investigation via measurements of free-carrier absorption inside the heterostructure of the laser diode pumped with short (100 ns) high current (up to 100 A, current density 50 kA/cm^2) pulses.

The method is as follows. A test light beam is coupled into the waveguide of the laser diode through its cavity mirror. The output of the test beam is collimated, selected from the laser self emission and registered. The test beam photon energy is well below all the bandgaps inside the laser diode structure so the beam is not affected by the band-to-band absorption but is still absorbed by free-carriers.

While the laser is pumped with the current pulse, the free-carrier absorption of the laser heterostructure layers rises and the test beam intensity decreases. This decrease with relation to the laser cavity length allows us to calculate the internal optical loss change, see equation (1).

$$\alpha_1 - \alpha_0 = \frac{1}{L}\ln\left(\frac{Int_0}{Int_1}\right), \quad (1)$$

where α_1 is the internal optical loss while the laser is pumped, α_0 is the internal optical loss while the laser is not pumped, L is the laser cavity length, Int_0 is the test beam intensity while the laser is not pumped and Int_1 is the test beam intensity while the laser is pumped.

The method presented provides the ability to measure internal optical loss change in a wide range of current levels and at different temperatures. It allows us to measure the active region free-carrier absorption while the laser is driven under its threshold. The measurements of the internal optical loss rise inside the heterostructure layers of high-power semiconductor lasers (spectral range 1.0-1.1 mkm) enabled us to explain the laser light-current curve saturation both under pulse-pumped and continuous-wave modes of operation. The internal optical loss measurements of the AlGaInAsP/InP lasers (spectral range 1.4-1.6 mkm) also have been carried out and allowed us to divide the contributions to the light-current curve saturation from the internal optical loss rise and from Auger recombination in the quantum well rise. The new technique helps us in designing new laser heterostructures with low internal optical loss.

[1] D.A.Veselov, V.A.Kapitonov, N.A.Pikhtin, A.V.Lyutetskiy, D.N.Nikolaev, S.O.Slipchenko, Z.N.Sokolova, V.V.Shamakhov, I.S.Shashkin, I.S.Tarasov, Quantum electronics, **44**, 993 (2014)
[2] N.A.Pikhtin, S.O.Slipchenko, I.S.Shashkin, M.A.Ladugin, A.A.Marmalyuk, A.A.Podoskin, I.S.Tarasov, Semiconductors, **44**, 1411 (2010)
[3] N.A.Pikhtin, S.O.Slipchenko, Z.N.Sokolova, A.L.Stankevich, D.A.Vinokurov, I.S.Tarasov, Zh.I.Alferov, Electronics Letters, **40**, 1413 (2004)

Huge Intensity gain of Group-IV LEDs on Si substrates by using MQW

B. Schwartz[1]*, M. Reiche[2], and M. Kittler[1]
[1] Institut für Physik, BTU Cottbus-Senftenberg, 03046 Cottbus, Germany
[2] MPI für Mikrostrukturphysik, 06120 Halle, Germany
*Bernhard.Schwartz@B-TU.de

The implementation of an integrated light source on Si substrate belongs to the most interesting research activities for group-IV photonics during the last years. The MIT group demonstrated for the first time a Ge-LED on silicon substrate with intensive luminescence of the direct transition around 0.8 eV by using tensile strained Ge layers with a high phosphorus concentration [1]. The high donor concentration shifts the Fermi level of the conduction band above the L-point towards the Γ-point where the direct Ge transition occurs.

We analyzed LEDs with 300 nm thick Ge layers and different antimony concentrations. The highest electroluminescence (EL) intensity was found for the LED with [Sb] = 3×10^{19} cm^{-3}. The intensity was about four times higher than the reference i-Ge LED without intentional doping, see Fig. 1. More details can be found in reference [2], for example. Furthermore, band structure calculations support an increase of the luminescence intensity caused by tensile strain.

Recently, we have demonstrated that the EL of LEDs on Si substrate, with GeSn-Ge MQW (multi quantum wells) as active structure, is intense compared to the above mentioned Ge LEDs [3]. The luminescence of the MQW stems from GeSn wells embedded in Ge barriers. Spectrum deconvolution yields three lines with the direct transition Γ > hh (heavy holes) as the most intensive peak. The intensity of the MQW LED with ten 12 nm thick GeSn wells, shown in Fig. 1, is again about four times higher than to the n^+-Ge LED. Correction for the thickness of the active layers yields an intensity increase of more than one order of magnitude.

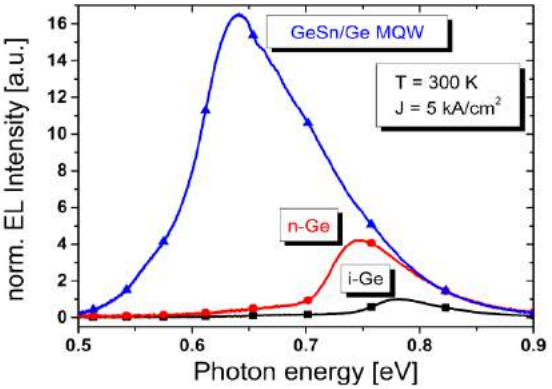

Fig. 1 EL spectra of different LEDs normalized to the intensity of the i-Ge LED. All spectra were taken at 300 K with 5 kA/cm² forward current density. The top structure of all LEDs was identical. Accordingly, the light extraction is comparable.

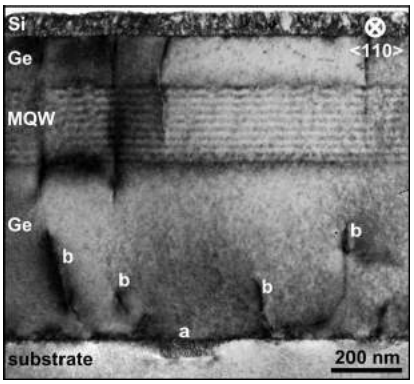

Fig. 2 Bright field TEM image of the cross-section of a GeSn-Ge MQW LED. The different layers are well distinguishable. A high density of threading dislocations can be seen.

It should be noted that the MQW and Ge LEDs contain a huge density of threading dislocations, see Fig. 2. Avoidance of threading dislocations is expected to improve the behavior of MQW LEDs. This could be realized by using Ge-Si MQW on Si containing ultra-thin Ge wells, for example.

We acknowledge the Institut für Halbleitertechnik (IHT) of Universität Stuttgart for providing samples in the framework of the DFG project KI 561/5-1; OE 520/5-1.

[1] X. Sun, J. Liu et al., Optics Letters **34**, 1198 (2009)
[2] B. Schwartz, A. Klossek et al., Phys. Status Solidi C **11**, 1686 (2014)
[3] B. Schwartz, M. Oehme et al., Optics Letters **40**, 3209 (2015)

Fountain Detectors Are Go
- Low Energy Secondary Electron Imaging for Various Semiconductors

T. Sekiguchi[1,2]*, H. Iwai[1], T. Kimura[1], and T. Agemura[2]
[1]National Institute for Materials Science (NIMS), Tsukuba 305-0044, Japan
[2]Graduate School of Pure and Applied Sciences, University of Tsukuba, Tsukuba 305-0044, Japan
*Sekiguchi.takashi@nims.go.jp

The modern scanning electron microscopy made it possible to obtain fruitful information of the semiconductor specimens, not only morphology and composition but also surface potential, electrical field etc. Such development is brought about by the energy filtered secondary electron detectors attached in the electron gun (inlens detector). On the other hand, the outlens detector was left behind such evolution. Recently, we have developed low-pass secondary electron detector (LPSED) for outlens SEM and named “Fountain Detector (FD)”. This detector is composed of bias grid above and electron detector below the specimen. The bias voltage and the geometry of the detector limit the energy and acceptance angle of SE, respectively. The biggest advantage of FD is that we can easily trace the trajectories of the secondary electros. Fig. 1 shows the schematic of FD. The subtraction of the images taken at different bias voltages gives the energy filtered images. Using this detector, we have characterized various semiconducting materials as well as metals and insulators.

In this presentation we confirm the performance of FD by getting SE spectra of Si specimens. Then, we show surface potential variation of p-n junction in SiC wafer. Fig. 2 shows a FD image and line profile of SE signals. These data give us the detailed information of band bending of p-n junction.

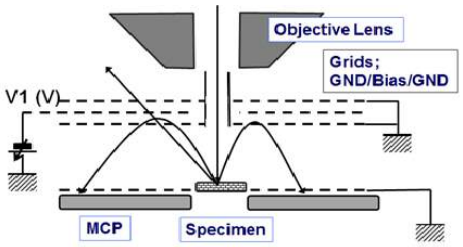

Fig.1. Schematics of fountain detector.

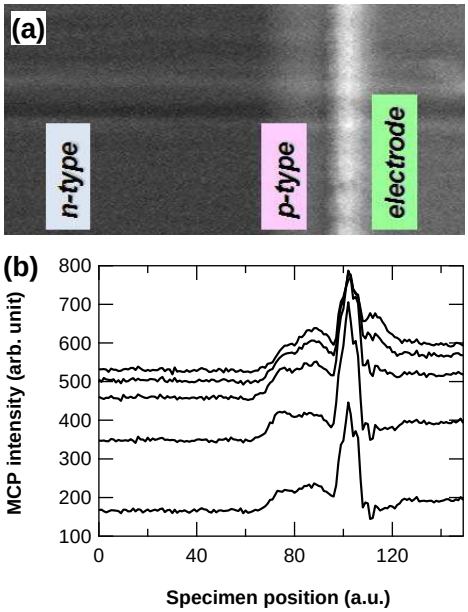

Fig.2. (a) FD image of pn junction in SiC and (b) its line profiles.

[1] T. Sekiguchi, H. Iwai, Jpn. J. Appl. Phys. 54 (2015) 088001.

Thursday June, 9 - ThB - Oral Session

11:00-12:20

Nano-materials

Chair: Brigitte Sieber, *Université des Sciences et Techniques de Lille, France*

Dual Probe Imaging: Combining Electron Beam Excitation and Near Field Scanning Optical Microscopy to Visualize Carrier Transport

N. M. Haegel, Chuanxiao Xiao, C.-S. Jiang, H. R. Moutinho and Mowafak Al-Jassim
Materials Science Center, National Renewable Energy Laboratory, Golden, CO USA
*Nancy.Haegel@nrel.gov

Integration of near-field scanning optical microscopy (NSOM) with the imaging and localized excitation capabilities provided by incident electrons in a scanning electron microscope (SEM) offers new opportunities for the direct observation of spatially resolved energy transport. We utilize the flexibility inherent in the independent, high resolution placement of the electron beam, in combination with scanning of an NSOM tip, to enable unique types of dual-probe experiments. This "transport imaging" is related to, but different from standard cathodoluminescence, because it maintains the spatial information in the emitted light. One can "see" the transport of carriers and determine minority carrier or exciton diffusion lengths from a single image and map spatial variations in drift and diffusion behavior properties. While carrier transport has traditionally been considered as a limit to the spatial resolution of CL imaging, dual beam transport imaging allows us to exploit that behavior to directly visualize the combined influences of diffusion, drift, surface recombination and photon recycling on energy transport in luminescent materials, from the nano to the micron scale.

Figure 1 illustrates examples of transport imaging for minority electron diffusion in GaInAs (near-field), minority electron drift in GaAs (far-field) and combined carrier diffusion and photon waveguiding in a GaN nanowire (near-field). We will illustrate the power of this approach, and its ability to complement other e-beam techniques, with examples from solar cell materials (GaInP and GaAs) and nanostructures (GaN and ZnO) [1-3]. A new system is being developed at NREL to provide near-field transport imaging with a focus on solar cell and other energy-relevant materials. Initial results from near-field imaging near grain boundaries in CdTe will be presented as the technique expands to study localized recombination behavior in polycrystalline materials.

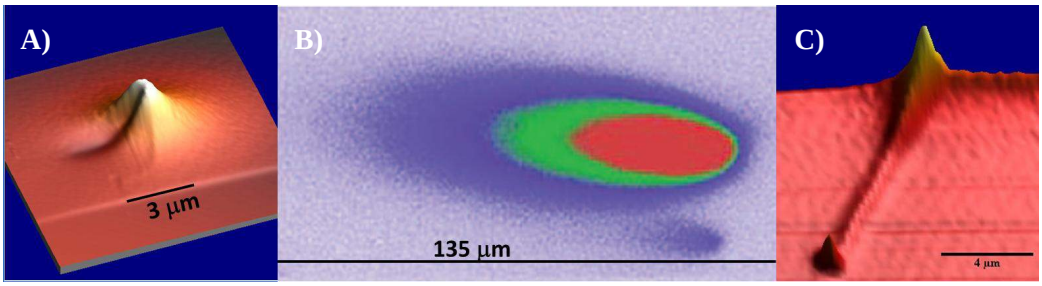

Figure 1: Examples of direct imaging of spatially resolved light emission from point source excitation illustrating (left to right) A) minority electron diffusion in GaInAs, B) minority electron drift in a GaAs double heterostructure (E ~ 520 V/cm) and C) carrier diffusion and photon waveguiding in a GaN nanowire. In all cases, the point of e-beam excitation is at or adjacent to the highest intensity emission (red in B).

[1] N. M. Haegel, T. Christian, C. Scandrett, A. G. Norman, A. Mascarenhas, Pronab Misra, Ting Liu, Arsen Sukiasyan, Evan Pickett and Homan Yuen, Appl. Phys. Lett.105, 202116 (2014).
[2] N. M. Haegel, Nanophotonics **3**, 75-89 (2014).
[3] L. Baird, C. P. Ong, R. A. Cole, N. M. Haegel, A. A. Talin, Qiming Li and George T. Wang, Appl. Phys. Lett. 98, 132104 (2011).

Beam injection techniques in the control and micropatterning of phase transitions in TiO_2 nanoparticles

G. C. Vásquez[1,] M. A. Peche-Herrero[2], D. Maestre[1], J. Ramírez-Castellanos[2],A. Cremades[1], J. M. González-Calbet[2] and J. Piqueras[1]
1Dpt. de Física de Materiales, Facultad de CC. Físicas, Universidad Complutense de Madrid, 28040, Spain.
2 Dpt. de Química Inorgánica I, Facultad de CC. Químicas, Universidad Complutense de Madrid, 28040, Madrid, Spain.
cremades@fis.ucm.es

The suitability of TiO_2 in different advanced applications is strongly dependent on the ability to control not only size, structure of defects and doping, but also on its crystallographic phase [1], as anatase is a metastable phase which transforms irreversibly into rutile with different properties and applicability.

In this work, anatase TiO_2 nanoparticles with average sizes around 5 nm have been doped during growth with Al or Fe up to 30 cationic per cent. The influence of Al and Fe doping in the structural and luminescent properties of anatase TiO_2 nanoparticles has been analyzed, with special attention focused on the effect of doping in the anatase-to-rutile transition (ART) induced by thermal annealing or local laser irradiation. The phase transition can be thermally-driven and it is either promoted or inhibited by Fe or Al doping, respectively, as measured by thermodiffraction. For Al doped samples the anatase phase has been stabilized up to temperatures above 900 °C [2], which increases significantly the working temperature of this metastable phase. In addition, the ART can be also controlled by laser irradiation and rutile or mixed anatase/rutile phases have been generated with micrometric resolution, thus performing micropatterning based on titania polymorphs [3]. Achieving a suitable control of the anatase to rutile phase transformation and micropatterning assures the spatial and quantitative on-demand design of mixed TiO_2 phases [4,5]. The results of this study provide relevant new insights that can help to explain the ART process, such as the influence of dopants (Al, Fe) in the kinetic of the ART, the key role played by the Ti-O bonding at the surface, the relevance of Ti^{3+} and oxygen deficiency, or the formation of rutile nucleation points at twinned regions.

The characterization of the samples have been carried out using different beam injection techniques such as x-ray diffraction (XRD), scanning electron microscopy (SEM), conventional and high resolution transmission electron microscopy (TEM, HRTEM), x-ray energy dispersive spectroscopy (EDS), cathodo- and photo-luminescence (CL and PL), Raman spectroscopy, XPS and x-ray absorption spectroscopy (XAS) at the Elettra Synchrotron.

[1] G. C. Vásquez, M.A. Peche-Herrero, D. Maestre, A. Cremades, J. Ramírez-Castellanos, J.M. González-Calbet, J. Piqueras. J. Phys. Chem. C **117**, 1941 (2013)
[2] G. Cristian Vásquez, M. Andrea Peche-Herrero, David Maestre, Belén Alemán, Julio Ramírez-Castellanos, Ana Cremades, José M. González-Calbet and Javier Piqueras, J. Mater. Chem. C **2**, 1037 (2014)
[3] G. Cristian Vásquez, M. Andrea Peche-Herrero , David Maestre, Alessandra Gianoncelli, Julio Ramírez-Castellanos, Ana Cremades, José María González-Calbet, and Javier Piqueras J. Phys. Chem. C **119** ,11965 (2015)
[4] OEPM Patent P201400722
[5] OEPM Patent P201400759

Cathodoluminescence study of photonic structures fabricated by dry etching on InP with InAsP quantum wells

A.Torres[1], V.Hortelano[1,2], J.Jimenez[1], J.P. Landesman[3], C.Frigeri[4], F.Pommereau[5]

[1]GdS Optronlab, Física Materia Condensada, Universidad de Valladolid, ed. i+d, Paseo de Belén 11, 47011 Valladolid, Spain
[2]Humboldt-Universität zu Berlin, Institut für Physik, Newtonstr. 15, D-12489 Berlin, Germany
[3]Institut de Physique de Rennes, CNRS-UMR 6251, Université Rennes 1, F-35042 Rennes, France
[4]CNR-IMEM Istituto, Parco area delle Scienze 37/A, 43010 Parma, Italy
[5]III-V Lab, Route de Nozay, F-91461 Marcoussis, France
*jimenez@fmc.uva.es

Dry etching is one of the main tools for the fabrication of photonic integrated circuits especially with compound semiconductors like GaAs or InP. The dry etching process can introduce defects, which can substantially modify the electro-optic properties of the devices (1-4). Therefore, the understanding of the defects introduced by the dry etching process is relevant for the control of the properties of photonic structures. Multilayer structures formed by a series of buried InAsP Quantum Wells (QWs) of different composition with InP spacers were etched by inductively coupled plasma (ICP) using Cl gases. Ridge waveguides of different dimensions (width and depth) were fabricated and studied by hyperspectral CL imaging. The CL measurements reveal significant changes in the QW emission as a consequence of the etching process. The CL spectra show a series of peaks corresponding to the emission of the different QWs, which the spectral features (intensity, peak wavelength and width) change depending on the etching conditions and the dimension of the waveguide structures. The initial strain conditions allowed providing a picture of the distribution of the defects generated by the etching process, showing differences between the etched floor, the sidewalls of the waveguides and the unetched top surface protected by the mask. The results are discussed in terms of the penetration of the etching species, more specifically chorine, which was estimated from micro SIMS measurements. Quantum confined Stark effect induced by the built in electric field and its modification by the etching process is also considered. The CL hyperspectral images in both top view and cross section permits to establish the distribution of residual stresses consequence of the etching, and also allow to determine the influence of the waveguide width and height in the distribution of the perturbation induced by the dry etching process. The possible mechanisms for defect formation, as well as the possible identity of the defects are discussed. The role of the diffusing species, mainly chlorine is considered in both the etched floor, and the lateral surface of the waveguides.

1)M.Avella, et al; Appl. Phys. Lett. 90, 223510 (2007)
2)M.Avella, et al; Appl. Phys. Lett. 93, 131913 (2008)
3)R.Chanson, et al.; J.Electron. Mater. 39, 688 (2010)
4)J.P. Landesman, et al; Microelectronics Reliability 55, 1750 (2015)

Tuesday June, 7 - Poster Session - TuP

16:00-18:00

Tuesday June, 7 - Poster Session - TuP-I

Cathodoluminescence

Cathodoluminescence Classification of Threading Dislocations in bulk GaN

T. Sekiguchi*, Y. Ohshima, Y. Cho, and X.J. Luo
National Institute for Materials Science, Tsukuba, Ibaraki 305-0044, Japan
* Sekiguchi.takashi@nims.go.jp

Not only optoelectronic applications, GaN is expected to be used for power devices. As for this application, the high quality GaN wafer is necessary to be developed because the crystal defects may suppress the performance of power devices and often cause the device failures. Thus, the characterization of extended defects becomes much more important.

Different from the heteroepitaxially grown GaN wafers, the bulk grown GaN includes several type of dislocations. Thus, the classification of dislocation is first importance. In this study, we have applied chemical etching technique and cathodoluminescence (CL) to distinguish dislocations. The etch pit patterns show slight difference according to the character of dislocations. Contrarily, using the as polished wafers, CL image of band edge emission is rather difficult to distinguish the dislocation character. However, we have found that the CL spectra show slight difference at certain dislocations in etched GaN wafers. Fig. 1 shows the CL image of band edge emission (a) and the 3-dimeisional outputs of the low energy shoulder of band edge emission (b, c). These two outputs clearly show the difference of shallow level distribution around dislocation probably due to the shallow impurity decoration.

In this presentation, we correlate the dislocation character and the characteristic CL features. The goal of this study is to distinguish the killer defects of power devices in GaN.

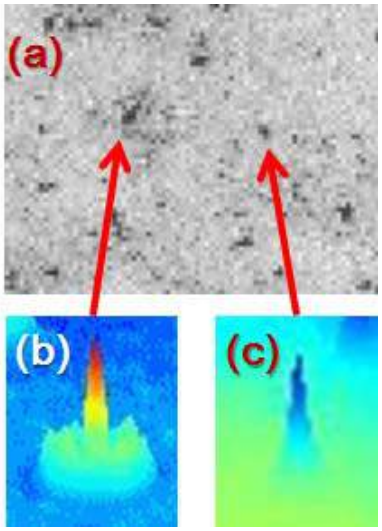

Fig. 1. CL image of band edge emission (a) and the 3-dimeisional outputs of the low energy shoulder of band edge emission (b, c) in etched GaN wafer.

Quantum dot-like emission from branched InGaN quantum discs in GaN nanowires

D. Stowe[1], B. Lassiter[1], K. Scudder[1], A. Howkins[2], D. Anjum[3], A. Prabaswara[3], B. Ooi[3]
[1]Gatan Inc., 25 Nuffield Way, Abingdon, Oxon., UK
[2]ETC, Brunel University, Uxbridge, London, UK
[3]KAUST, Jeddah, Saudi Arabia
*dstowe@gatan.com

Nanowires based on III-nitride semiconductors have significant potential in optoelectronic and energy storage applications. However, in order to realize the full potential of these materials characterization and correlation of individual nanowire (NW) morphology, microstructure, composition and optical and electronic properties is required. This has been enabled by the recent development of cathodoluminescence (CL) detectors suitable for (scanning) transmission electron microscopes (STEM) where the thin sample and high energy electron beam enable luminescence information to be gathered at a spatial resolution approaching 1 nm [1-3].

Cathodoluminescence performed in the STEM was used to analyze the anomalous emission from InGaN quantum discs inside GaN nanowires. Photoluminescence measurements revealed strong emission at the expected wavelength of 540 nm, however, an additional emission band at 430 – 460 nm was observed at liquid-nitrogen temperatures. CL spectrum-imaging performed at 100 K revealed that the low temperature emission band was due to quantum dot-like emission at sites where a single quantum disc branched into two arms; analysis of individual NWs revealed intense, narrow emission lines (FWHM <5 nm) associated with the center of the branching site. The central wavelength of the quantum dot-like emission was found to vary continuously (± 15 nm) between NWs that contained such branching defects explaining why a broad emission peak was observed when a non-spatially localized excitation source was used (PL or CL with a scanned probe).

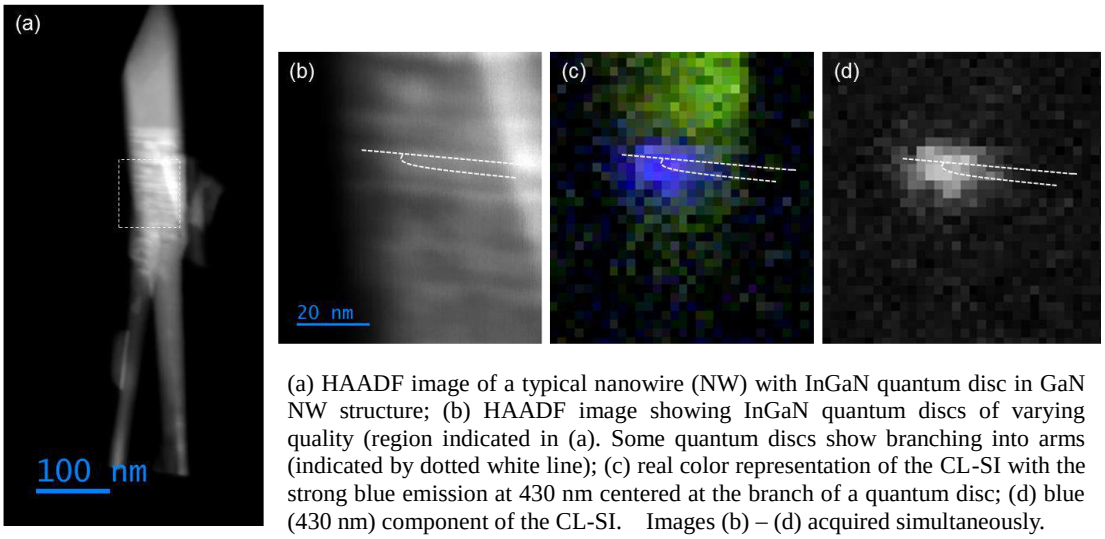

(a) HAADF image of a typical nanowire (NW) with InGaN quantum disc in GaN NW structure; (b) HAADF image showing InGaN quantum discs of varying quality (region indicated in (a). Some quantum discs show branching into arms (indicated by dotted white line); (c) real color representation of the CL-SI with the strong blue emission at 430 nm centered at the branch of a quantum disc; (d) blue (430 nm) component of the CL-SI. Images (b) – (d) acquired simultaneously.

[1] Kim S. K., Brewster M., Qian F., Li Y., Lieber C. M. and Gradecak S., Nanoletters 9, 3940, 2009
[2] Zagonel L. F., Mazzucco S., Tence M., March K., Bernard R., Laslier B., Jacopin G., Tchernycheva M., Rigutti L., Julien F. H., Songmuang R. and Kociak M., Nanoletters 11 (2011) p568
[3] Stowe D.J., Microscopy and Microanalysis 19, (2013)

Effects of the Recombination Velocity on the Cathodoluminescence of a Semiconductor Nanowire

A. Lahreche[1,2], Y.Beggah[1], and R-J.Tarento[3]*
[1]Physics Department, Jijel University, Jijel, Algeria
[2]Faculty of Technology, A.Mira University, Bejaia, Algeria
[3]Laboratoire de Physique des Solides ,UMR8502 Université de Paris Sud , Orsay, France
*tarento@lps.u-psud.fr

The cathodoluminescence signal of a semiconductor nanowire is modelled taking into account the recombination velocity which has a value Vr on the curved lateral surface of the cylinder or Vs at the top basis.

The distribution of charge carrier is governed by the continuity equation. For n-type semiconductor, the following equation has to be solved.

$$D\left(\frac{1}{r}\frac{\partial}{\partial r}(r.\frac{\partial p(r,\theta,z)}{\partial r})+\frac{\partial^2 p(r,\theta,z)}{\partial z^2}\right)-\frac{1}{\tau}p=-g(r,z)$$

g(r,z) is the generation rate of minority carriers, Ű is the life time and D is the diffusion coefficient. The boundary conditions are:

$$D\frac{\partial p}{\partial z}=v_s\,p(r,z)\ \text{at}\ \ z=0$$

$$p=0\ \text{at}\ \ z=h$$

$$D\frac{\partial p(r,z)}{\partial r}=v_r\,p(r,z)\ \text{at}\ r=r_a$$

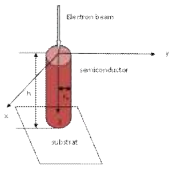

The minority carrier concentration p(r,ɗ,z) is obtained with the Green function technics. In the present study, we assume a uniform generation sphere of radius R centered on the nanowire axis The carrier distribution yielded by the incident electron beam is investigated versus the shape of the nanowire (the length h and the radius Ra) and the semiconductor parameters (the recombination velocity Vs and Vr, the diffusion length L é .).

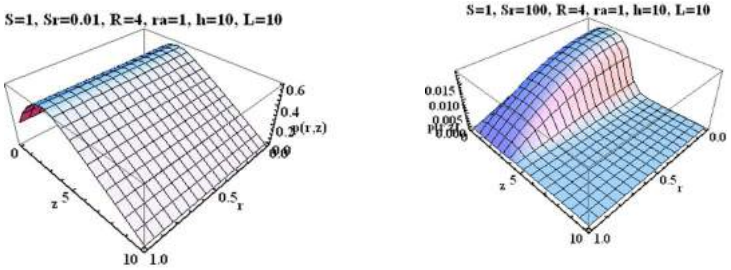

Minority carrier concentration in the nanowire for different parameters

The final part deals with the catholuminescence intensity versus the nanowire, semiconductor and generation characteristics.

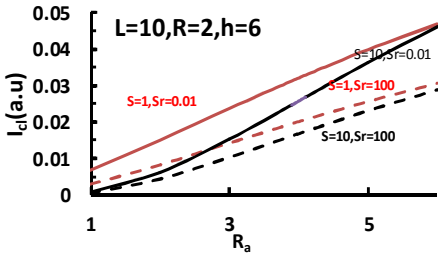

Fig. Effect of the recombination velocity on the cathodoluminescence dependence versus the nanowire radius.

Cathodoluminescence mapping on cross-sectional epitaxial GaN grown on Si-based substrates and TEM/CL correlation

L. Piot [1], N. Mante [1], N. Rochat [1], G. Feuillet [1], P. Vennégues [2], F. Semond [2], E. Frayssinet [2]
[1] Univ. Grenoble Alpes, F-38000 Grenoble, France,
CEA, LETI, MINATEC Campus, F38054 Grenoble, France
[2] CRHEA-CNRS, Rue Bernard Gregory, 06560 VALBONNE, France
*nevine.rochat@cea.fr

Gallium nitride is a widely used material in optoelectronic devices like LEDs. The LED structures are mostly grown by epitaxy onto sapphire substrates, but, for cost reasons, silicon is a possible contender. Nevertheless, the large misfit and the difference in coefficient of thermal expansion between silicon and the nitrides lead to numerous dislocations and possible cracks during cooling down from the growth temperature, both being detrimental for LED applications. The samples of this study are grown by MOVPE and MBE on Si-based substrate in CRHEA-CNRS.

The cathodoluminescence (CL) technique constitutes a fast and highly relevant way to investigate the above material properties. Indeed, besides the distribution of dislocations can be visualized due to their higher rate of non-radiative recombination, emission lines give us an access to several punctual defects identification as well as variation of strain, doping, growth direction and carrier concentrations.

In this work, we performed low temperature high spatial resolution cathodoluminescence by hyperspectral imaging on lamellas prepared by tripod polishing. The cross-sectional imaging on the GaN layers gives us an insight into the thickness of the samples and provides direct information on interfaces roles as the growth proceeds. Development of an innovative cryogenic sample holder compatible with both CL and TEM equipment allowed us to couple cathodoluminescence and TEM diffraction on the same sample. This method allows the correlation between optical properties and structural information such as strain determined from TEM contrast analysis together with nano-diffraction. Such fine characterization is a chance to improve nitride layers quality for LED applications.

Acknowledgments: This work was supported by the National Research Agency (ANR) through the French "Recherche Technologique de Base" Program, and CL experiments were performed in the frame of the joint development program with Attolight and the Nanocharacterisation platform (PFNC) at MINATEC.

Tuesday June, 7 - Poster Session - TuP-II

Nano-materials

Sn-catalyzed silica and alumina nanowires and their optical properties

N. Jeong*, Soon-cheol Park, Moon-seog Jang
Jeju Global Research Center, Korea Institute of Energy Research, Jeju, Republic of Korea
*njjeong@kier.re.kr

One-dimensional (1D) nanostructures such as wires, tubes, and belts have drawn tremendous interest because of their unique properties and numerous potential applications.[1] Among many possible production methods, catalyst-assisted growth is one of the most powerful for the synthesis of various kinds of 1D nanostructures, notably of carbon, semiconductor, and oxide materials.[2] In this approach, the nanowires form mostly via vapor-liquid-solid (VLS) growth,[3] in which the catalyst particles provide effective active sites, absorbing gas-phase reactants and facilitating their diffusion for nanowire growth once supersaturated. Therefore, the diameter, morphology and structural properties of the nanowires strongly depend on the chemical and physical state and properties of the catalysts. Also, the direct fabrication of macroscopic arrangements of such 1D nanostructures, which is essential for practical applications, is a challenge that has yet to be met.

Herein, we report the growth of alumina and silica nanowires and their optical properties. Our work focuses on the catalytic synthesis of the nanowires on commercial substrates, namely porous discs, foams, and monoliths, using Sn particles in a very simple method that facilitates both large-scale and substrate-independent nanowire growth. In particular, we characterize the growth mechanism of these nanowires experimentally and highlight the key role of the Sn catalysts in the branching, amalgamation, and packing of the nanowires. Finally, we investigate their light emitting properties through cathodoluminescence studies.

[1] Y. Xia, P. Yang, Y. Sun, Y. Wu, B. Mayers, B. Gates, Y. Yin, F. Kim, H. Yan, Adv. Mater., **15**, 353 (2003).
[2] V. Jourdain, C. Bichara, Carbon, 58, 2 (2013).
[3] R.S. Wagner, W.C. Ellis, Appl. Phys. Lett., 4, 89 (1964).

Structural and optical properties of TM doped ZnO elaborated by ultrasonic spray paralysis method

B. Kharroubi[1]*, B. Mohamed[1], A. Bezzerrouk[1], , A. Zeinert[2], M. El Marsi[2], and R.Baghdad[1]

[1]LGP, Departement of Physics, Ibn Khaldoun University-Tiaret-Algeria

[2]LPMC, Faculty of Sciences, Picardie Jules Verne University, Amiens, France

*E-mail bachir.kharroubi@gmail.com

Diluted magnetic semiconductors (DMSs) based on ZnO have recently been attracting much attention, because transition metal (TM) doped ZnO DMSs exhibit ferromagnetism at room temperature (RT) in contrast to those based on III– V semiconductors such as GaAs and InAs,

A detailed investigation on the effect of the Cobalt and Mn doping on the structural and optical properties of zinc oxide thin films deposited by ultrasonic spray pyrolysis for eventual applications as DMS materials

Co and Mn-doped ZnO nanostructured thin films with doping levels (0, 1,3,5, 7, 9, 11, 13 at%) and Ts = 350°C; were synthesized via ultrasonic spray pyrolysis method under atmospheric pressure, To study the properties of the films we have used to do several characterisations this non expensive and simple technique is very flexible to adjust the doping level in the films with good and controlled way confirmed by the EDAX characterisations, the structure of the as-prepared samples was characterized by Raman spectroscopy and Fourier Transform infrared spectroscopy (FTIR). Compared with the Raman spectra for ZnO pure films, the Mn-doping effect on the spectra is revealed by the presence of two additional peaks around 235 and 538 cm-1 due to Co incorporation. These results show that cobalt ions, in the oxidation state of Co2+, replace Zn2+ ions into the ZnO lattice without changing its wurtzite structure. The optical properties of the samples were studied by ultra-violet visible near infrared (UV-VIS-NIR) spectroscopy.

Electron beam modification and patterning of 2D hexagonal boron nitride.

C. J. Lobo[1*], C. Elbadawi[1], I. Aharonovich[1] and M. Toth[1]
[1]School of Mathematical and Physical Sciences, University of Technology Sydney, Ultimo, New South Wales 2007, Australia
[*]charlene.lobo@uts.edu.au

Group III-nitrides incorporate a wide range of materials with numerous applications in high performance electronics and optoelectronics. In particular, the two-dimensional (2D) material hexagonal boron nitride (hBN) has recently attracted considerable interest as a polaritonic and hyperbolic metamaterial[1]. Here, we demonstrate high resolution etching of hBN mono- and multilayers using electron beam irradiation in a background atmosphere of water vapour. ThehBN undergoes denitrogenation under electron beam induced etching in H_2O, forming volatile NO and NO_2 and leaving behind Boron nanoparticles. Under continued irradiation, the dissociated H_2O molecules react with NO and NO_2 species to produce nitric acid, which etches the deposited boron nanoparticles[2],resulting in highly localized, clean etching of the hBN (Fig. 1a). Raman analysis demonstrates that the surrounding hBN material is not damaged by the etch process (Fig 1b), enabling damage-free electron beam fabrication of well-defined hBNnanoribbons, holes and other geometries.

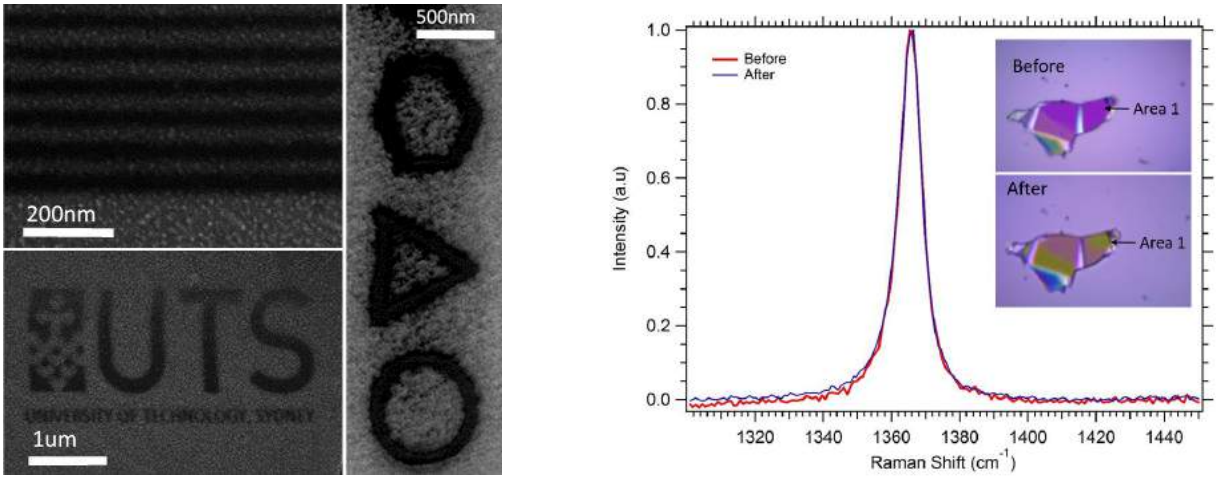

Figure 1. (a) High resolution etch patterns in hBN sheets, (b) Raman spectrum of the surrounding region.

(1) Caldwell, J. D., Kretinin, A. V., Chen, Y., Giannini, V., Fogler, M. M.*et al* Sub-diffractional volume-confined polaritons in the natural hyperbolic material hexagonal boron nitride *Nat Comms***2014**, *5*, 5221.

(2) Liao, Y., Tu, K., Han, X., Hu, L., Connell, J. W.*et al* Oxidative Etching of Hexagonal Boron Nitride Toward Nanosheets with Defined Edges and Holes *Scientific Reports***2015**, *5*, 14510.

Experimental Investigations on the Physical Properties of Tin Doped Indium Oxide Thin Films

H. Gueddaoui[1], H. Zerrouki[1], B. Sebboua[1] and A. Elyossoufi[1]
[1] LMSOM Laboratory of Physics Faculty, USTHB University, Algiers, Algeria
*hgueddaoui@yahoo.fr

Multi-layered tin indium doped oxide (ITO) films were deposited onto glass substrates by sol-gel spin coating process. The number of deposited layers was optimized in order to decrease the reflectance and to improve the optical transmittance in the visible range

Films properties were analysed with X-ray diffraction, optical and electrical measurements were also performed. A systematic investigation on the physical properties of ITO films was reported with respect to the number of deposited layers. Structural characterisation showed that obtained films were crystallized in cubic phases with 9–10 nm crystallite size and the determined lattice constant was nearly 10,1 Å, with orientation along the (222),(400), and(110) planes for all deposited films indicating stable cubic phase as reported in [1, 2].

Optical analysis of ITO showed high transparency and low reflectance in the visible range. The energy band gap of the multi-layered films as determined from absorption spectrum was ~ 3.7eV. The Drude-Lorentz classical model has been also used to fit the optical reflectance and transmittance.

Electrical measurements showed a clear dependence between sheet resistance and the deposited layers, the sheet resistance decreased from 114.5 MΩ to 4.35 MΩ for respectively 1 and 5 deposited layers.

[1] F. Davoine, P. A. Galione, J. R. R. Barrado, D. Leinen, F. Marin, E. A. Dalchiede, and R. E. Marotti, Solar Energy **91**, 316 (2013) .
[2] J. Hotovy, J. Hupkes, W. Bottler, E. Marins, L. Spiess, T. Kups, V. Smirnov, I. Hotovy, and J. Kovac, Appl Sur Sci **269**, 81 (2013) .

Annealing Effects on Silicon Oxy-Nitride Thin Films: Optical, Structural and Morphological Properties

M. Perani[1], N. Brinkmann[2], A. Hammud[2], B. Terheiden[2], D. Cavalcoli[1*]
[1]Physics and Astronomy Department, University of Bologna, Bologna, Italy
[2]Physics Department, University of Konstanz, Konstanz, Germany
*daniela.cavalcoli@unibo.it

Photovoltaic (PV) technology is nowadays an essential answer to the request of providing alternatives to fossil fuels: PV is easily available, it can be integrated with buildings and presents limited environmental issues [1]. Silicon Oxy-Nitride (SiO_xN_y) thin films have been investigated in view of the application in thin-film as well as in wafer based silicon solar cells, like Silicon HeteroJunction (SHJ). The optical and electronic properties, the composition and structure of the film have been investigated to gain a deep understanding of SiO_xN_y [2]. In addition, the role of deposition conditions and precursor gas concentrations on these properties have been clarified.

SiO_xN_y thin films have been deposited by Plasma Enhanced Chemical Vapor Deposition (PECVD) and subsequently annealed in order to increase the silicon crystallized fraction of the layers. The formation of nanocrystals have been studied through structural, compositional and optical methods. The characterization techniques used are Fourier transform infra-red, Raman and energy dispersive X-ray (EDX) spectroscopy. The morphology of the layers have been investigated using quantitative Atomic Force Microscopy (AFM) studies [3]. The influence of annealing time and the N_2O dilution ratio during PECVD deposition on the properties of the layers (such as silicon crystallized fraction) have been investigated.

During the annealing process, the material undergoes a phase transition from a homogeneously distributed material in terms of Si-Si and Si-O-Si bonds towards a two phase material consisting of Si-rich and O-rich clusters. Moreover, the Si crystallized fraction increases upon annealing and an enhancement of the dark conductivity is observed. The increase of N_2O dilution during PECVD deposition causes an enhancement of crystal disorder, revealed through a decrease of the Si crystallized fraction and an evolution of the surface morphology of the layers, with an increase of the lateral correlation length.

The layers exhibit interesting properties for the application in the field of SHJ solar cells. In particular, an optical band gap E_{Tauc} of (2.5 ± 0.1) eV, as well as very high dark conductivity of σ_{dark} of (44 ± 4) S/cm have been observed for the layer with higher crystallized fraction (88 ± 2)%, annealed for three hours.

[1] Q. Schiermeier, J. Tollefson, T. Scully, A. Witze, O. Morton, Nature **454**, 816 (2008).
[2] M. Perani, N. Brinkmann, A. Hammud, D. Cavalcoli, B. Terheiden, J. Phys. Chem. C **119**, 13907 (2015).
[3] M. Perani, S. Carapezzi, G.R. Mutta, D. Cavalcoli, Nanostructured surfaces investigated by quantitative morphological studies, submitted.

Structural and Photoluminescence Properties of Silicon Nanocrystals Embedded in SiN_x Matrix Prepared by Plasma Enhanced Chemical Vapor Deposition

S. Meziani*[1], A. Moussi[1], L. Mahiou[1], M. Mebarki[1], K. Djelloul[1], R. Outemzabet[2].

[1]CRTSE, Division Développement des Dispositifs de Conversion à Semi-conducteurs. 2, Bd Frantz Fanon, BP 140 Alger 7- Merveilles 16038, Algérie.

[2]Laboratoire des semi-conducteurs et oxydes métalliques, Université des Sciences et de la Technologie Houari Boumediene. BP 32 El Alia, Bab Ezzouar. Alger. Algérie.

mezianisamir@crtse.dz

Abstract

The effects of the annealing temperature on photoluminescence (PL) of non-stoichiometric silicon nitride(SiN_x) thin films deposited by plasma enhanced chemical vapor deposition (PECVD) using ammonia and silane mixtures at 380 °C were investigated. The optical property and the chemical composition of the films annealed at different temperatures were investigated by Photoluminescence (PL) spectroscopy and Fourier transform infrared absorption spectroscopy (FTIR), respectively. Based on the PL results and the analyses of the bonding configurations of the films, the light emission is attributed to the quantum confinement effect of the carriers inside silicon nanocrystals (Si-NC) and radiative defect-related states. The evolution of Si nanocrystals from amorphous to crystalline ones during high temperature treatment was examined by Raman scattering (RS) spectroscopy and X-Ray Diffraction (XRD). The amorphous Si clusters were already revealed in as-deposited SiN_x while the annealing results in their crystallization. These results provide a better understanding of optical properties of Si-NC embedded in silicon nitride films and are useful for the application of 3rd generation solar cells.

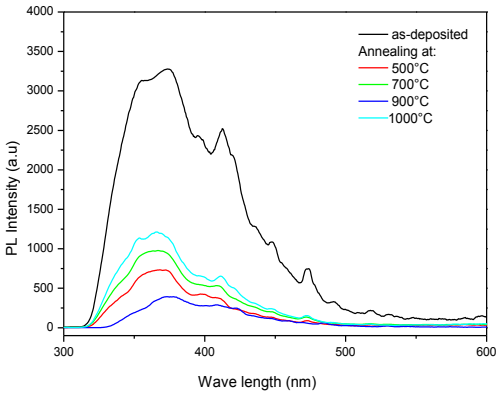

Fig. 1: PL spectra of Si-NC in SiN_x films, annealed at 500°C, 700°C, 900 and 1000°C.

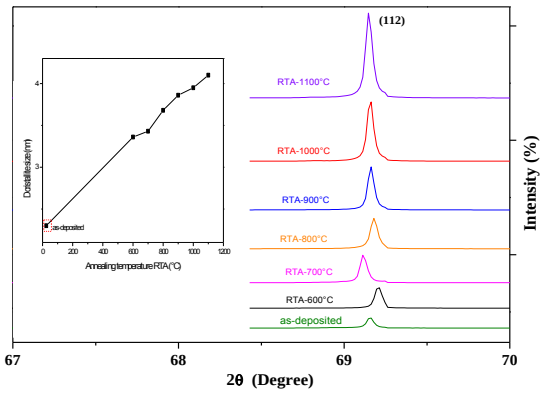

Fig. 2: XRD patterns for samples as deposited and annealed at different RTA for 50s. Figure inset show the evolution of Si-NC size with annealing temperature.

Strain-Assisted Self-Assembling of Graphene-like Nanoflakes in Si/SiGe/Si Layers

P.I.Gaiduk
Department of Physical Electronics and Nanotechnology, BSU, Minsk, Belarus
gaiduk@bsu.by

We report on the segregation of carbon atoms and structural transformations in strained multilayered Si/SiGe/Si structures after molecular-beam epitaxial (MBE) growth, carbon ion implantation and thermal treatment at different conditions. The idea behind this study is that due to their specific strain distribution, layers of Si/SiGe promote spatial separation of vacancies and interstitials, and segregation of foreign dopant atoms. If the dopant has a low solubility in Si (like carbon) and the dopant concentration is high, then there is a tendency for dopant precipitation near the strained regions and around structural defects.

High temperature ion implantation was used for injection of carbon atoms as well as point defect generation in the strained layers. The defects were investigated by transmission electron microscopy (TEM), dopant depth profiles by secondary-ion-mass spectrometry (SIMS), and optical properties by Raman scattering measurements. Based on SIMS data we will demonstrate that the redistribution of the implanted carbon atoms around the strained SiGe/Si layers results in carbon accumulation on the Si side and reduction on the SiGe side. The TEM study demonstrates formation of plate-like defects, stacking faults and thin carbon-precipitated flakes distributed along the Si/SiGe interfaces. Raman spectra reveal peaks at 1600 and 2700 cm^{-1} which might be associated with carbon-related phases. We will then demonstrate that the phase and structural state of the carbon precipitates depend on the configuration of the strain field. The concept of strain-enhanced separation of point defects and dopants will be discussed.

Electrodeposition ofMoS_2 and WS_2 Thin Filmsfor Photovoltaic Application

Md. Anower Hossain[1, 2]*, Belabbes A. Merzougui[1, 2], Abdelhak Belaidi[1, 2],Fahhad Hussain Al Harbi[1, 2], and Nouar Tabet[1, 2]*
[1]Qatar Environment and Energy Research Institute, Doha,Qatar
[2]Hamad Bin Khalifa University, Doha, Qatar
*E-mail: mdhossain@qf.org.qa, ntabet@qf.org.qa

Abstract.

Transition-metaldichalcogenides, such as molybdenum disulfide (MoS_2), and tungsten disulfide (WS_2) have shown much attention recently due to their unprecedented electronic characteristics, *i.e.*, high carrier mobility of >200 $cm^2V^{-1}S^{-1}$, suitable direct and indirect band gap energies of ~1.8eV, and ~1.3 eV, respectively, and high light absorption coefficient which are much beneficial for the photovoltaic application [1-3].In addition, these materials are abundant in earth's crust, cheaper, environmentally friendly, and have suppressed dangling bonds because of layered structure [4].However, only two-dimensionalMoS_2 and WS_2 layers have been investigated as absorber in solar cells, which are capable of absorbing around 10% of the incident light, implying a huge transmission loss. Therefore, we report here thegrowth of the MoS_2 and WS_2 bulk materials onto conducting FTO, Mo, and W substrates by electrodepositionapproach for fabrication of the Schottky-barrier solar cells.The as-deposited and post-treated MoS_2 and WS_2 materials characterized by XRD, SEM, UV-vis, Raman, Photoluminescence, *etc.*, will be presented. All the stack materials are optimized to obtain optimum electronic properties for fabricating high efficiency solar cells both in substrate and superstrate configurations.

References.

[1]. M.-L. Tsai, S.-H. Su, J.-K. Chang, D.-S. Tsai, C.-H. Chen, C.-I. Wu, L.-J. Li, L.-J. Chen and J.-H. He, *ACS Nano*, 2014, **8**, 8317-8322.

[2]. M. Chhowalla, H. S. Shin, G. Eda, L.-J. Li, K. P. Loh and H. Zhang, *Nat Chem*, 2013, **5**, 263-275.

[3]. Q. H. Wang, K. Kalantar-Zadeh, A. Kis, J. N. Coleman and M. S. Strano, *Nat Nano*, 2012, **7**, 699-712.

[4]. J. Pu, Y. Yomogida, K.-K. Liu, L.-J. Li, Y. Iwasa and T. Takenobu, *Nano Letters*, 2012, **12**, 4013-4017.

Microstructural Properties of ZnO Powder Nanostructures Prepared by Mechanical Alloying

Oudjertli Salah [1,*], Bensalem Rachid [1], Alleg Safia[2], J. J. Suñol[3], Mohamed Bououdina [4], Miloud Ibrir[5]

[1]Laboratoire des Nanomateriaux- Corrosion et Traitements de Surfaces, Département de Physique
Université de Annaba B. P. 12 (23000) Algeria.
[2]Laboratoire de Magnétisme et Spectroscopie des Solides, Département de Physique
Université de Annaba B. P. 12 (23000) Algeria.
[3]Dep. de Fisica, Universitat de Girona, Campus Montilivi, Girona 17071, Spain
[4] Nanotechnology Centre, University of Bahrain, P.O. Box 32038, Kingdom of Bahrain.
[5] Dép. de Biologie, Faculté des Sciences, Université de M'Sila, B.P. 166, 28000 M'Sila, Algérie
[*] E-mail: salah.oudjertli@gmail.com

INTRODUCTION

The wide bandgap semiconductors (ZnO) have been studied for several years in a highly competitive international environment given their wide range of applications. In our work we prepared powder nanoparticles mechanically alloyed .

EXPERIMENTAL/THEORETICAL STUDY

ZnO powder nanoparticles mechanically alloyed were doped with iron to investigate their structural and microstructural properties using X-ray diffraction (XRD) , scaning electron microscopy (SEM) [1,2] and differential scanning calorimetry (DSC) for examined pur ZnO and 5% Fe doped ZnO.

RESULTS AND DISCUSSION

The ZnO starting pure powder exhibited a hexagonal crystal structure with space group p63mc of ZnO, however with the introduction of 5%Fe in the ZnO milled powder, the hexagonal ZnO phase remained unchanged, whereas the microstructural parameters were subject to significant variations due to the introduction of Fe atoms into the ZnO hexagonal matrix to replace oxygen ones [3]. The size of crystallites and microstrains are found milling time dependent.

CONCLUSION

This product exhibited a hexagonal crystal structure with space group p63mc of ZnO and with c-axis preferential orientation, however with the introduction of 5 % Fe in the ZnO milled powder, the hexagonal ZnO phase remained unchanged,whereas the microstructural properties were subject to significant variations due to the introduction of Fe atoms into the ZnO hexagonal matrix to replace oxygen ones.

REFERENCES

[1] B. Weintraub, Z. Zhou, Y. Li, and Y. Deng, "Solution synthesis of one-dimensional ZnO nanomaterials and their applications," *Nanoscale*, vol. 2, no. 9, pp. 1573-1587, 2010.
[2]Look, D.C. (2006) 'Progress in ZnO materials and devices', Journal of Electronic Materials Vol. 35, pp. 1299-1305.
[3]S Q. B. Ma, Z. Z. Ye, H. P. He, L.P. Zhu, J.Y. Huang, Y. Z. Zhang and B. H. Zhao, Scripta Materialia.vol. 58 21-24, 2008.

Tuesday June, 7 - Poster Session - TuP-III

EBIC & light injection

Investigation of GaN Nanowires containing AlN/GaN Multiple Quantum Discs

V. Piazza[1*], A. Babichev[2], N. Guan[1], M. Morassi[1], V. Neplokh[1], P. Quach[1], F. Bayle[1], L. Largeau[3], F.H. Julien[1], J.-C. Harmand[3], N. Gogneau[3], M. Tchernycheva[1]

[1] Institut d'Electronique Fondamentale, Université Paris Sud XI, 91405 Orsay Cedex, France
[2] St. Petersburg Academic University, Nanotechnology Research and Education Centre, Russian Academy of Science, Khlopina 8/3, 194021 St. Petersburg, Russia
[3]Laboratoire de Photonique et Nanostructure-CNRS, Route de Nozay, 91460 Marcoussis, France
*e-mail: valerio.piazza@u-psud.fr

In this work we investigate single GaN nanowires with GaN/AlN multiple quantum discs (MQDs) insertion using electron beam induced current (EBIC) microscopy. The structures were grown by plasma-assisted molecular beam epitaxy (PAMBE) on Si (111) substrate with a thin AlN layer, consisting of an n-GaN base with a thin AlN external shell, of an active region with 20 periods of 0.6 nm GaN discs / 6 nm Al barriers and of an n-GaN cap, as confirmed by SEM and TEM. Single NWs were dispersed on Si/SiO_2 substrates with alignment marks and contacted using electron beam lithography and Ti/Au metallization. Structural results were used to build a band gap-vs-position simulation with NextNano© software which showed the presence of a triangular confining potential well at the AlN/n-GaN interface (similar to the 2D electron gas in HEMT transistors induced by the polarization discontinuity between AlN and GaN). The position of this potential well is different from the thin film case since the nanowires exhibit N polarity instead of Ga-polarity [1].

To investigate experimentally the band gap profile, EBIC mapping was used since, being a charge collection microscopy technique, it allowed the detection of peculiar band gap features within the wire [2] (such as for example the electron accumulation region at AlN/n-GaN interface). A bias ranging from -4 V to 4V was applied to study the evolution of EBIC signal and of parameters such as doping level and diffusion length.

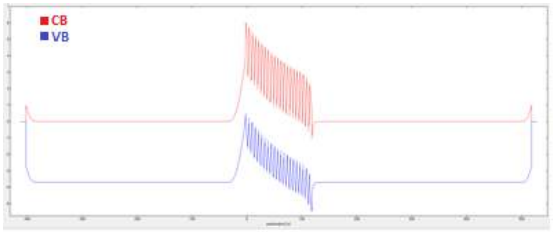

Figure 1 Band profile performed with NextNano© software, showing the confining potential well at the AlN/n-GaN interface.

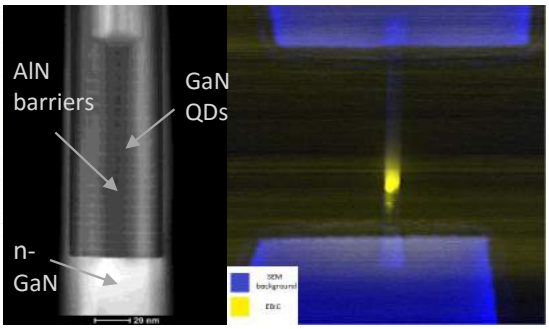

Figure 2 On the left, TEM image showing the internal nanowire structure; on the right, EBIC map (in yellow) overlapped with SEM image (in blue), showing the signal coming from the MQDs region.

[1] Sergei Lopatin, Florian Furtmayr, Carlos J. Fernández-Rojas, Bo Peng, Joan Ramon Morante, Riccardo Rurali, Martin Eickhoff, Anna Fontcuberta i Morral, Qihua Xiong, and Jordi Arbiol, Nano Lett., **12**, 2579−2586 (2012).
[2] Jian Xiong Wang, Vladimir Neplokh, Maria Tchernycheva, Joaquim Nassar, Pere Roca i Cabarrocas, and Rusli,, J. Phys. Chem. C, **120**, 2962−297 (2016).

EBIC Investigation of Dislocation Loops in $SrTiO_3$

J. Chen[1,*], S. Ito[2], J. Y. Li[3], X. J. Luo[1], T. Sekiguchi[1]
[1]National Institute for Materials Science, Tsukuba 305-0044, Japan
[2]Institute for Materials Research, Tohoku University, Sendai 980-8577, Japan
[3]Fukushima Renewable Energy Institute, Koriyama 963-0215, Japan
*CHEN.Jun@nims.go.jp

Niobium doped strontium titanate ($SrTiO_3$:Nb) has now been focused on resistance switching. It was reported that the motion of oxygen vacancies along dislocations may account for the resistance switching. [1] On the other hand, the electron-occupation kinetics at defects inside the depletion layer were also considered to affect switching phenomena.[2] Recently, we found that dislocations in Nb-doped $SrTiO_3$ were associated with different energy levels depending on their characters, and some dislocations may affect the resistance switching.[3]

In this study, we will report interesting EBIC behaviors of dislocation loops. Figure 1 shows two EBIC images of dislocation loops at fresh state (a) and after electron beam scanning for a few minutes (b). At first, bright contrast was observed inside loops. It should be noted that the loops themselves still have weak dark contrast. During the acquisition of EBIC images, strong dark loops became visible and their contrast increased with the acquisition time. Experimental and theoretical studies have revealed that dislocations in $SrTiO_3$ tend to be oxygen-deficient.[4] The initial bright contrast is probably halo pattern due to the gettering of oxygen vacancies by dislocation loops. The dark contrast appeared later shows the presence of recombination centers at dislocation loops. It is suggested that e-beam irradiation may introduce deeper defect levels. Our study indicates that dislocation loops may also contribute to the resistive switching phenomena.

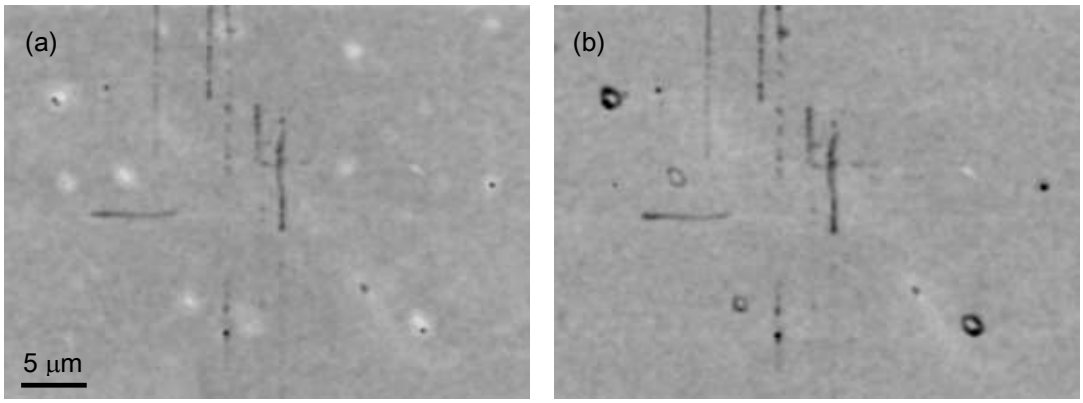

Figure 1. EBIC images of dislocations in (100) $SrTiO_3$ at initial state (a) and after electron beam scanning (b). Bright contrast was observed inside dislocation loop at initial state, while dark loops became visible after e-beam irradiation.

[1] K. Szot, W. Speier, G. Bihlmayer, and R. Waser, Nature Materials **5**, 312 (2006);
[2] J. Y. Li, N. Ohashi, H. Okushi, and H. Haneda, Phys. Rev. B **83**, 125317 (2011);
[3] J. Chen, T. Sekiguchi, J. Y. Li, S. Ito, W. Yi, and A. Ogura, Appl. Phys. Lett. **106**, 102109 (2015).
[4] D. Marrocchelli, L. Sun, and B. Yildiz, J. Am. Chem.Soc. **137**, 4735 (2015).

Prediction of Betavoltaic Battery Output Parameters Based on SEM Measurements

E.B. Yakimov
Institute of Microelectronics Technology RAS, Chernogolovka, Russia
National University of Science and Technology MISiS, Moscow, Russia
yakimov@iptm.ru

In betavoltaic batteries a nuclear radiation energy is directly converted to electric power using a semiconductor convertor. For a successful design and optimization of effective converters methods for their testing and output parameters prediction should be developed. A good idea is to use for this purpose e-beam of SEM, which could imitate beta radiation. However, as our Monte Carlo simulation have shown, the depth-dose dependence for beta particles emitted from radioisotope ^{63}Ni of finite thickness decays approximately exponentially with a depth and thus it differs qualitatively from that for monoenergetic electron beam. Therefore beta-irradiation cannot be directly imitated with SEM by a choice of one or a few beam energies.

A different approach is proposed here for a prediction of betavoltaic battery output parameters. This approach to the problem is based on a calculation of current induced in the semiconductor converter by beta-irradiation and consists of three parts: (1) a Monte Carlo simulation that predicts the depth dependence of excess carrier generation rate inside the semiconductor converter, (2) a determination of collection probability based on the electron beam induced current (EBIC) measurements and a calculation of induced current, and, (3) SEM measurements of output parameters using the calculated induced current value.

The home-made Monte Carlo program was used, the calculation algorithm being specially adapted for the fast simulation of multilayer structures. The structure simulated consists of two principal layers: a thick semiconductor structure and the radioisotope Ni layer (the beta particle source), whose thickness can be varied. In turn, the semiconductor structure consists of one or a few layers, i.e. it can include upper metallization and/or passivation layers. The electron trajectories were assumed to start uniformly over the Ni layer thickness and isotropically along the electron emission direction. For the initial electron energy the spectrum of beta particles for ^{63}Ni is used. It should be stressed that such simulation allows to calculate directly the energy losses in the depth of the semiconductor for any source thickness and specific activity. The electron-hole (e-h) pair generated rate dependences on a depth is obtained from the energy losses using the average energy E_i necessary for the e-h pair creation.

The induced in the semiconductor converter current can be calculated as a convolution of the generation function with the collection probability. The collection probability can be calculated as a solution of diffusion equation with appropriate boundary conditions but without the generation term. For such calculations a few parameters such as the width of the space charge region, the diffusion length, the depth of the p-n junction, etc. should be known. It is proposed to obtain these parameters for any particular structure by fitting the collected current experimental dependence on beam energy measured in SEM by simulated one. Other characteristics of convertor, such as open-circuit voltage, filling factor and maximum power can be easily measured in a scanning electron microscope using beam current, which produced the calculated value of collected current. Experiments with the real ^{63}Ni source show that for Si- and SiC-based structures the difference between the measured and predicted parameters does not exceed 10%.

Manufacturing Reliability of Via-First Through Silicon Via using Scanning-Laser-Beam-Induced Current Method

Woon Choi*, and Hajime Tomokage

Department of Electronics Engineering and Computer Science, Fukuoka University,
8-19-1 Nanakuma, Jonan-ku, Fukuoka 814-0180, Japan
*choi@fukuoka-u.ac.jp

Recently, high bandwidth memory (HBM) which is the next generation high-performance DRAM, has been announced. This is connected vertically and horizontally between the dies of the SDRAM stacked using through silicon via (TSV) technique.

A TSV of copper interconnects enables vertical connection between layers without wire bonding. The depth of a TSV, which corresponds to the thickness of a chip or interposer of a TSV, is the same role as the length of a bonding wire. Therefore, advantages of TSV interconnect enables high-speed signal transmission and volume reduction of electronic devices. However, the manufacturing processes of TSVs for 3D integration are complex, and a high yield for each process is required. Failure analysis for improvement of the wiring reliability is important.

In this study, for the manufacturing reliability of TSV, the filling state of electroplating copper was investigated using the scanning-laser-beam-induced current (SLBIC) method. After reactive etching of via holes with a diameter of 50 μm and the depth of 100 μm, a copper seed layer was deposited by sputtering, metal filling of the via is performed by electroplating, and planarization by chemical mechanical polishing. The wiring of the top surface for the SLBIC measurement was formed by photolithography after the second times copper electroplating. This was used a sample. An infrared laser beam with a wavelength of 1064 nm scanned upwards from the back surface of a sample, and the induced current between the copper layer and silicon back surface was measured to obtain the current image and optical image. By changing the focal point of the laser beam, the copper filling state of the TSV was analyzed non-destructively in the direction of depth.

Tuesday June, 7 - Poster Session - TuP-IV

Miscellaneous

Development of a low energy secondary electron detector for out-lens SEM and its application of semiconductor heterostructures

T. Agemura[1]*, H. Iwai[2], T. Kimura[2] and T. Sekiguchi[1,2]
[1]Graduate School of Pure and Applied Sciences, University of Tsukuba, Tsukuba, Japan,
[2]Nano-Electronics Material Unit, National Institute for Materials Science, Tsukuba, Japan
* AGEMURA.Toshihide@nims.go.jp

Scanning electron microscopes (SEMs) are widely used to observe surface structures of various materials on the nanometer scale. To improve the image resolution, several modifications are implemented; the immersion objective lens, the superimposition of electrostatic and magnetic fields, the retarding voltage, and so on. However, it must be pointed out that SEM users cannot estimate the energy, angle, and number of electrons emitted from the specimen, because those complicated systems give strong modification on secondary electrons. Thus, the secondary electrons are not effectively used to characterize the physical/chemical properties of materials. To overcome such difficulties, we have developed a detector which can be mounted on out-lens type SEM. [1]. This detector is composed of a planar bias filter above and a micro-channel plate (MCP) below the specimen. The SE trajectories become parabolic which can be simulated easily. The angular selective detection is also realized by sectoring MCP.

However, it has been found that there exist many tertiary electrons (TEs) which increase the noise level of the detector. The backscattered electrons (BSEs) emitted from the specimen hit the filter grid and yield significant TEs. In order to overcome this problem, we have developed a new detector with a spherical energy filter. Based on the trajectory simulation, the SE detection efficiency can be three times higher.

In the presentation, we show the improvement of detector performance and give the instances of SE observation using this detector. We will show SEM images of semiconductor hetrerostructures and homostructure with different doping levels.

[1] T. Sekiguchi and H. Iwai, Japanese Journal of Applied Physics **54**, 088001 (2015).

Mechanical Properties of Hydrogenated-Amorphous Silicon Thin Films on Crystalline-Silicon Substrates

A. Abdallah[1]*, A. UI-Hamid[2], S.A. Said[3] and N. Tabet[1]
[1]Qatar Environment and Energy Research Institute, Hamad Bin Khalifa University, Doha, Qatar
[2]Center for Engineering Research, King Fahd University of Petroleum and Minerals, Dhahran, Saudi Arabia
[3]Mechanical Engineering Department, King Fahd University of Petroleum and Minerals, Dhahran, Saudi Arabia

*aabdallah@qf.org.qa

, , ,

Hydrogenated amorphous silicon (a-Si:H) solar cells show high potential for replacing the conventional crystalline silicon solar cells with a large optical absorption coefficient and direct bandgap. However, the main challenge is to improve the cell efficiency which is approximately 50% lower than those made of multi-crystalline silicon solar cells. The low efficiency of a-Si:H thin film solar cells is attributed to low carrier mobility [1].
One of the innovative methods available to overcome this shortcoming is to engineer residual stresses in a-Si:H films in a controlled manner. Previous work suggests that the ability to tailor residual stress during film growth could reduce the density of hole traps, potentially enhancing the transport properties of a-Si:H thin films, and as a consequence, improving the solar cell efficiency [2]. Beyond this, in order to produce successful, long lasting solar cells, these films should exhibit good mechanical properties such as mechanical stability and adhesion between layers (measured by scratch hardness). Residual stresses induced in thin film during deposition may affect the integrity of the layered structure dramatically. This may result in film cracking and/or interfacial failure (buckling and delamination), and as a consequence, deterioration of physical and optoelectronic properties of the film.
Plasma Enhanced Chemical Vapor Deposition (PECVD) has been used to grow hydrogenated amorphous silicon thin films (a-Si:H) on crystalline silicon substrates coated with a silicon oxide insulating layer. Mechanical properties of a-Si:H films obtained from load-displacement curves via nanoindentation, and results from nanoscratch experiments are presented as a function of residual stresses induced in the film during deposition. Residual stresses varying from compressive to tensile were obtained by modifying the process pressure from 100 mTorr to 600 mTorr. FTIR analysis showed films with compressive residual stress expressed hydrogen bonding dominated by silicon monohydride, whereas tensile stress samples exhibited a dominance of hydrogenated voids. In addition, Film buckling and delamination were observed in films with a compressive residual stress above -1000 MPa. Experimental results indicate that residual stresses induced in the films during deposition have a strong effect on film elastic modulus, as well as scratch and indentation hardnesses. The film indentation hardness decreases from high compressive residual stress to a low tensile residual stress in the films.

[1] J. Mattheis, J. r. H. Werner, and U. Rau, Phys. Rev. B **77**, 085203 (2008).

[2] E. Johlin, N. Tabet, S.C.-Galnares, A.A. Abdallah, M.I. Bertoni, T. Asafa, J.C. Grossman, S.A. Said, T. Buonassisi, Physical Review B **85**, 075202 (2012).

List of Contributors

K

L

M

N

O

P

R

S

T

U

V

W

X

Y

Z

BIAMS 2016

Sunday June, 5	16:00-19:00	Registration and welcome party at Versailles university
Monday June, 6	8:00-8:50	Registration
	8:50-9:00	Opening remarks
	09:00-10:40	**Cathodoluminescence - part 1** Chair: Anna Cavallini, *University Bologna, Italy*
	10:40-11:00	Coffee break (20min)
	11:00-12:20	**Beam-induced modifications** Chair: Eugene Yakimov, *Institute of Microelectronics, Chernogolovka, Russia*
	12:20-14:00	Lunch break (100min)
	14:00-15:40	**LBIC and EBIC** Chair: Takashi Sekiguchi, *National Institute for Materials Science Tsukuba, Japan*
	15:40-16:00	Coffee break (20min)
	16:00-17:00	**Excitation processes** Chair: Martin Kittler, *IHP Frankfurt & IHP/BTU Joint Lab Cottbus, Germany*
	18:00-20:00	Mayor reception at Espace Richaud
Tuesday June, 7	09:00-10:40	**Photovoltaic materials** Chair: Otwin Breitenstein, *MPI of Microstructure Physics, Halle, Germany*
	10:40-11:00	Coffee break (20min)
	11:00-12:20	**Cathodoluminescence - part 2** Chair: Javier Piqueras, *University Complutense, Madrid, Spain*
	12:20-14:00	Lunch break (100min)
	14:00-15:40	**EBIC and CL** Chair: Nouar Tabet , *Qatar Energy and Environment Research Institute, Qatar*
	15:40-16:00	Coffee break (20min)
	16:00-18:00	**Poster Session**
Wednesday June, 8	09:00-10:40	**Cathodoluminescence - part 3** Chair: Matthew Phillips, *University of Technology, Sydney*
	10:40-11:00	Coffee break (20min)
	11:00-12:20	**Miscellaneous** Chair: Maria Zamoryanskaya, *Ioffe Institute, St Petersburg, Russia*
	12:20-14:00	Lunch break (100min)
	14:00-14:40	**Plasmonic** Chair: Matthieu Kociak, *Laboratoire de Physique des Solides, France*
	16:15-18:00	Castle visit
	18:00-19:30	Garden visit (free time)
	19:30-23:00	Conference dinner (inside the garden)
Thursday June, 9	09:00-10:40	**Devices** Chair: Hajime Tomokage, *Fukuoka University, Japan*
	10:40-11:00	Coffee break (20min)
	11:00-12:20	**Nano-materials** Chair: Brigitte Sieber, *Université des Sciences et Techniques de Lille, France*